UNIVERSITÀ
DEGLI STUDI
DI TRIESTE

UNIVERSITÀ DEGLI STUDI DI TRIESTE

XXXIV CICLO DEL DOTTORATO DI RICERCA IN

MOLECULAR BIOMEDICINE

miR-200c prevents and reverts Lung Fibrosis by downregulating *Flt1* and promoting lung regeneration.

Settore scientifico-disciplinare: **Med/10**

DOTTORANDA
Maria Concetta Volpe

COORDINATORE
PROF. Germana Meroni

SUPERVISORE DI TESI
PROF. Marco Confalonieri

ANNO ACCADEMICO 2020/2021

CONTENTS

Abstract

Idiopathic pulmonary fibrosis (IPF) is a devastating progressive fibrotic disease affecting the lungs and causing chronic respiratory failure. In IPF, adult alveolar type II stem cells (ATII) cannot trans-differentiate to alveolar type I cells (ATI), and therefore, represents a relevant target in the progression of lung fibrosis. There are only two FDA-approved drugs for the treatment of IPF, which can only ameliorate the disease, but a permanent cure is not yet available. In this work, we showed that human ATII cells isolated from IPF patients displayed impaired trans-differentiation *in vitro.* When transfected with miR-200c the ability of trans-differentiation was restored. The administration of miR-200c into mice lungs was performed using an aerosol delivery system, which resulted in an inhibited fibrosis in bleomycin-induced lung fibrosis mouse model. This data confirms miR-200c to be a powerful anti-fibrotic treatment in conditions of early onset fibrosis and when fibrosis was already established. We investigated if ATII differentiation could be rescued upon down-regulation of *Flt1* a miR-200c target and highly expressed in endothelial cells. For this reason, we performed co-culture assays between endothelial cells from both Wild type (WT) and Cdh5 -ERT2-CreFlt1$^{flox/flox}$ mice, depleting *Flt1* in endothelial cells, and ctrl and bleomycin ATII cells. We observed that the knock-out of *Flt1* in endothelial cells prevented disease progression in a murine model of lung fibrosis, through releasing an increased amount of angiocrine factors, such as SerpinC1, Haptoglobin, Itih2 detected by mass spectrometry analysis of the secretome.

This work importantly contributed to the discovery of a new potential IPF treatment, such as miR-200c, and to the underlying molecular mechanisms involved in both lung fibrosis and lung regeneration.

1 Introduction

1.1 The Lung regeneration

Respiratory disease is one of the leading causes of mortality world-wide in aged people. About 65 million people suffer from pulmonary diseases and 3 million die each year due these pathologies, making the respiratory disease the third leading cause of death worldwide (World Health Organization; 2021). Several lung respiratory diseases are treated with palliative cures due to lack of available treatments, indicating an urgent need for the discovery of novel therapeutics (Calvert and Firth; 2020). Replacing damaged cells in the lung to restore the functionality of the epithelium, could be a very promising therapeutical approach for several lung diseases. It is known that adult tissue has a decreased ability to repair the damage upon an injury. On the one hand, tissues like the gastrointestinal tract, the skin, or the hematopoietic system, have a high cellular turnover sustained by stem cell niches that promote rapid regeneration after a damage (Parekh et al., 2020). On the other hand, organs, such as the heart and the brain, have a no regenerative capacity. In brain it has been known that there were identified stem cell populations in the hippocampus and in the olfactory bulbs that have a pivotal role in supplying pleiotrophin factors to the neurons during adult neurogenesis (Tang et al., 2018). In the heart, there was no identified stem cell population. In these organs, cellular injuries are repaired by the formation of scars of non-functional tissue (Tzaor and Poss; 2017). In the lung, the airway and the alveolar regions are relatively quiescent, exhibiting low cellular turnover and proliferation at homeostasis, but with a remarkable capacity to regenerate in response to injury. This regeneration could rescue the airway function or could repair the formation of a fibrotic scar that, if not cured, would cause a chronic disease. This regenerative capacity is due to the presence of progenitor cells, that are recruited after the injury and can differentiate into adult and fully committed cell types, thus promoting effective lung regeneration (Hogan et al., 2014).

1.2 The respiratory system

Anatomically, the respiratory system is divided into 2 different parts: the upper and the lower portions. The first one includes the nose, the nasal cavity, mouth and throat (pharynx) and terminates at the voice box (larynx), while the trachea and lungs represent the lower respiratory tract. Lungs are further subdivided into respiratory airways and terminal portion, in which peripheral alveoli perform gas exchange, the main function of the lung (Zepp and Morrisey., 2019) (Fig.1A).

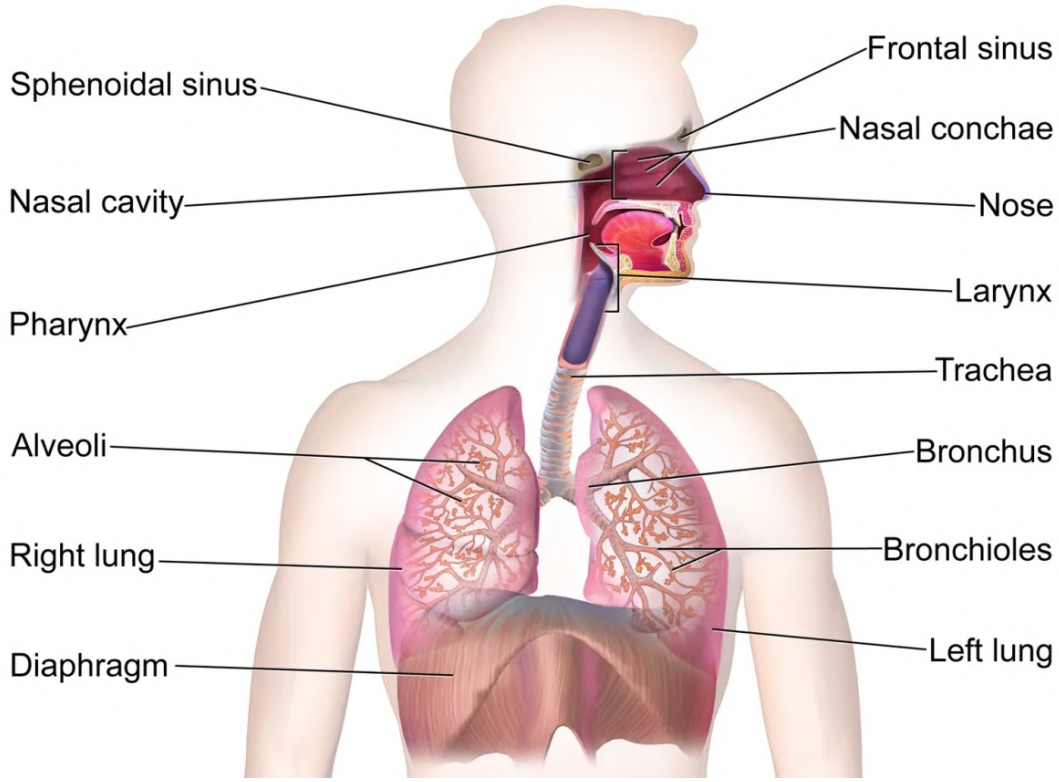

Figure 1: The respiratory system. *Representative image of the respiratory system divided in the nasal, the pharynx and the larynx cavities represented the upper respiratory system and the lower part of the respiratory system composed of trachea, bronchi and Alveoli (taken from owlcation.com).*

The development of the respiratory system has been studied and explored. It is composed of many steps including lineage specification, branching morphogenesis, sacculation and alveologenesis (Morrisey and Hogan., 2010). Defects in any of these processes can result in a severe reduction in respiratory function leading to various respiratory diseases. All lung compartments have distinct stem cell lineages, necessary for tissue regeneration after injury or while chronic and inflammatory diseases occur. The entire respiratory system is composed of several integrated compartments that together with the cardiovascular system allows efficient blood oxygenation (Cross et al., 2020). For this purpose, lungs are populated by several types of epithelial, endothelial, mesenchymal and

immune cells, critical for the functioning of each specific compartment. The branched structure of the airways is in close contact with the pulmonary vasculature, which intersects with cells in the alveolus to form the gas diffusible interface.

1.2.1 The epithelial cell types: role and function

The airway epithelium is composed of a continuous layer of cells that extends from the nasal cavity to the alveolar compartment. Proximal airway or bronchi cells could be columnar, pseudostratified, secretory cells and goblet cells (Zepp and Morrisey., 2019). Mucus-secreting goblet cells and multiciliate cells represent the first line of defense for trapping inhaled particulates or microorganisms. The distal airway is constituted by a single layer of secretory cells and fewer ciliated cells. In their relative positions, all cells contribute to the conductance of the air to alveolus and maintenance of the barrier against inhaled agents. Since the entire epithelium is constantly exposed to the external environment and subject to potential injury in the trachea and bronchi, basal stem/progenitor cells, can repopulate the pseudostratified epithelium during homeostasis and after injury. Other epithelial cells are the pulmonary neuroendocrine cells (PNEC), which are found in clusters at bronchiolar branch junctions, in neuroepithelial bodies or as solitary cells in the upper airways and trachea. PNECs act as sensory cells, harboring secretory granules loaded with a variety of neurotransmitters. It has been shown that PNECs modulate the immune response to allergens and can influence elevated mucus production (Barrios et al., 2018). Finally, the last and the most important portion of the lung is represented by alveoli that are distinct in their structure and development. Alveoli are lined by a continuous epithelium composed of intermixed Alveolar Type 1 (ATI) and Alveolar type 2 (ATII) epithelial cells (Gillich et al., 2020). ATI cells are large, thin and highly extended cells that cover 95% of the respiratory surface across which gas diffusion occurs. The main function of ATI cells is collaborating with the endothelial cells, to perform gas exchange and thereby play a critical role in barrier integrity. ATII cells are cuboidal cells that secrete surfactant proteins for preventing alveolar collapse during the respiratory act. ATII cells can also act as adult stem/progenitor cells, as it is known to occur after lung injury, ATII cells can activate themselves and trans-differentiate into ATI cells and promote lung regeneration (Ruaro et al., 2021).

1.2.2 The endothelial cells in the lung: role and function

During the last decades, much progress has been made in understanding the development, maintenance and repair of the alveolar epithelium, whilst the cells of the alveolar endothelium have received less attention (Gillich et al., 2020).

Pulmonary endothelial cells (EC) are an essential component of the gas exchange machinery of lung alveolus. Small blood vessels called capillaries are in close contact with the alveoli, allowing oxygen to be extracted from the air into the blood, while carbon dioxide can be released from the blood into the air, which makes the endothelial cells important actors in the gas exchange. Moreover, endothelial cells form a specific microenvironment, named vascular niche, in which endothelial cells interact with other resident cells to regulate development, homeostasis and regeneration (Rafii et al., 2016). The pulmonary vascular tract acts with ATI cells to constitute a very thin gas-diffusible interface, while endothelial cells perform other important roles, as controlling barrier integrity and functionality, and regulation of the pulmonary vascular tone (Ryan and Ryan., 1984). Furthermore, the pulmonary endothelium works as an active and dynamic receptor-effector tissue and responds to different chemical, physical or mechanical stimuli by secreting substances that maintain vasomotor balance and vascular-tissue homeostasis. Indeed, endothelial cells are highly metabolically active, sensing and responding to signals from extracellular environments (Eelen et al., 2018). Defects of the pulmonary endothelium play a central role in the pathogenesis of several chronic and acute lung diseases, such as acute respiratory distress syndrome (ARDS) or chronic obstructive pulmonary disease (COPD).

Pulmonary dysfunction may lead to:

- increased permeability that can be followed by vascular leakage and edema formation, acquisition of a pro-inflammatory phenotype with increased expression of adhesin molecules for inflammatory cell recruitment.
- release of inflammatory mediators and oxidative stress.

Endothelial cells are also involved in angiogenesis, microcirculation, coagulation and inflammation in the local tissue (Cines et al., 1998). Therefore, it has been shown that tissue regeneration in the lung requires neovascularization of the alveolar region (Niethamer et al., 2020), but it is still unclear how pulmonary endothelial cells participate in the lung regeneration process upon damage or injuries.

1.3 The Alveolar regeneration

1.3.1 The cellular crosstalk between Alveolar Epithelial cells and Endothelial cells

In adult alveolus, the alveolar membrane is composed of ATI cells interposed by ATII cells, intermediate basement membrane and capillary endothelial cells. Following, there is the presence of an alveolar interstitium, that consists of stromal cells, like fibroblasts, pericytes and macrophages, fibrillar extra-cellular matrix and separated capillaries (Vaccaro and Brody.,1981) (Fig. 2). It has been demonstrated that endothelial cells maintain the homeostasis of alveoli, contributing to the regeneration of the alveoli (Friedrich et al., 2019). However, alveolar endothelial cells may also regulate the behavior of alveolar epithelial cells by supplying extracellular matrix components in the alveoli (Witjas et al., 2019). As described before, ATI cells have a thin and flat shape with multiple branches spread over a large area of the alveolar membrane, facilitating contact with the endothelial cells and promoting an efficient gas exchange (Mammoto and Mammoto., 2019). The cellular crosstalk between ATII and endothelial cells is not completely understood, but many studies suppose that they may communicate through the basal membrane, by ATII cells acting as an anchor for various growth factors (Lawler et al., 2009). In fact, *in vitro* co-culture of ATII cells and endothelial cells demonstrated that physical contact between ATII cells and endothelial cells is crucial for the expansion of ATII cells (Ding et al., 2011). A recent publication by Gillich and colleagues showed that the alveolar endothelium is composed of two intermingled cell types with different morphologies and a distinct function (Gillich et al., 2020). The first cell type, named Aerocytes (aCap), specific for the lung, is specialized for gas exchange and the trafficking of leukocytes. The second type, General capillary (gCap), is specialized in the regulation of vasomotor tone and functions as a stem progenitor cell in capillary homeostasis and repair (Gillich et al., 2020). Additionally, they found that aCap and ATI are complex cells that are tightly apposed in the thinnest regions of the gas exchange surface. Moreover, aCap cells emerge as ATI differentiation begins, highlighting coordination between the two cell types, critical for gas exchange (Ellis et al., 2020). During adulthood, the alveolar endothelium is maintained and repaired by gCap cells, that like ATII cells, are bifunctional stem progenitor cells. Yet, further studies need to be performed to better understand and characterize the relationship between ATII cells and endothelial cells in alveolar regeneration (Ding et al., 2011).

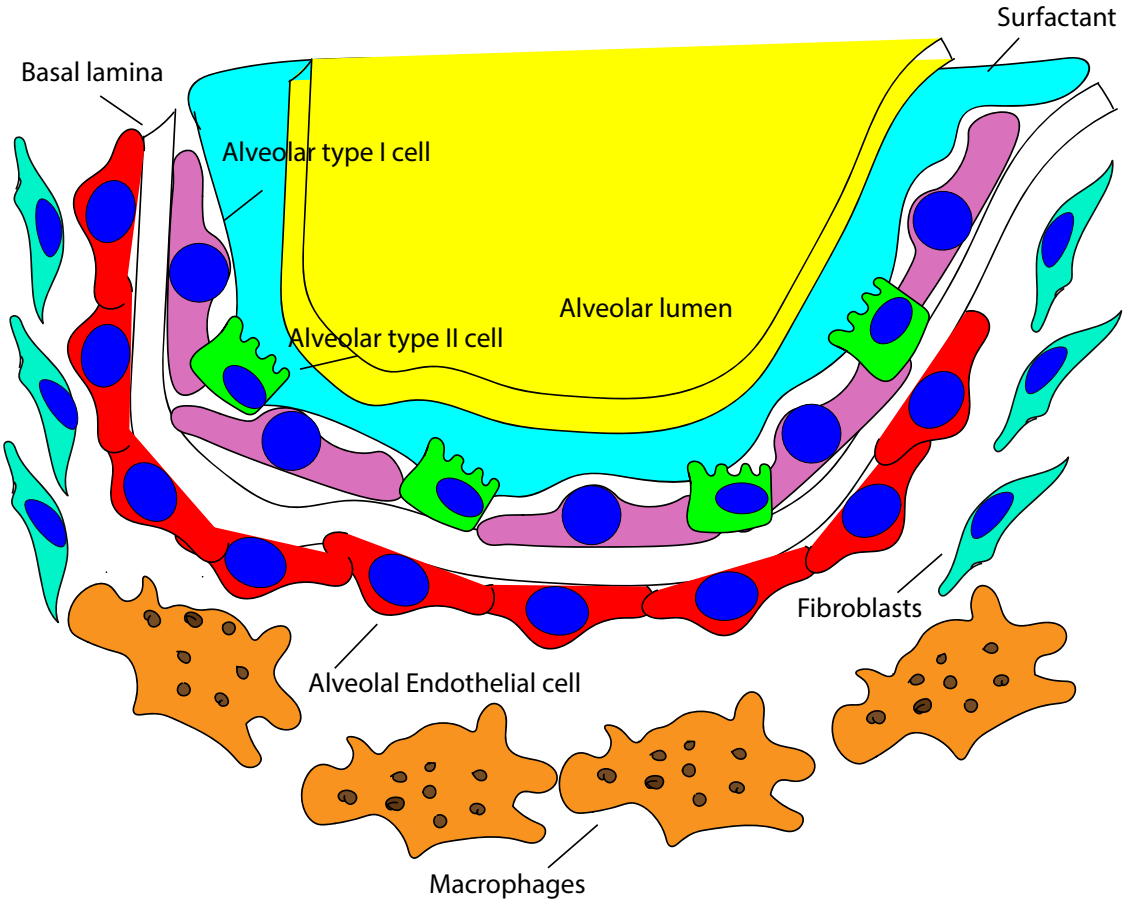

Figure 2: ***Cell types populating Alveolus.*** *Representation of the alveolar compartment: alveolar lumen is in the proximity of Alveolar type I cells (pink cells), Alveolar type II cells (green cell) that secreted surfactant (blue space). The basal lamina (the portion in white) separated Epithelial cells from Endothelial cells (red cells), Fibroblasts (blue cells) and macrophages (orange cells).*

1.3.2 Animal model of lung regeneration

The degree of lung regeneration differs among animal species and their age. Small animals, like rodents, have a better capacity for lung regeneration because their somatic growth lasts throughout their life (Wright et al., 2008). Studies in animal models are essential to study the pathophysiology of lung regeneration and the development of novel therapeutic approaches for human lung diseases that do not have a permanent cure (Nikolic et al., 2019). Nowadays, animal models are well characterized for lung regenerations, like alveolar regeneration in lung emphysema and compensatory lung growth after pneumonectomy (PNX) (Ding et al., 2011). Importantly, there are many transgenic mice available for lineage tracing, gene over-expression and targeted gene deletion of genes related to lung regeneration (Rawlins and Perl., 2011).

1.3.3 The compensatory lung growth after pneumonectomy

PNX is an experimental method performing the removal of a left lung lobe in mice that leads to species-specific and age-dependent compensatory growth of the remaining right lung lobe. PNX mimics the loss of functional gas exchange units observed in several chronic destructive lung diseases, like Idiopathic Pulmonary Fibrosis (IPF) (Paisley et al., 2013). This regenerative process is driven by alveologenesis, a process that is dependent on the proliferation of epithelial progenitor cells (Rock and Hogan, 2011). In 2011, Ding and colleagues showed that endothelial cells, covering the lung microvasculature, form a specialized vascular niche to modulate the function and the activation of alveolar progenitor cells. Following PNX, the membrane-type metalloprotease 14 (MMP14) in endothelial cells becomes up-regulated, which leads to the release of cryptic epidermal growth factor (EGF) like ligand, causing the propagation of alveolar progenitor cells, such as ATII cells, thus allowing the regenerative alveolarization (Ding et al., 2011). However, the precise mechanism by which PNX initiates and sustains regenerative alveologenesis and the role of endothelial cells in guiding the alveolarization and trans-differentiation of alveolar epithelial cells is still unknown. This makes PNX a potentially useful model for the study of the cellular and molecular events which occur during re-alveolarization.

1.4 The angiogenesis in lung regeneration

Angiogenesis is the process by which new capillary blood vessels can form from preexisting vasculature. It is an important physiologic process during development, tissue injury, repair and healing. Angiogenesis commonly occurs in response to local tissue hypoxia through both sprouting and non-sprouting processes involving endothelial cells. (Burri et al., 2004). Endothelial cells play a predominant role in angiogenesis, as they are the main target for molecular signals for cells growth, proliferation and migration. At the most basic level, tissues secrete pro-angiogenic molecules, due to the need for oxygen and basic nutrients. endothelial cells respond to growth factors by becoming invasive and developing protruding filopodia (Gerhardt et al., 2003). There are two different types of endothelial cells: 1) the stalk cells, that proliferate, elongate their sprouts, forming lumens and generate blood circulation under suitable conditions; 2) tip cells, are in the distal end of each sprout, are motile, invasive and highly polarized with many long filopodial protrusions which can extend, lead and guide endothelial sprouts (Carmeliet and Jain., 2000) (Fig. 3). Tip cells can connect with neighboring tip cells and form new vessel circuits. The tip-stalk cell equilibrium is essential for the angiogenesis process, as it regulates the balance between the secretion of pro-angiogenic and anti-angiogenic factors and consequently the activation of their downstream signaling network (Carmeliet and Jain., 2000). Adult endothelial cells are quiescent with a long half-life, due to the protection mechanisms induced by vascular endothelial growth factor (VEGF), NOTCH, angiopoietin 1 (ANG1) and fibroblasts growth factor (FGF) pathways. Moreover, endothelial cells present oxygen sensors like prolyl hydroxylase domain-containing protein (PHD) 1,2 and 3, that can regulate members of the hypoxia-inducible factors (HIF) family and respond to hypoxic stimuli from the blood (Bruick et al., 2003).

Due to the complexity the lung, studies of lung angiogenesis and its role in lung disease appear to have lagged those in other organs (Eldridge and Wagner; 2019). However, the angiogenic process is very complex and requires the coordinated action of several molecules, among those, the VEGF-A plays the most crucial role.

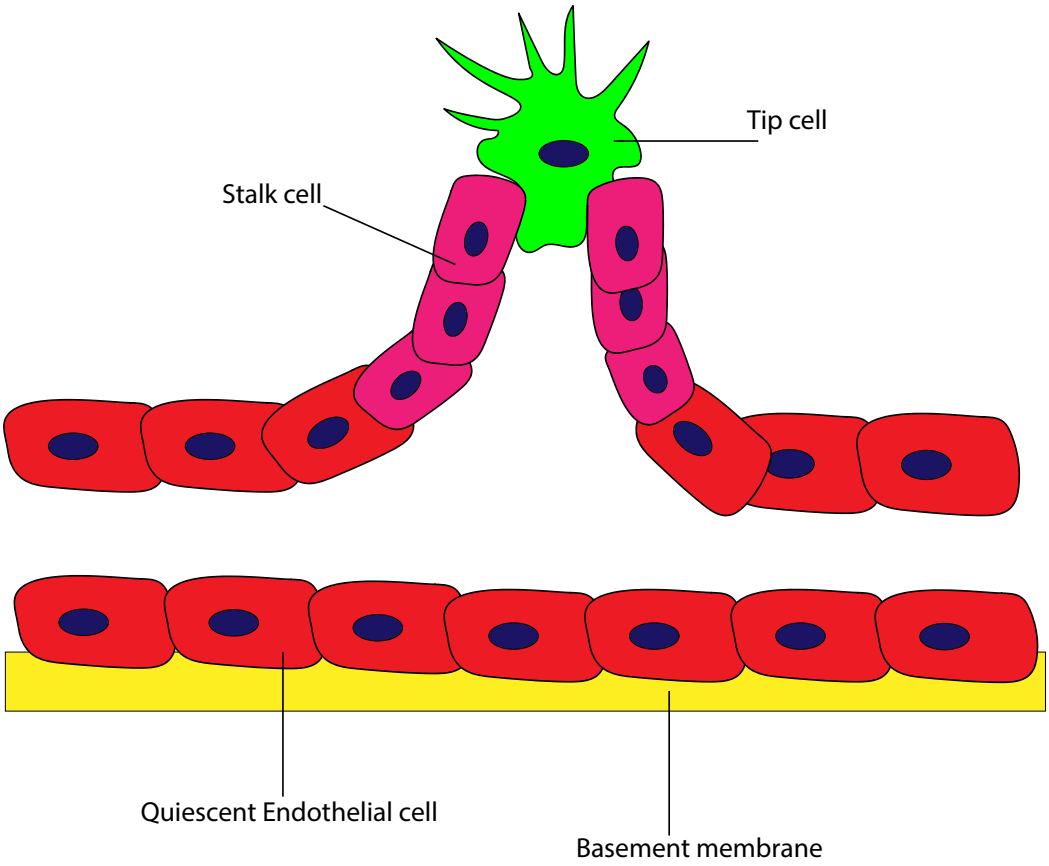

Figure 3: Model of endothelial cells. The tip cells (in green) present many protruding filopodia. The following stalk cells (in pink) proliferate and form a new vessel lumen. Quiescent endothelial cells (in red) are attached to the basement membrane.

1.4.1 The role of VEGF in Lung

VEGF-A is a 34-46 kDa glycoprotein that belongs to a superfamily of structurally and functionally related proteins, encoded by different genes, which also include VEGF-B, VEGF-C, VEGF-D and placental growth factor (PIGF) (Giacca et al., 2010). They all share a common receptor-binding domain. Among all the factors, VEGF-A, due to its proliferative potential, is described as a key regulator of angiogenesis (Tetzlaff and Fisher., 2018). It can form heterodimer complexes with other family members to activate VEGF receptors and modulate downstream signaling. The process of alternative mRNA splicing generates 7 different isoforms of VEGF-A containing 206, 189, 183, 165, 148, 145 and 121 amino acids (Giacca et al., 2010). The most abundant and biologically active splicing isoform is VEGF165 (Jia et al., 2006). Airway epithelial cells are the predominant source of VEGF-A especially during the development, alveolarization and lung maturation (Barratt et al., 2018). Significant amounts of VEGF-A persist in the normal adult lung, where the alveolar epithelium appears to be the major source, although smooth muscle cells, macrophages, endothelial cells and fibroblasts also express VEGF-A (Barratt et al., 2018). The classical processes linked to VEGF-A activity are extremely limited in the mature lung. While the exact role of VEGF-A in the lung has not been fully defined, it has been proposed that compartmentalization of VEGF-A within the alveolar space is essential to maintain normal lung structure and function (Balberova et al., 2021). VEGF-A has been observed to stimulate ATII growth, surfactant production and angiogenesis of the systemic vasculature with reports suggesting an additional anti-apoptotic and survival role for epithelial and endothelial cells (Barratt et al., 2018).

1.4.2. The VEGF Receptors

The biologic activities of VEGF-A are mediated through its interaction with specific receptors. Three VEGF tyrosine kinase (TK) receptors (VEGFRs) have been identified to date: VEGFR1 (or Flt1) and VEGFR2 (or Flk1) and VEGFR3 (Plate et al., 1992). *Flt1* and *Flk1* are mainly expressed on endothelial cells and are linked to endothelial differentiation and vascular organization (Shibuya; 2006) (Fig. 4). Flk1 binds VEGF-A and appears to be the major transducer of VEGF signals in endothelial cells mediating all endothelial cells responses to VEGF. The binding of VEGF to its receptor results in a variety of biological responses such as proliferation, due to the inhibition of endothelial cell apoptosis, migration and differentiation (Shibuya; 2011).

Last, VEGFR3 is described as a member of tyrosine kinases receptors, without binding VEGF165 (Robinson et al., 2001). It is especially expressed in lymphatic endothelial cells, generating the main signal for lymphangiogenesis. Besides the VEGF3 receptor, there are also members of the neuropilins family, as Neuropilin 1 (NRP1), that act as co-receptors of VEGF, promoting the binding and increasing the affinity of VEGF with the VEGFR2 (Carmeliet et al., 2011).

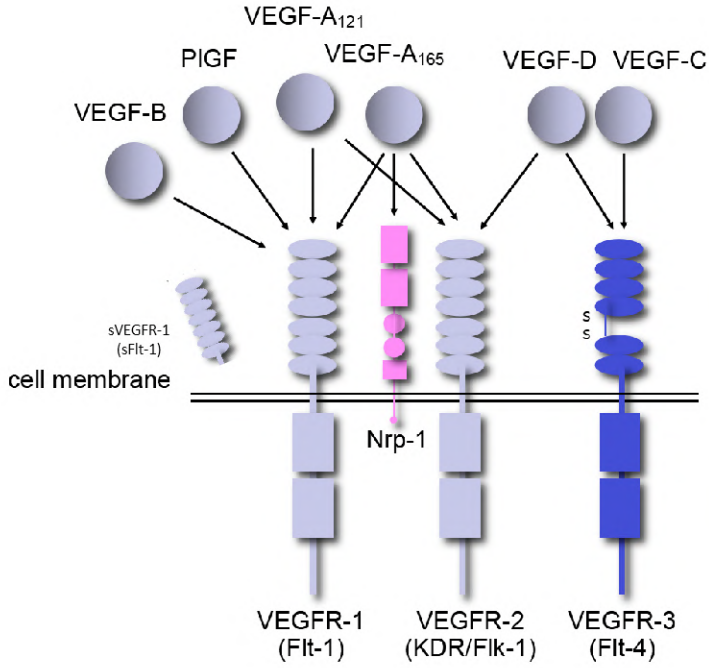

Figure 4: Interactions between VEGF family members with their receptors and NRP1 co-receptor (taken from Giacca et al., 2010).

1.4.3: The role of VEGFR1 in the lung

VEGFR1 is expressed not only by endothelial cells but also on the membrane of macrophages lineage cells, such as monocytes. Its role stands in recalling signals for the migration and cytokine/chemokine production of endothelial cells. *VEGFR1* expresses two mRNA isoforms: the full-length VEGFR1/Flt-1 receptor with tyrosine kinase; and the other one, encoding for a soluble protein form, carrying only the ligand-binding region (Fig. 4) (sFlt-1/soluble VEGFR1) (Shibuya; 2011).

Flt1 consists of 1338 amino acids and can be separated into four portions: the extracellular domain, transmembrane domain, tyrosin kinase domain and the carboxy-terminal region (Shibuya et al., 1992). The extracellular domain carries 7 immunoglobulin-like domains, but the ability to bind ligands is localized in the second

and the third domain. The affinity for VEGF-A is very high, with a Kd of about 2-10 pM, which is at least one order of magnitude higher than that of VEGFR2 (Mamer et al., 2020). However, the functionality of downstream signaling of VEGFR1 is not fully understood. Despite its high affinity, studies on the tyrosine kinase activity of VEGFR1 showed that it is relatively weak in the stimulation of the VEGF-A to activate the proliferation of endothelial cells. On the other hand, it can efficiently promote the migration of endothelial cells (Shibuya; 2006). These data suggest that VEGFR1 acts as both, a negative regulator by sequestering VEGF via the ligand-binding domain of its soluble form, and a positive regulator for the signaling towards migration/proliferation via its tyrosine kinase activity. In 1995, Fong and colleagues reported that VEGFR1 null mutant mice die in the embryonic stage, not because of poor vascularization, but due to an overgrowth of disorganized blood vessels (Fong et al., 1995). This demonstrated that in the angiogenesis process, VEGFR1 in the embryonic stage acts as a suppressor of pro-angiogenic signals establishing a crucial balance, which is essential for the correct vascular formation (Fallah et al., 2019). A recent study in mice showed that VEGFR1 expression increases three days after PNX (Chamoto et al., 2015). Therefore, it has been demonstrated that when soluble VEGFR1 is administered to mice after PNX, it prevents VEGF from binding to its cognate cell surface receptors, leading to the suppression of compensatory lung growth and repair (Been et al., 2009). These findings could indicate that VEGFR1 has other functions beyond its role in lung alveolarization after PNX.

1.5 Interstitial lung diseases

Interstitial lung diseases (ILDs) are a group of diffuse parenchymal lung disorders (DPLD) associated with elevated morbidity and mortality worldwide (Antoniou et al., 2014). The American Thoracic Society estimated the prevalence of these disorders on 80.9 cases per 100.000 men and 67.2 cases per 100.000 women worldwide (Travis e al., 2013). In Europe the incidence is estimated to be 0,33 to 2,51 per 10.000 people (Maher et al., 2021). Those pathologies are also known as fibrotic lung diseases, which are composed of a group of more than 100 heterogeneous disorders. They are characterized by similar clinical and radio-pathological patterns of aberrant inflammation and fibrosis of the lung parenchyma. Diseases causes and prognoses are very variable and not completely defined (American Thoracic Society; 2001). Accurate diagnosis depends on the assessment of potential contributing etiologies, including drugs, granulomatous disease, occupational or environmental exposures and connective tissue disorders (Corrin et al., 2011). However, many symptoms, named Idiopathic ILDs, can have an unknown cause and can occur after the disease diagnosis. Some symptoms can be potentially reversed, like the acute respiratory distress syndrome (ARDS), while others are progressive, such as Idiopathic Pulmonary Fibrosis (IPF). ILDs have in common overlapping clinical, radiographic, physiologic and pathologic manifestations, usually leading to decreased lung volume and compliance, and eventually to insufficient oxygenation due to both impaired ventilation and gas exchange (Martinez et al., 2017). The symptoms can subsequently lead to scarring and fibrosis of the lungs, resulting in progressive and irreversible lung damage. The most common symptom of all ILDs is shortness of breath, accompanied by dry cough, chest discomfort, fatigue, weight loss, associated with bilateral abnormal opacities of various types on conventional chest radiographs or high resolution computed tomographic (HRCT) scans (Lynch III and Belperio; 2011). ILDs usually have a gradual onset but can also occur in an acute form. Different risk factors could increase the probability to get ILDs (Ryu et al., 2001):

- Genetic predisposition
- Medical treatment such as radiation or chemotherapy.
- Exposure to dangerous materials, like asbestos or cigarette smoke.

From the biological point of view, ILDs are characterized by expansion of the interstitial compartment, which is the portion of the lung parenchyma between the epithelial and

endothelial basement membranes, with an infiltrate of inflammatory cells. The inflammatory infiltrates are often associated with fibrosis, either in the form of abnormal collagen deposition or proliferation and activation of fibroblasts in myofibroblasts capable of collagen synthesis (Visscher and Myers., 2006).

Today, major ILDs include more than 300 different disorders divided into ILDs with a known aetiology, which represent 35% of all cases, and ILDs with unknown aetiology, representing the remaining 65%. Recently, the American Thoracic Society (ATS) and the European Respiratory Society (ERS) consensus classification identify Idiopathic Pulmonary Fibrosis (IPF) as the most common of ILDs (Raghu et al., 2018).

1.5.1 Idiopathic Pulmonary Fibrosis

Idiopathic Pulmonary Fibrosis (IPF) affects 1-30 per 100.000 people worldwide. There are approximately 130.000 patients in the USA, 300.000 in Europe and 640.000 in East Asia (Ley and Collard., 2013). Altogether, IPF affects 3 million people worldwide and the incidence is increasing dramatically with age. IPF is estimated to affect 400 people in 100.000 over 65 population (Raghu et al., 2014). Most studies report that there is a predominance of male patients, however, it is unclear if these findings are correlated with a biological predilection or if it is a result of environmental factors (Raghu et al., 2014). Usually, IPF patients have a progression of symptoms ranging from cough and dyspnea to end-stage respiratory insufficiency. Therefore, patients have an extremely decreased life quality with a life expectancy of 3-5 years after diagnosis (Nureki et al., 2018). IPF is defined by the presence of a radiographic and histopathological pattern of usual interstitial pneumonia (UIP), leading to lesion composed of temporally and spatially heterogeneous areas of fibroblast and myofibroblast accumulation coupled with extracellular matrix deposition, disruption of alveolar architecture and subpleural honeycomb (Fig.5) (Katzenstein A-L., 1998). It usually presents as honeycombing cystic airspaces with well-defined walls, traction bronchiectasis (dilatation of the bronchi) and complete absence of the peripheral alveolar septal thickening. It has been reported that progressive fibrosis begins at the base and periphery of the lungs and gradually affects all lung tissues (Martinez et al., 2017). IPF is a complex disease where environmental and genetic factors contribute to disease susceptibility. Therefore, it can be classified into two different forms of the disease: sporadic or genetic form (Barros et al., 2019). Several rare variants were found in patients genes encoding telomerase RNA component such as Telomerase Reverse Transcriptase (TERT) and Telomerase RNA Component (TERC),

as well as other genes related to telomere maintenance such as Ring Finger Protein 2 (RNF2), Dyskerin Pseudouridine Synthase 1 (DKC1), Regulator of Telomere Elongation Helicase 1 (RTEL1), Poly(A)-Specific Ribonuclease (PARN) and Nuclear Assembly Factor 1 Ribonucleoprotein (NAF1), especially in Alveolar Epithelial cells (Alter et al., 2008). Other important genes found mutated in IPF patients are genes encoding for surfactant proteins, that are secreted primarily by alveolar epithelial type II cells. The mutation of the *surfactant protein C* gene (*SFTPC*) causes a deficient folding and therefore, inefficient processing of surfactants, dysregulated proteostasis, endoplasmic reticulum stress and might promote epithelial de-differentiation and death (Martinez et al., 2017). Therefore, molecular signatures of cellular stress, apoptosis and foreshortened telomeres, associated with genetic mutations, have been found also in sporadic IPF cases (Kropski et al., 2013). However, the causes of IPF sporadic forms are not clear yet. The lungs are constantly exposed to many injuries such as environmental exposures, smoking, viral infections, pollution, agriculture, livestock and metal dust. All these factors could affect aging, leading to pro-fibrotic reprogramming, epithelial cell senescence, excessive production of pro-fibrotic mediators and activation of mesenchymal cells leading to the eventual development of fibrosis (Salton et al., 2019). Although evidence is required to support the correlation between risk factors and the pathogenesis or the progression of the disease (Martinez et al., 2017).

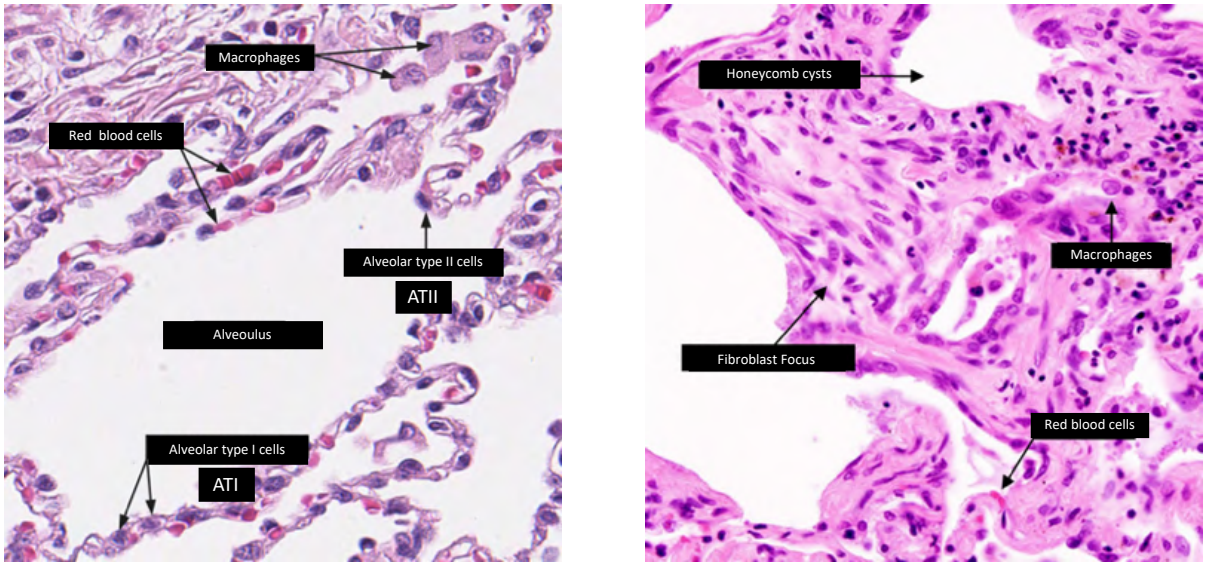

Figure 5: Histological pattern of IPF parenchyma. Representative images of a normal alveolus in the left from a healthy person, in which is possible to appreciate different types of cells as ATII, ATI and macrophages. On the right, a histological section of lung parenchyma from an IPF patient in which fibroblast focus and honeycomb cysts replace the alveoli space.

1.5.2 The role of Alveolar Epithelial cells in Idiopathic Pulmonary Fibrosis

For years, IPF was considered a devastating disease in which inflammatory or mesenchyme cells represented the main drivers of IPF, due to the high amount of inflammation and the consistent amount of collagen deposition in the lungs (Todd et al., 2012). However, in the last years, evidence showed that IPF is an epithelial-driven disease, and therefore, ATII could have a central role in the pathogenesis of IPF, due to a loss of regenerative potential (Naikawadi et al., 2016). Further, mutations in genes specifically expressed in ATII were identified in patients with familial pulmonary fibrosis (Moimas et al., 2019), linking a pathogenic relationship between ATII cells dysfunction to the development of scars. IPF lungs show an aberrantly activated lung epithelium, in which injured ATII cells may produce mediators of fibroblast migration, as well as the release of TGF-β and recruitment of inflammatory cells, leading to fibroblasts proliferation and activation into myofibroblasts (Salton et al., 2019). These myofibroblasts secrete extensive amounts of extracellular matrix (ECM) that subsequently remodel the lung architecture (Wang et al., 2015) (Fig 6). ATII cells are small, cuboidal cells with the anatomic features of active metabolic epithelial cells. They contain a high density of mitochondria and are distinctive by their apical microvilli (Barkauskas et al., 2013). They account for about 15 % of the total lung cells, but only 5 % is composing the alveolar area. ATII cells have four main functions: the production and secretion of surfactant proteins, the trans-epithelial movement of water and ions for regulating the volume of the alveolar surface liquid, the expression of immunomodulatory proteins necessary for host defense the regulation of innate immunity and finally the regeneration of alveolar epithelium after injury (Ruaro et al., 2021). The impairment in the normal functional capacity of ATII cells could lead to the development of a pro-fibrotic phenotype. Moreover, during IPF onset, increased apoptosis and senescence of ATII cells were observed in areas with both fibrosis and without it (Filho et al., 2001).

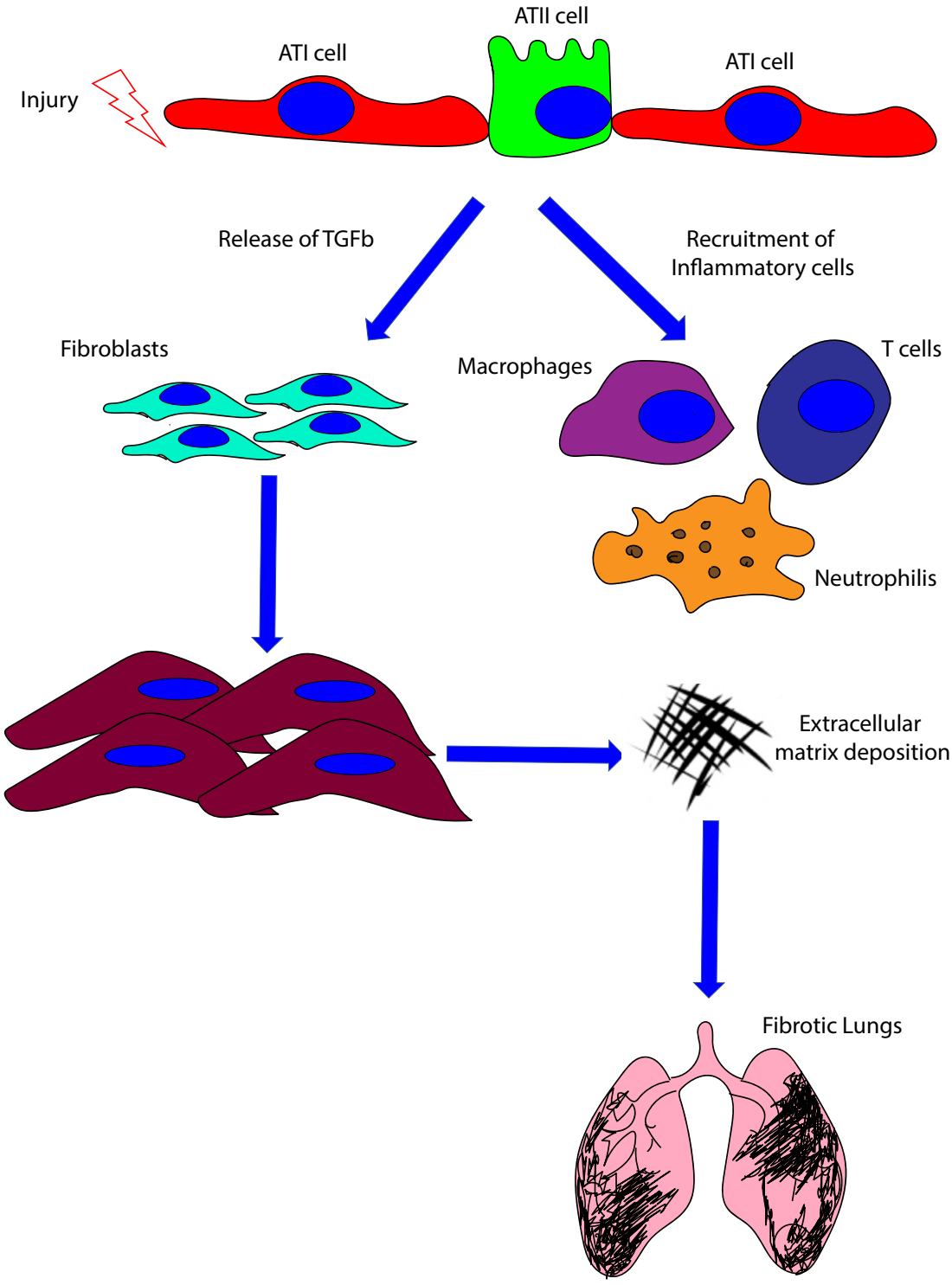

Figure 6: The key role of ATII in the development of fibrotic tissue.

1.5.3 Current treatments for Idiopathic Pulmonary Fibrosis

The pathogenesis of IPF remains poorly understood with a not precise method for diagnosing the disorder. It represents another important obstacle in the development of pharmacological and non-pharmacological therapies capable of stabilizing or improving lung function in patients (Barkauskas et al., 2013). Clinical trials using anti-inflammatory drugs like corticosteroids, immunosuppressive agents and cytokine modulators, showed low efficacy or even toxic effects (Takeda et al., 2014). However, there are two FDA-approved anti-fibrotic agents, named Pirfenidone and Nintedanib, for the treatment of IPF patients. Nintedanib is a tyrosine kinase inhibitor that acts in the growth factor pathways, targeting the vascular endothelial growth factors receptors 1, 2 and 3, fibroblast growth factor receptors 1, 2 and 3 and platelet-derived growth factor receptor (Wollin et al., 2015). However, patients, taking nintedanib, reported cases of drug-induced liver injury, increased risk of bleeding and thrombotic events, leading, in some cases, to myocardial infarction (Grzesk et al., 2021). The other drug, Pirfenidone, reduces the inflammation and the fibrotic effect, by down-regulating the TGF-β pathway and tumor necrosis factor alpha (TNF-a) (Lopez- de la Mora et al., 2015). Even if the molecular mechanism by which the drug is acting on fibrosis and inflammation is not well understood, it is known that it acts on collagen synthesis and in the myofibroblasts activation (Fig. 7). Again, patients after treatment with Pirfenidone reported side effects as anorexia, nausea, vomiting and liver damage (King et al., 2014). Unfortunately, these two drugs are shown to only slow down the rate of deterioration of the pulmonary function, not improving IPF progression or resolution. Both have shown some efficacy in reducing severe respiratory events, such as acute exacerbations and in many cases hospitalization for respiratory problems (Gulati and Luckhardt., 2020).

Despite the progress being made in recent years in the treatment of IPF, it remains a progressive and fatal disease with a poor prognosis and high mortality. Currently, IPF is the main cause of lung transplantation worldwide, which represents the best treatment option for patients affected by this disease (Hernandez et al., 2018). Even if only a minority of IPF patients receive the transplantation, lung transplantation still represents the only treatment significantly improving survival rate (Hernandez et al., 2018). However, mortality of patients when they are on the waiting list is high, as many patients are indicated for the transplant in an advanced disease stage (3 years after the diagnosis). Lung transplantation is also a very risky procedure leading to side effects, like graft

dysfunction, acute and chronic forms of allograft rejection, cytomegaloviral infections and cancer (Hernandez et al., 2018; Valapour et al., 2021). International guidelines for IPF treatment are indicating that currently there are no pharmacological therapies that would lead to an improvement in IPF survival (Abuserewa et al., 2021). Also, the progress in the development of new treatments has been hampered by the lack of understanding of the IPF pathogenesis (Williamson et al., 2014), which is a consequence of the absence of preclinical models that fully recapitulate the clinical features of IPF (Blackwell et al., 2013).

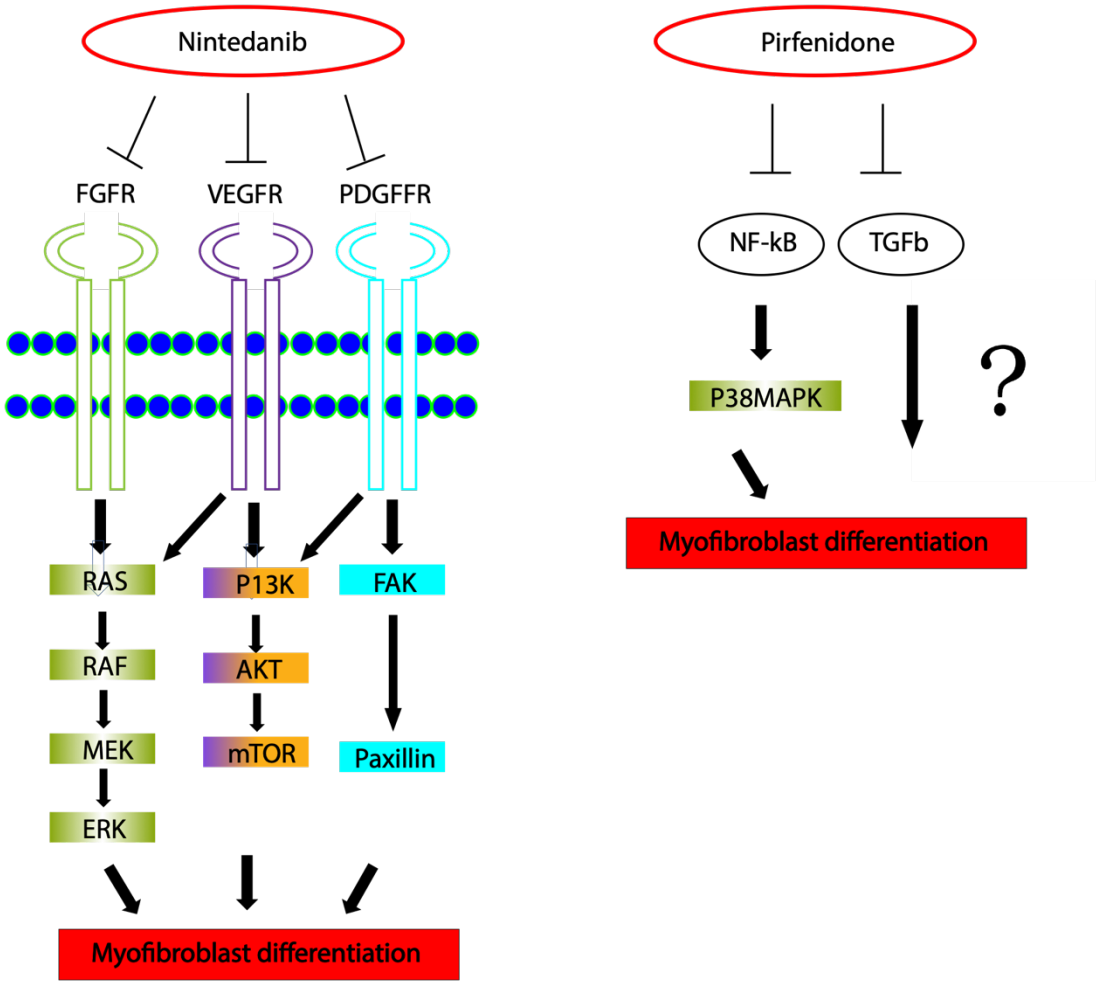

Figure 7: Molecular mechanism of Nintedanib and Pirfenidone in inhibiting Myofibroblast differentiation.

1.5.4 Animal model of Idiopathic Pulmonary fibrosis

A single model system may never fully recapitulate all the aspects of the human IPF, as it is characterized by progressive and irreversible clinical problems, with a sex predilection for older males (Jenkins et al. 2017). Murine models do not fully mimic classical IPF histopathology, probably due to anatomic differences between murine and human lungs, while rats may be more reminiscent to recapitulate IPF lung histopathology. However, direct comparisons between rats and mice suggest similar responses to lung injury. Pigs and ferrets are more similarly to humans anatomically but are harder to maintain under laboratory conditions compared to mice or rats (Tashiro et al., 2017).

Animal models of IPF disease can be divided into those with a strong and lower inflammatory injury. Use of bleomycin, radiation, silica, asbestos, FITC and many cytokine overexpression systems lead to fibrosis after a robust inflammatory response, whereas transgenic animal model targeted depletion of alveolar epithelial cell genes are less dependent on inflammation (Jenkins et al., 2017). American thoracic society recommends that mice are considered the best animal model for pre-clinical studies today (Jenkins et al., 2017).

1.5.4.1 The bleomycin-induced lung fibrosis animal model

Among various models of IPF (Bleomycin, FITC, Silica and radiation), the bleomycin model is the most used (Walters et al., 2008). Bleomycin is part of complex glycopeptide antibiotics family isolated from *Streptomyces verticillus.* It is clinically used as a chemotherapy drug for head and neck carcinomas and lymphomas (Moeller et al., 2008). Bleomycin is causing cell cytotoxicity by inducing double-stranded DNA breaks (Huang et al., 1981), leading to cell death by apoptosis. In the lungs and skin, the bleomycin-induced toxicity is higher, due to the lack of the bleomycin-inactivating enzyme called Bleomycin hydrolase, an intracellular cysteine protease (Yagoda et al., 1972). Therefore, in the lung, the persistence of the compound is prolonged and consequently increasing bleomycin-induced lung injury and lung toxicity. Analyses of patients' lungs, that died from bleomycin-induced pulmonary fibrosis, have reported ATI loss, vascular endothelial cell damage, ATII hyperplasia, alveolar immune cell infiltration, intra-alveolar collagen deposition and diffuse alveolar and sub-pleural fibrosis (Simpson AB et al., 1998). Since the recognition of bleomycin as a cause of pulmonary fibrosis, it has become the agent of choice for modeling pulmonary fibrosis in rodents.

In general, the lung injury progresses through three main steps:

- Acute injury and inflammation, a result of widespread damage of the alveolar epithelium, vascular leak and upregulation of pro-inflammatory cytokines (Moore et al., 2008).
- The transition phase from inflammation to active fibrosis, in which there is an increase in fibroblasts proliferation and myofibroblasts activation (Chaudhary et al., 2006).
- Chronic fibrosis stage, characterized by myofibroblast expansion and increased deposition of extracellular matrix (Moore et al., 2008)

  The bleomycin model is a self-limiting model of fibrosis which contrasts with the progressive chronic fibrosis typical of the human IPF (Moore et al., 2008). The bleomycin model is a non-progressive model, with a tendency toward spontaneous resolution. This is a potential disadvantage since in humans with IPF the disease progresses relentlessly, which usually leads to end-stage lung damage with honeycombing structures and no evidence of spontaneous resolution of fibrosis. Another limitation of the model is its significant chronic inflammation during the development of fibrosis in mice, which is relatively lower or absent in human IPF (Lawson et al., 2005). Despite these limitations, the bleomycin model remains the most widely used model for studies of chronic progressive lung diseases today, due to its easy fibrosis induction requiring short timepoints. Studies assessing bleomycin treatments in older mice revealed more aggressive fibrosis, which is associated with enhanced inflammatory responses and is not able to resolve spontaneously (Redente et al., 2011). Hecker and colleagues found that aged mice suffer from impaired resolution or regeneration after injury (Hecker et al., 2014). In addition, the animal model mimics the hyperplasia of ATII cells, which is an important feature particularly for the development of new drugs for IPF patients.

1.6 The angiogenesis in Idiopathic Pulmonary fibrosis

IPF is based on a complex and not completely understood pathogenesis. However, some of the cellular and molecular mechanisms of vascular remodeling have been explored and it has been shown that alterations of micro-vessels are involved in IPF (Hanumegowda et al., 2012). In order to understand the process of vascular integrity and repair, it is necessary to identify the factors associated with angiogenesis in IPF (Hanumegowda et al., 2012). Angiogenic factors (stimulatory and inhibitory growth factors) need to be in a precise balance to regulate vessel homeostasis in normal physiologic conditions in the lungs (Fallah et al., 2019). When this balance is disturbed, as it happens during tissue injury, the result can be either an increased or decreased angiogenesis (Polverini et al., 2017).

Several studies support the evidence that the IPF lungs capillary density is increased, as compensatory response, in areas of minimal fibrosis or normal lung tissue. On contrary, the most extensive fibrotic lesions show low level of VEGF expression and are usually associated with a very low capillary density (Ebina et al., 2004). Similar evidence have been found in autopsies of IPF lungs that were characterized by reduced vascular density, as well as diminished total vascular area, loss of vessels close to alveolar space (Hanumegowda et al., 2012). This data is suggesting the destruction of the pulmonary system in fibrotic lungs of IPF patients (Renzoni et al., 2003). Also, it has been suggested that the poor regenerative capacity in aged lungs may influence lung repair and consequently fibrosis resolution (Meiners et al., 2015). Although the role of the lung vasculature in IPF and repair mechanisms in aging lungs is not yet completely studied (Caporarello et al., 2020).

1.6.1 The role of Endothelial cells in Idiopathic Pulmonary fibrosis

Endothelial cells together with the ATI cells have a pivotal role in permitting gas exchange (Aird., 2007). Endothelial cells are important regulators of lung homeostasis releasing angiocrine factors that regulate alveologenesis, both in lung development, as well as in the regeneration process in adult mice (Ding et al., 2011). The dysfunctionality of endothelial cells increases with aging, and it may be a cause for the development of chronic lung diseases (Polverino et al., 2018). In IPF, capillary irregularities, vessel dilatation and loss of microvasculature have been observed (Barrat and Miller; 2014), but the role of endothelial cells in IPF disease remains unknown (Caporarello et al., 2020). In 2018, Kato and colleagues showed that in mouse model of bleomycin-induced lung

fibrosis the lung microvasculature goes through extensive remodeling (Kato et al., 2018). Importantly, the depletion of the VEGFR pathway, in the early phase of the inflammatory process upon bleomycin treatment, inhibits the activation of fibroblasts (Iyer et al., 2015). In the lungs, a subset of bone marrow-derived stem cells, named Endothelial progenitor cells (EPCs), may be essential in parenchymal repair and reconstitution of the damaged vascular bed (Yamada et al., 2005). EPCs are divided into two different groups: the first one is represented by late EPCs that differentiate into mature endothelial cells and are involved in the repair of injured blood vessels (Faldini et al., 2007). The second group is represented by early EPCs that have the angiogenic capacity by secreting cytokines and VEGF (Urbich et al., 2005). It was described that in IPF lungs the number of EPCs is reduced in comparison to healthy controls. However, fewer reports are containing IPF patient's data.

1.6.2 The VEGF factor in Idiopathic Pulmonary fibrosis

Over the last decade, there has been an emerging interest in researching the role of VEGF in IPF, especially with the development of Nintedanib (Barratt et al., 2018). VEGF is one of the most potent angiogenic factors known to date, and as such, is a common target for antiangiogenic therapies (Niu and Change., 2010). An imbalance of angiogenic mediators, such as VEGF, has also been found in the lungs of IPF patients, where many studies have shown a decrease in lung VEGF protein levels (Willems et al., 2013). However, other groups have observed that VEGF is unaltered or even elevated in IPF patients (Anto et al., 2010). Therefore, the association between the disease and this growth factor remains matter of scientific debate. Currently, it has been demonstrated that Platelet-derived growth factor (PDGF), VEGF, and fibroblast growth factor (FGF) have all an implication in the IPF pathogenesis (Hanumegowda et al., 2012). Overexpression of VEGF in the lungs increases pulmonary vascular permeability, which results in edema (Kaner et al., 2000). Normally, in lungs, VEGF performs many functions that are associated with IPF disease, such as the stimulation of epithelial proliferation, prevention of epithelial cell apoptosis, which was demonstrated both *in vitro* and *in vivo* studies (Roberts et al., 2007) and protecting endothelial cells by reducing vascular remodeling (Farkas et al., 2009). VEGF has also a relevant function in promoting the type-2 inflammation that may increase the severity of an existing fibrotic response (Lee et al., 2004). Accordingly, anti-VEGF gene therapy approaches have been purposed as potential treatment to attenuate lung injury and lung fibrosis (Kulkarni et al., 2016). In

conclusion, alteration in the angiogenic pathway might be related to IPF phenotypes. However, since there are reported different explanations, further studies need to be addressed in the research of the role of VEGF in IPF (Murray et al., 2017).

1.6.3 The role of VEGFR1 in Idiopathic Pulmonary fibrosis

As described above, VEGF interacts with 3 Tyrosine-Kinase receptors, VEGFR1, VEGFR2 and VEGFR3. Nintedanib acts an inhibitor of VEGF receptors 1-3, PDGF receptors and FGF receptors 1-3, which results in the inhibition of cell proliferation, migration and fibroblasts differentiation (Sato et al., 2017). Interestingly, under both, hypoxic and hyperoxia conditions, the expression of VEGFR1 is increased in the lungs (Barratt et al., 2018). Interestingly, macrophages isolated from both mice and rats, showed increased expression of VEGFR1 upon bleomycin treatment, thus confirming the hypothesis that VEGF signaling plays a relevant role in lung fibrosis (Hara et al., 2005) (Amano et al., 2021). However, the key role of VEGFR1 is not well understood, as not many studies have been performed. The main findings are suggesting that its depletion can rescue lung fibrosis (Amano et al., 2021; Amano et al., 2019). In conclusion, future studies need to be done in order to better understand the key role of VEGFR1.

1.7 MicroRNAs Biology

It's commonly accepted that MicroRNAs (miRNAs or miRs) play a critical role in the pathophysiology of a wide range of chronic respiratory diseases (Hoefel et al., 2019). MiRNAs are small non-coding RNA molecules (about 22 nucleotides in length) situated in introns and sometimes in exons. Pri-miRNA expression is mainly driven by RNA Polymerase II and in fewer cases by RNA Polymerase III. Pri-miRNA are further processed in the nucleus by the Microprocessor, containing Drosha (RNase III enzyme) and DGCR8 (dsRNA-binding protein), allowing formation of pre-microRNAs, short stem-loop structures of 65–75 nt. Pre-miRNA are translocated, by the exportinV, from the nucleus to the cytoplasm, where Dicer, a cytoplasmic RNase, generates the mature 22 nucleotides long dsRNA by cleaving the loop structure of the pre-miRNA (Joshi et al., 2011). The leading strand of the microRNA is loaded onto the RNA-induced silencing complex (RISC) in order to silence the target mRNA through sequestration, translational repression or mRNA degradation (Wang et al., 2007) (Fig. 8). Unlike the process involving siRNAs, microRNAs do not require perfect pairing to induce silencing, therefore miRNAs can modulate several transcripts by binding to the complementary sequences of the mRNA in their 3' untranslated region. In particular, the interaction occurs through complementary binding of the seed sequence of miRs, located between nucleotides 2 and 8 at the 5' end of the miRs, to the target mRNA (Gebert et al., 2019). miR dysregulation can potentially influence the function of multiple genes, and therefore it can lead to pathologic conditions (Hoefel et al., 2019).

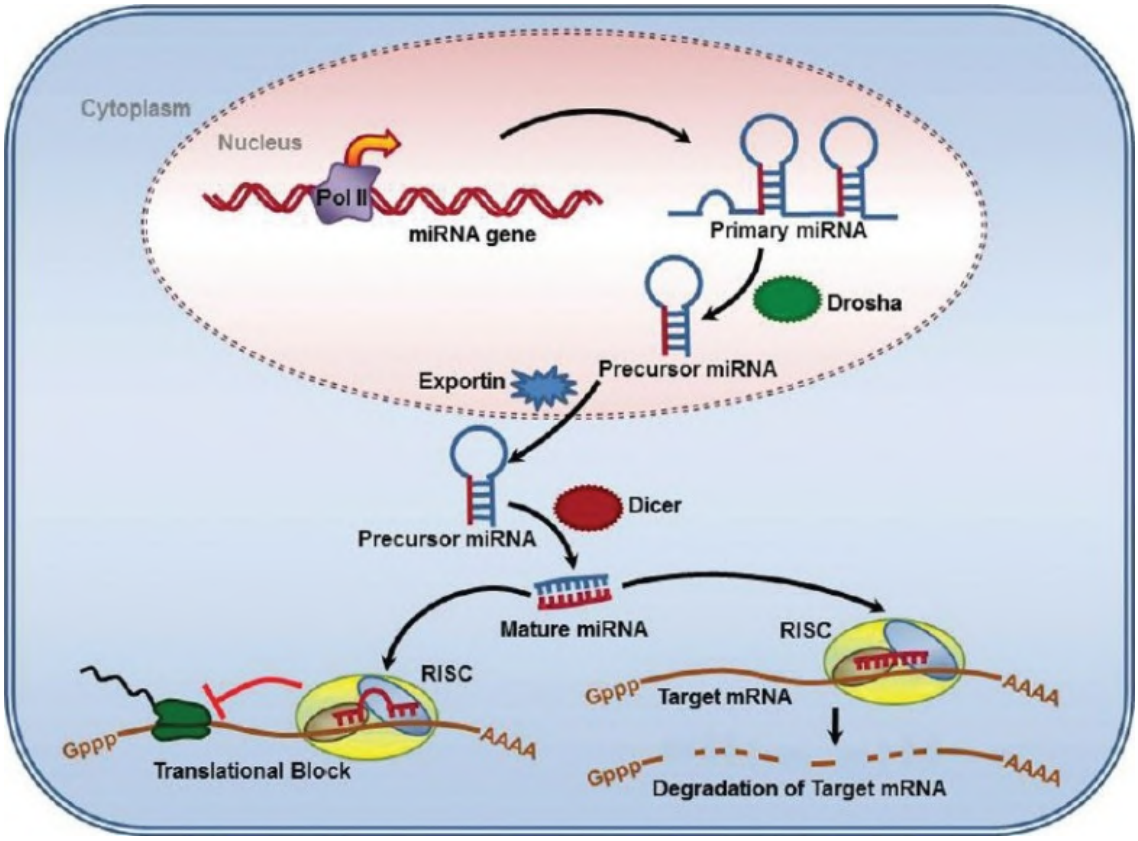

Figure 8: MiRNA synthesis and degradation of target mRNA (taken from Joshi et al., 2011).

1.7.1 MicroRNAs in lung function

The important role of different microRNAs in lung cell differentiation, lung regeneration and lung diseases has been extensively investigated (Boateng and Krauss., 2020; Takagi et al., 2019; Sato et al., 2017). The pivotal role of microRNAs in lung function is evident when *Dicer1* was silenced in the mouse lung epithelium in both the developing and adult lung, leading to decreased branching morphogenesis and a severe ECM production with fibrosis progression (Herrera et al., 2018; Harris et al., 2006). Furthermore, many studies of gain- and loss-of-function have highlighted microRNA member families or single microRNAs involved in IPF, raising the possibility to use these microRNAs as either biomarkers or targets for novel therapies (Gao et al., 2021; Li et al., 2016). Several microRNAs have been described to regulate specific processes in lung regeneration, including alveolar differentiation as miR-26 (Sun et al., 2018), miR-142, miR-17, miR-92 that play crucial role in ATI and ATII cell maturation in the developing alveolar epithelium (Guo et al., 2016; Shrestha et al., 2019; Wang et al., 2016). However, miRNAs have been implicated in the pathogenesis of lung disease as IPF (Stolzenburg et al., 2018).

miR-326 (Das et al., 2014), let-7d and miR-200 (Pandit et al., 2010; Yang et al., 2013), miR-153 (Liang et al., 2015) and miR17-92 (Dakhlallah et al., 2013) have an anti-fibrotic effect in IPF. To date, no one microRNA for the treatment of any lung disease has undergone human clinical investigation.

1.7.2 MicroRNAs in Idiopathic Pulmonary fibrosis

Epithelial injury in IPF seems to be the first initiator that regulates the development of fibrotic lesions (Pandit et al., 2010). Recent studies have been devoted to elucidating the participation of miRNAs in tissue fibrosis, which demonstrated having either a pro-fibrotic or anti-fibrotic effect (O' Reilly., 2016). Furthermore, it has been shown that miRNAs, in the pathological mechanisms of IPF, have an impact on the lung epithelial repair, the epithelial-mesenchymal transition, alveolar epithelial cells and collagen production (Miao et al., 2018). Indeed, microarray analysis of lung samples, from patients affected by IPF and healthy individuals, are indicating a significant difference in the expression of miRNAs between patients and controls (Fan et al., 2017). In the past years, many miRNAs have been studied in order to better understand the molecular mechanism of IPF, aiming at finding an eventual therapy for treating this incurable disease. The main factor studied in IPF is the transforming growth factor b (TGF-β), which is released in response to injury in the lung tissue. Released TGF-β stimulates fibroblast activation and differentiation in myofibroblasts to promote wound healing (Pandit et al., 2010). In 2010, Pandit and colleagues showed that in IPF patients miR-let-7d and miR-26 are both downregulated (Pandit et al., 2010). This is causing a negative regulation of the epithelial-mesenchymal transition, blocking TGF-β expression in alveolar epithelial cells and upregulating high-mobility-group-A2 protein (HMGA2), which consequently induces EMT and increases the deposition of collagen promoting pulmonary fibrosis (Pandit et al., 2010). Similarly, it has been seen that miR-29 has also been downregulated in IPF lungs (Cushing et al., 2015). The main targets of miR-29 are the proteins related to Extracellular Matrix (ECM), such as elastin, fibronectin and collagens, suggesting that this miR-29 is involved in the regulation of the ECM accumulation in lungs. Due to its downregulation in IPF patients, when it was instilled in a bleomycin-induced mouse model of fibrosis, it showed to have an antifibrotic effect (Herrera et al., 2018).

1.7.2.1 MiR-200 in Idiopathic Pulmonary fibrosis

Among the microRNAs families, the molecules that belong to the miR-200 family, appear particularly relevant in fibrosis regulation. This class of microRNAs is downregulated both in human individuals affected by IPF and in the bleomycin-induced mouse model of fibrosis (Moimas et al., 2019). MiR-200 family is composed of 4 components, with a seed sequence shared between miR-200a and miR-141, and also by, miR-200b and miR-200c. The inhibition of miR-200s miRNAs is known to affect a variety of cell functions, such as the epithelial-mesenchymal transition and angiogenesis induction in the lung. MiR-200 family and its target proteins are fundamental during primary and secondary alveolarization, as they suppress several pathways including TGF-β, Wnt and Notch (Caprioli et al., 2015). These pathways play relevant roles in human lung repair and differentiation (Caprioli et al., 2015) and are abnormally activated both in human pulmonary fibrosis and a bleomycin-induced mouse model of fibrosis. Additionally, intra-tracheal administration of miR-200c into the mice's lungs diminished experimentally induced pulmonary fibrosis, suggesting its anti-fibrotic role (Yang et al., 2012). In particular, it has been shown that miR-200c is regulating epithelial-mesenchymal transition (EMT), by targeting and downregulating Zinc finger E-box-binding homeobox 1 and 2 (ZEB1 and ZEB2) and upregulating E-cadherin and promoting the activation of ATII cells (Moimas et al., 2019). Besides directly targeting epithelial cells, miR-200c is silencing Vascular Endothelial Growth Factor Receptor 1 (VEGFR1 or FLT-1) (Mezquita et al., 2014) (Shibuya et al., 2006), thereby preventing VEGFR2 signaling activation. VEGFR2 signaling is the most important signaling of the endothelium and is crucial during adult angiogenesis to prevent tissue fibrosis. In conclusion, miR-200c is known to affect different pathways such as chemosensitivity, programmed cell death, cell growth and proliferation, epigenetic regulators and migration and invasion pathways (Fig.9). Being IPF a multi-factorial disease, all these pathways make it a relevant target to study for the treatment of IPF. Therefore, a relevant mechanism that should be studied in IPF pathogenesis is the dysfunction of the endothelium (Kivela et al., 2019; Hanumegowda et al., 2012), as it is also essential for the maintenance of programmed cell death and chemosensitivity (Fig. 9).

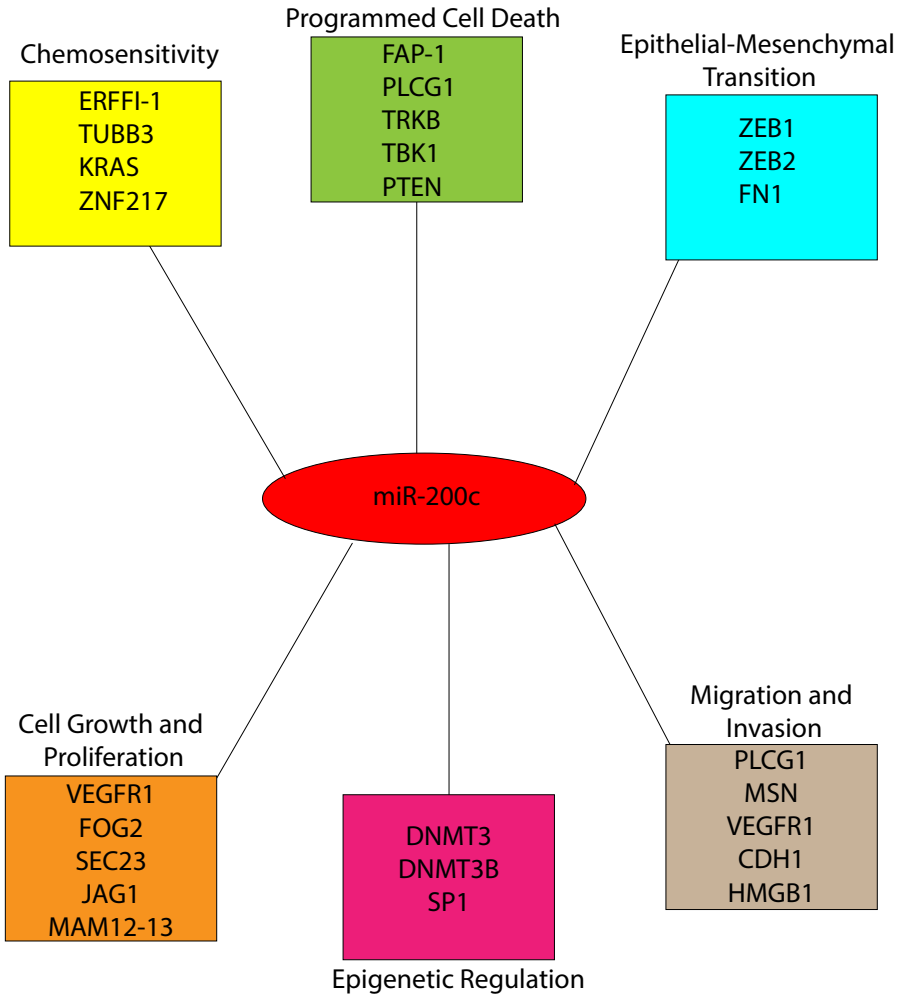

Figure 9: The main targets family of miR-200c.

1.7.3 Potential therapies using MicroRNAs

An increased number of new discovered microRNAs showed to be involved in several respiratory diseases, like IPF (Brown et al., 2014). Furthermore, specific miRNAs could also be used as potential biomarkers for the diagnosis and disease prognosis, as they may indicate the severity and type of the disease (Condrat et al., 2020). However, off-target effects may predispose to cancer, alteration in immunity, alteration in metabolism and other abnormalities (Heyn et al., 2020). Another challenge is the delivery of microRNAs, as they can be quickly degraded by nucleases before acting on the target. There are various therapeutic options to delivery microRNAs employing different vehicles like local or systemic delivery associated with viral vectors, nanoparticles or liposome (Dua

et al., 2017). A possible solution could be in the use of more stable miRNA molecules, as *in vivo* studies have shown, that microRNA stability and half-life are enhanced with chemically modified oligonucleotides (Cheng et al., 2013). In the past few years, pharmaceutical companies have already started clinical trials for microRNA-based therapies. Santaris Pharma developed Miravirsen, used against hepatitis C infection, to inhibit miR-122 which is upregulated in patients affected by hepatitis C virus (Hoffmann et al., 2012). For cancer treatment, there has been developed miR34, which is downregulated in several cancer types. Even if several clinical trials using microRNAs were halted due to immunologic adverse effects or to lack of efficacy, they are still a very promising therapeutic tool. A complementary approach may be to identify the critical targets of the relevant miRNAs and develop small molecules to modulate these downstream factors (Hoefel et al., 2019). However, there is no microRNA treatment approved for the IPF disease. Targeting specific miRNA has great potential in the treatment of IPF and represent the most exciting intervention target of the last ten years. In the future, there is the need to develop new clinical trial using microRNAs for an effective treatment to alleviate the suffering of IPF patients (Li et al., 2016).

1.7.4 Epithelial-Mesenchymal Transition in Idiopathic Pulmonary Fibrosis

In IPF lung, stem cell exhaustion after epithelial damage drives an abnormal repair and failure of alveolar regeneration with aberrant activation of Wnt/β-catenin (Salton et al., 2019). This creates a pro-fibrotic environment, in which collagen is produced by fibroblasts that differentiate into myofibroblasts, followed by the transition of bone-marrow-derived fibrocytes, or other circulating progenitors, that will lead to Epithelial-Mesenchymal Transition (EMT) (Salton et al., 2019).

EMT is a biological process in which epithelial cells lose contact adhesion and apical-basal polarity, acquiring certain mesenchymal features including invasion, migration and production of ECM (Acloque et al., 2009). EMT is a physiological and often reversible process necessary for normal embryonic development, but it also can occur as a response to injury, carcinogenesis and fibrosis. The main hallmarks of EMT processes are defined by the loss of epithelial phenotype and the gain of the mesenchymal one, namely proteins involved in cell contact, cytoskeletal proteins, and luminal proteins secreted by the original cells with loss of surfactant production and gain of extracellular matrix or metalloproteinases secretion (Salton et al., 2019). There are three different types of EMT:

- Type I is associated with physiological processes involved in tissue and organ formation during embryogenesis
- Type II refers to normal wound healing and has a role in excessive tissue repair, as has been seen in IPF.
- Type III involves the acquisition of a migratory phenotype by malignant epithelial cells associated with tumor invasiveness and metastasis.

IPF has long been categorized as a type II EMT. It is physiologically induced in response to injury and stops when tissue repair leads to wound healing and subsequent regeneration (Kalluri et al., 2009). During fibrosis, the persistence of EMT-inducing signals creates abnormal ECM accumulation causing tissue remodeling and organ pathology (Kalluri et al., 2003). It has been seen that EMT contributes to the early development of interstitial fibrosis via the paracrine signaling, directed from the alveolar epithelium to underlying fibroblasts (Yao et al., 2018). EMT of ATII cells mainly sustained by the aberrant activation of specific EMT-related pathways such as Wnt, Sonic Hedgehog and TGF-β signaling pathways). These pathways crosstalk to each other and converge to key transcription factors, as SNAIL1/2 and ZEB1/2, inducers of epithelial mesenchymal transition and inhibitor of the E-cadherin promoter, to initialize and maintain the process

of EMT (Zhang et al., 2016). In particular in EMT, Wnt signaling promotes induction and stabilization of β-catenin. It activates the SMAD pathway contributing to the cytosolic accumulation of β-catenin and translocation factors into the nucleus, causing modifications of cytokeratin expression and reorganization of the cytoskeleton (Salton et al., 2019). The TGF-β is one of the most studied growth factors involved in EMT. It activates SMAD2/3 which form a complex with SMAD4 and participate directly in the transcriptional regulation of SNAIL1/2. Finally, the Shh pathway contribute to the maintain of EMT process at different levels, promoting transcriptional changes that lead to loss of the adherents junction complex, breakdown of the apical-basal polarity and cytoskeletal rearrangement (Nieto et al., 2016).

In fibrotic conditions it is over-expressed in ATII cells adjacent to sites of ECM deposition, leading to an EMT state. This event may create a profibrogenic microenvironment due to the loss of epithelial phenotype, the acquisition of mesenchymal phenotype and the activation of myofibroblasts, leading later to the development of fibrosis (Yao et al., 2018) (Fig.10). Currently, further deeper studies need to be performed to understand if EMT is a valid anti-fibrotic target. However, it has been demonstrated its involvement in multi-organ fibrosis through TGF-β and inflammatory processes (Di Gregorio et al., 2020).

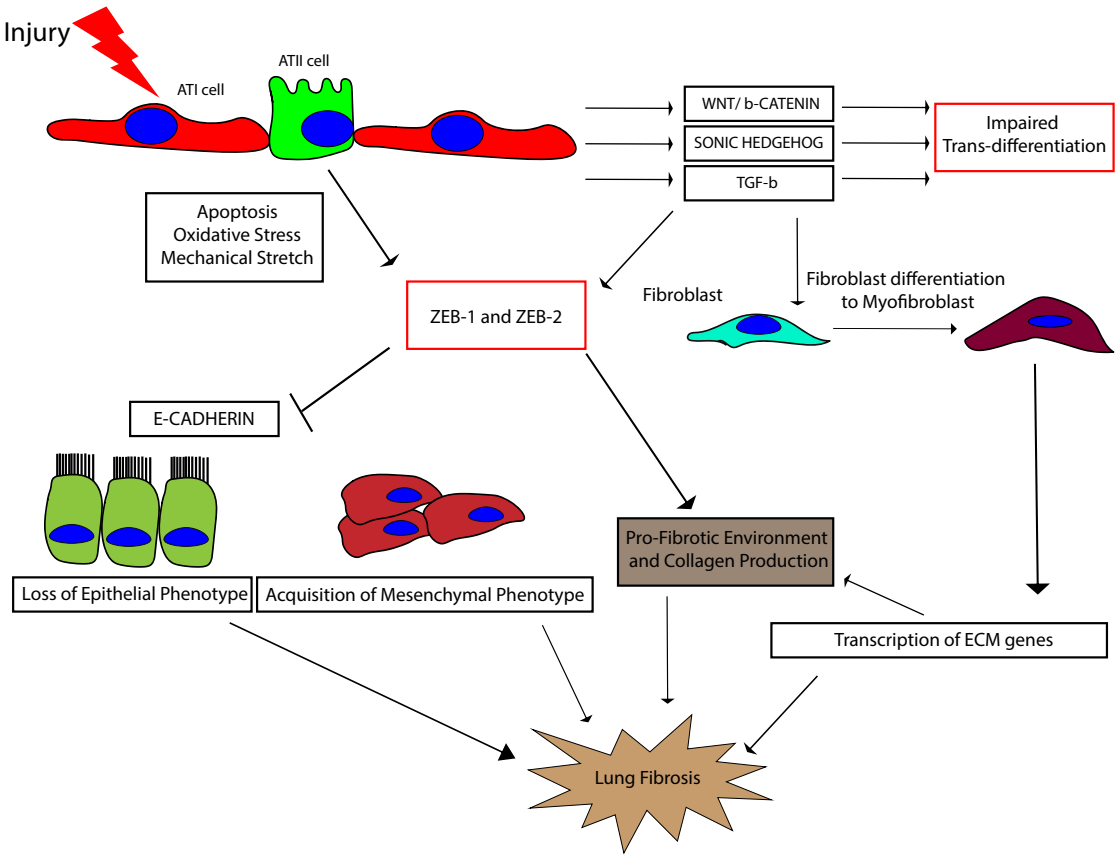

Figure 10: The role of EMT in lung fibrosis.

2. Aim of the thesis

The aim of my thesis resided in the discovery of the molecular mechanisms that halt lung regeneration in a model of lung injury that mimics IPF. Considering the importance of ATII cells in promoting lung regeneration after injury, by trans-differentiating into ATI cells (Barkauskas et al., 2013), we assessed the phenotypic characteristics and trans-differentiating ability of both human and murine ATII cells harvested from IPF patients and bleomycin-treated animals, demonstrating for the first time that in either case, ATII cells present an impaired trans-differentiation. Based on this achievement, during the course of my thesis, my work has focused on the role of miR-200c that can induce trans-differentiation of human IPF ATII cells to ATI cells (Moimas et al., 2019). Therefore, we optimized an *in vivo* translational method to deliver miRNA to ATII cells through aerosol by using a fluorescent miRNA. Then, we assessed whether aerosol administration of miR-200c into lungs was able to inhibit bleomycin-instilled lungs compared to controls. Bleomycin-instilled mice who received miR-200c mimics either, during early onset of fibrosis or when fibrosis was already established, displayed attenuated collagen deposition. Following, in order to better study the molecular mechanism through miR-200c as inhibitor of lung fibrosis, we define target genes that can indirectly drive the trans-differentiation of ATII cells to ATI cells using two prediction tools to scan the genome for putative miR-200c binding sites, both in human and mouse. Among several genes, we selected a gene that can improve cell growth and proliferation: *Flt1* gene. Since it is highly expressed by endothelial cells, in order to understand the role of *Flt1* in promoting trans-differentiation, we performed different types of co-culture assays (direct, indirect and contacting) between ATII cells isolated from either ctrl or bleomycin-treated mice and endothelial cells isolated from either WT or Cdh5-ERT2-CreFlt1$^{flox/flox}$ mice, a genetic model of *Flt1* conditional knock-out. Using these models, we therefore exploited the negative effect of *Flt1* in promoting trans-differentiation. Moreover, the depletion of *Flt1* was tested both in a model of lung regeneration induced by partial pneumonectomy (PNX) and in bleomycin-induced lung fibrosis, showing increased trans-differentiation of ATII to ATI cells *in vivo*. To assess the hypothesis that endothelial cells from Cdh5-ERT2-CreFlt1$^{flox/flox}$ mice act as sensors, releasing paracrine factors, that in turn activate ATII cells and thus promote the trans-differentiation to ATI cells, we performed a Mass Spectrometry analysis on the secretome of endothelial cells from Cdh5-ERT2-CreFlt1$^{flox/flox}$ and WT endothelial cells. We identified differentially secreted factors that

modulate trans-differentiation. In this respect, my work has shown that the Haptoglobin and the Serpinc1 are the best candidates in promoting trans-differentiation, leading to the identification of the key players promoting lung regeneration in the absence of *Flt1,* mediated by the over-expression of miR-200c.

In conclusion, we can therefore divide the work of my thesis into 5 main projects:

- Characterization of primary human and murine ATII cells and determination of defective ATII trans-differentiation.
- Determination of the effect of miR-200c on the fibrosis phenotype in the bleomycin model and analysis of miR-200c targets.
- Study the impact on ATII trans-differentiation to ATI by control and bleomycin mice in co-culture with endothelial cells from WT and *Flt1* KO under endothelium specific promoter *in vitro and in vivo*.
- Validation of secreted factors that can modulate the trans-differentiation of ATII cell to ATI and promote lung regeneration.
- Characterization of lung cells from Pneumonectomy mice in order to establish the primary sensor cells that start the activation of ATII cells during a regenerative process.

3 Material and Methods

3.1 Cell culture

3.1.1 Primary human Alveolar type II isolation

Human Alveolar type II cells were isolated from unidentified patients with IPF or recently deceased donors from the Lung Tissue Bank at Temple Lung Center (Department of Thoracic Medicine and Surgery at Temple University, Philadelphia PA). The organs were extracted, cut in small pieces and rinsed with calcium-and bicarbonate-free Hank's solution with HEPES (CBFHH). The tissue was digested with a solution composed by Collagenase-Elastase at the final concentration 2 mg/ml (Worthington-biochem #LK002067) and DNAse II (8mg/ml) for 30 min at 37°C in agitation. The solution was filtered using a 100 μm-pore size cell strainer (Falcon) in order to remove ATI cells and then using a 40 μm-pore size cell strainer (Falcon) for promoting single cell suspension. The pellet was then resuspended in a solution containing PBS/0,5% Bovine Serum Albumin (BSA, Sigma) and 0,5 M EDTA and incubated with 1:20 anti-EpCAM magnetic Microbeads (Miltenyi Biotec, # 130-061-101) for 20 minutes in the dark. The EpCAM+ cells were selected and washed through an LS column (Miltenyi Biotec #130-042-401) and subsequently placed in the magnetic field separator. Primary ATII cells were grown on plates coated with Collagen I (Cultrex #3447-020-01). The isolated ATII cells were resuspended in DMEM supplemented with 10% FBS, 2mM glutamine, 2.5 μg/ml amphotericin B, 100 U/ml penicillin, 100 μg/ml gentamicin (all reagents from Thermo Fisher Scientific; Whaltam, MA). The institutional Written informed consent was obtained for each lung specimen studied which was donated for lung research from patients undergoing lung transplantation for IPF, or from family members for brain dead normal subjects whose family members donated lung tissue for human research from the Gift of Life Donor Program (control). The study was approved by IRB at Partners Healthcare and Temple University and conformed to the Declaration of Helsinki protocols (IRB#4407).

3.1.2 Primary mouse Alveolar type II isolation

Murine Alveolar type II cells were isolated from adult lung of C57BL/6. Lungs were perfused and digested with Dispase (BD Biosciences) for 30 minutes at room

temperature. Then, lungs were mechanically dissociated using a McIlwain tissue chopper (Metrohm, USA) and treated with 20 μg/ml DNAse II (Sigma-Aldrich) for 10 minutes at 37°C. Cell suspension was filtered using a 100 μm-pore size cell strainer (Falcon) in order to remove ATI cells and then using a 40 μm-pore size cell strainer (Falcon) for promoting single cell suspension and centrifuged at 400 x g for 10 minutes. The pellet was then resuspended in DMEM supplemented with 10% FBS and antibiotics (pen/strept) in order to promote negative selection of mesenchymal cells (fibroblasts) and macrophages by 3 differential adherences on plastic culture dishes. Then, cells were centrifuged at 400 x g for 10 minutes and resuspended in a solution containing PBS/0,5% Bovine Serum Albumin (BSA, Sigma) and 0,5 M EDTA. Following, CD45-positive cells were removed by negative selection using simultaneous incubation with a Dynabeads Untouched Mouse T Cells Kit (Invitrogen, #11413D) and Dynabeads mouse DC Enrichment Kit (Invitrogen, #11429D). Recovered cells were grown on plates coated with Collagen I in order to promote trans-differentiation in ATI cells, in Pneuma-Cult medium (Stem Cell #005001).

3.1.3 Primary mouse Endothelial cells

Primary endothelial cells were isolated from adult lung of C57BL/6 mice. The organs were draw out, cut in small pieces and placed with CBFHH. The tissue was digested incubating with an enzyme mix following the manufacturer's instruction (Skeletal muscle dissociation kit, Miltenyi Biotec; #130-098-305), for 30 minutes at 37°C in agitation. The solution was filtered a 70 μm-pore size cell strainer (Falcon) and centrifuged at 400 x g for 10 minutes. The pellet was resuspended in a solution containing PBS/0,5% Bovine Serum Albumin (BSA) and 0,5 M EDTA and incubated 1:20 anti-CD45 magnetic MicroBeads (Miltenyi Biotec, #130-052-301) for 15 minutes in the dark in order to remove immune cells. Finally, negative CD45 cells were centrifuged at 400 x g for 10 minutes and incubated with 1:20 anti-CD31 magnetic MicroBeads (Miltenyi Biotec, #130-097-418) for 15 minutes in the dark. The CD31+ cells were selected and washed through an LS column (Miltenyi Biotec, #130-042-401) and subsequently placed in the magnetic field separator. Primary endothelial cells were grown on plates coated with a mixture of gelatin (Sigma, #G9391, final concentration 0,2 mg/ml) and fibronectin (Invitrogen, #33010-018, final concentration 1 mg/ml) in EGM-2 medium (Lonza, #CC-3162).

3.1.4. Transfection methods

3.1.4.1 Transfection of miRNA in human and mouse ATII cells

Human and mouse ATII cells and mouse endothelial cells were plated in 96-well plates (20.000) and cultured as described in the section 2.1.1. All miRNA (miRIDIAN miRNA mimics) and siRNA (siGENOME siRNA) were purchased from Dharmacon, Thermo Fisher Scientific. ATII cell transfection was performed using DMEM supplemented with 5% FBS without antibiotics and according to a standard transfection protocol with a scramble siRNA (siScr) (Dharmacon D-001210-0X), designed not to target any known human genes. As control transfection, I used a siRNA targeting the polyubiquitin-C gene (siUBC) (Dharmacon M-019408-01) at a final concentration of 50 nM. A mixture of transfection reagent (Lipofectamine RNAiMAX, Thermo Fisher Scientific) and OPTI-MEM (Thermo Fisher Scientific) was incubated at room temperature for 5 minutes. After 5 minutes, the miRNAs and controls were added into the mix and incubated for 30 minutes at room temperature. Then, mix was added dropwise to the cells. The day after, medium was replaced by fresh medium for one day to allow cells to recover.

3.1.4.2 Transfection of HEK-293T and production of enriched supernatant

HEK-293T cells were cultured until 70% of confluence and transfected as follows. A mixture of DNA (10µg in a 60 mm-dish), 60 µl of 2M $CaCl_2$ and water was added drop-wise to 500 µl of 2X HEPES Buffered Saline (HBS) in agitation. After 10 minutes of incubation at RT, the transfection mix was added drop-wise to the cells in antibiotic-free cell culture medium with 10% FBS. Transfection using a plasmid encoding for EGFP was used as a positive control to check transfection efficiency (consistently higher than 90%). One day after transfection, the cell culture medium was replaced with PNEUMA-cult medium supplemented with10% FBS and antibiotics and kept for one day to allow cells to recover. The enriched supernatant was recovered 24 hours later, centrifuged at 400 x g for 10 minutes to remove cell debris, filtered with 0,22 µm cell strainer and stored at -80°C.

3.1.4.3 Transfection of fibroblasts cell line

3T3 cells were cultured until 70% of confluence and transfected as follows. Lipofectamine 3000 reagent was diluted in OPTIMEM medium. The DNA (75ng) was

diluted in Optimem and P3000 reagent was added to the mixture. The diluted DNA was added to diluted Lipofectamine 3000 and the final mixture was incubated for 15 minutes at room temperature. After incubation, the transfection mix was added to 3T3 cells. Transfection using a plasmid encoding for EGFP was used as a positive control to check transfection efficiency (consistently higher than 90%).

3.1.5 Proliferation assay

Murine endothelial and ATII cells were seeded in 96 well-plates. After 2 days, medium was replaced with fresh medium containing 10 mM 5-ethynyl2'-deoxyuridine (EdU), to mark proliferating cells. Cells were fixed with 4% PFA for 20 minutes and then stained for primary antibodies, DAPI and EdU, using Click-it EdU Cell Proliferation Kit (Thermo Fisher, #C10338) following manufacturer instruction.

3.1.6 Co-culture assay

In order to understand the endothelial-epithelial crosstalk, I performed a physical or direct co-culture between murine endothelial cells, that were harvested as described in the paragraph 2.1.3, and 20.000 endothelial cells were seeded on 96 well-plates in mixed medium (EGM2 and Pneuma-Cult medium). After 1 days, the medium was replaced with fresh medium without antibiotics for allowing the miRNA transfection. After 2 days more, ATII cells were isolated from ctrl and Bleomycin mice. 20.000 cells for each condition were seeded on the top of endothelial cells for 4 days. After 2 days ATII cells isolation, medium was replaced with fresh medium with EdU. After 4 days, cells were fixed with 4% PFA for 20 minutes and stained. Transwell Membrane Inserts (0.4 μm) (Stemcell Technologies, #38023) were used to perform indirect co-culture between endothelial and alveolar epithelial cells. 100.00 ATII cells were seeded on the bottom of the plate coated with collagen I with Pneuma-Cult medium, while endothelial cells (100.000) were seeded in the upper part of the membrane in EGM2 medium. After 2 days, medium was replaced and EdU was added on the fresh medium. 2 days after, cells were fixed in PFA 4% and stained. Finally, it was performed a contacting co-culture assay, in which Endothelial cells (100.000 cells per well) were seeded on 10% Matrigel (diluted in DMEM) (Corning, #356230) for 6 hours in the bottom part of the trans well membrane in EGM2 supplemented with 10% FBS. The day after, ATII cells (50.000 cells

per well) were harvested from both Bleomycin and WT mice and seeded on the upper portion of trans well membrane in PNEUMA-CULT supplemented with 10% FBS.

3.1.7 Production of the extracellular matrix

The protocol was followed for matrix production from fibroblasts was published by Franco-Barraza (Franco-Barraza et al., 2016). The plates were pre-treated to stabilize anchoring of the matrix to the culture surface, then precoated with 0,2% gelatin for 1 hour at RT. After washing with PBS, 1% glutaraldehyde (dissolved in PBS) was added for 30 minutes at RT and then washed with PBS. The plates were incubated with 1 M ethanolamine (dissolved in water) for 30 minutes at RT and washed carefully with PBS. Fibroblasts were cultured for 9 days in DMEM supplemented by 10% FBS, antibiotics, and 50 μg/ml of ascorbic acid. 24h after cell seeding, fibroblasts were transfected with Col2a1 and Col3a1 plasmids as described in the section 2.1.4.2 of Material and Methods. The medium was replaced every 48 hours. To decellularize the matrix, the culture medium was carefully removed and rinsed twice with PBS, then incubated with an extraction buffered composed by 0,5% Triton X-100, 20 mM NH_4OH in PBS for 10 minutes at 37°C. Then, the extraction buffer was diluted with 100 μl of PBS and incubated overnight. The day after, the matrix was washed several times and ATII cells were seeded on top of it.

3.2 Animal experimentation

All animal experiments were conducted in compliance with the European guidelines and international laws and policies (*ECC Council Directive 86/609, OJL 348, 12 December 1987*), with the approval of ICGEB Animal Welfare Board, Ethical Committee, and Italian Minister of Health. Adult C57BL/6 and Cdh5-Cre; Flt1 fl/fl mice were used for animal experiments. We used experimental group of animals composed by males. They were housed under optimal environmental conditions in a temperature-controlled environment with 12/12 hours of light/dark cycles.

3.2.1 Bleomycin administration

Adult C57BL/6 mice received intraperitoneal injection of 30 μl of Ketamine and Xylazine. After 5 minutes, mice received 40 μl of Bleomycin (Biocen) intra-tracheally with different doses, 0,5 U/Kg, 1 U/Kg, 1.5 U/Kg. Animals were sacrificed after 14, 21,

30 and 60 days after Bleomycin injection in order to understand the available dose and time points. Animals were perfused with 10 ml of PBS from the right ventricle and with 10 ml of PBS intra-tracheally. Then lungs were fixed in 4% PFA and sucrose for immunostaining or in 50% ethanol for Masson trichrome.

3.2.2 MiR-200 administration

In order to study the effect of the miR200C in lung fibrosis. C57BL/6 3-month-old mice received 40 µl of Bleomycin intra-tracheally at the final dose of 1 U/Kg. in the same day, the same mice received in aerosol way 6 µg of miR200C. Mice were sacrificed after 30 days. Lungs were harvested and the left lung was placed in PFA 4% for immunostaining, while the right lung was used for RNA or protein extraction.

3.2.3 Knock-down of Cdh5-Cre; Flt1 fl/fl mice *in vivo*

Transgenic Cdh5-Cre; Flt1 fl/fl mice express the CRE under the control of the Cdh5 promoter (endothelial specific marker). After genotyping, CRE positive flox-flox mice were treated with 5 injection of Tamoxifen (Sigma, #10540-29-1) daily at the final concentration of 5 mg/ml intraperitoneally. After 1 week, mice were sacrificed, animals were perfused with 10 ml of PBS in the right ventricle and intra-trachea, and lungs were harvested for immunostaining, Masson Trichrome or for endothelial cells isolation.

3.3 Molecular Biology

3.3.1 RNA extraction

RNA extraction was performed from endothelial and alveolar epithelial cells seeded in 24-well plates. Cells were washed once with PBS, collected and centrifuged at 1200 RPM for 5 minutes at room temperature. Pellet was resuspended with 500 µl of Trizol reagent purchased from Invitrogen lnc. To each sample 100 µl Chloroform were added, in order to separate the homogenate into a clear upper aqueous phase, containing RNA, an interphase and red lower organic layers, which contains DNA and protein. After an incubation of 5 minutes at room temperature, cells were centrifuged at 13.000 RPM for 15 minutes at +4 °C. The aqueous phase, which contains RNA, was transferred in another tube and 250 µl isopropanol was added to precipitate the RNA. After 10 minutes of incubation at room temperature samples were centrifuged for 10 minutes at 13.000 RPM at +4°C. The RNA pellet was washed with Ethanol 70% and centrifuged at 13.000 RPM

for 5 minutes at +4 °C. Finally, pellet was resuspended with sterile H_2O (ddH_2O). The RNA quality was controlled on 1% agarose gel and by absorbance ratios 260/280 and 260/230 nm measured on a NanoDropTM 1000 spectrophotometer (Thermo Scientific) at 260 nm. The concentration was obtained by the same NanoDropTM measurement.

3.3.1.2 Dnase Treatment

To remove the genomic DNA, Dnase Treatment was performed (Thermo Fisher, #AM1907). A mixture of 1 µg of RNA, 1 µl of 1X Turbo Dnase Buffer and 1 µl of TURBO DNAse enzyme was performed. The solution was incubated at 37°C for 30 minutes. Then, 2 µl of the DNAse Inactivation Reagent was added to the solution in order to stop the reaction. Samples were incubated for 5 minutes at room temperature and centrifuged at 10.000 x g for 1.5 minutes.

3.3.1.3 Reverse Transcription

1 µg of total RNA was reverse-transcribed using M-MLV reverse transcriptase (Thermo Fisher #K1612) following manufacturer instruction. The mix included:

Total RNA	1 µg
Random Primers	1 µl
Water nuclease-free	To 11 µl

Samples were incubated at 65°C for 5 minutes and left cooling on ice for 2 minutes. Each sample received the second mix that included:

5X Reaction Buffer	4 µl
RiboLock RNase Inhibitor (20U/µl)	1 µl
10 mM dNTP Mix	2 µl
M-MulV Reverse Transcriptase (20U/µl)	2 µl

Table 1: Reagent used for Reverse Transcription

Samples were incubated at 25°C for 5 minutes and then at 37°C for 60 minutes. To inactivate the enzyme, samples were heated at 70°C for 15 minutes.

3.3.1.4 Real-time qPCR analysis

mRNA expression levels were measured with a quantitative RT-PCR using a C1000 Thermal Cycler CFX96 Real-Time System (Bio-Rad). A master mix with a final volume of 12 µl included:

SYBER Green Mastermix (Promega)	10 µl
ddH_2O	7,5 µl
Primer forward (10 µM)	1 µl
Primer reverse (10 µM)	1 µl
cDNA diluted 1:5	1.5 µl

Table 2: Master mix composition for Real-time PCR.

Samples were analyzed on a 96-well real-time PCR plate with the following conditions for 44 cycles:

95°C	5:00
95°C	0:10
61°C	0:30
61°C	0:05
95°C	0:05

Table 3: Degree used for qPCR analysis.

Data were analyzed using ΔΔCt method.

Primer list:

Gene	Forward primer	Reverse primer
hGAPDH	5'-AAGGTGAAGGTCGGAGTCAA-3'	5'-AATGAAGGGGTCATTGATGG-3'
hAQP5	5'-GCCACCTTGTCGGAATCTACT-3'	5'-GGCTCATACGTGCCTTTGATG-3'
hHOPX	5'-TTCAACAAGGTCGACAAGCACCC-3'	5'-CCAGGCGCTGCTTAAACCATTTCT-3'
hSFTPA1	5'-AGCCACACTCCACGACTTTAG-3'	5'-GGATTCCTTGGGACAGCAATG-3'
hSFTPC	5'-CTCATCGTCGTGGTGATTGTG-3'	5'-TGGAGAAGGTGGCAGTGGT-3'
hZEB1	5'-GGCATACACCTACTCAACTACGG-3'	5'-TGGGCGGTGTAGAATCAGAGTC-3'
hZEB2	5'- CCAGCGGAAACAAGGATTTCAG-3'	5'-AGGCCTGACATGTAGTCTTGTG-3'
hCDKNA1	5'-TGGAGACTCTCAGGGTCGAAA-3'	5'-GGCGTTTGGAGTGGTAGAAATC-3'
hCDKNA2	5'-ACCAGAGGCAGTAACCATGC-3'	5'-AAGTTTCCCGAGGTTTCTCAG-3'

Gene	Forward primer	Reverse primer
mGapdh	5'-TGACCTCAACTACATGGTCTACA-3'	5'-CTTCCCATTCTCGGCCTTG-3'
mβ-actin	5'-TGACGTTGACATCCGTAAAG-3'	5'-GAGGAGCAATGATCTTGATCT-3'
m18S	5'-GGCCCTGTAATTGGAATGAGT-3'	5'-CCAAGATCCAACTACGAGCTT-3'
mSftpc	5'-TGATGGAGAGTCCACCGGAT-3'	5'-TCTCCCGGAAGAATCGGACT-3'
mSftpa1	5'-GTTGCTGGCATCAAGTGCAA-3'	5'-GCAAGCTGAGGACTCCCATT-3'
mAqp5	5'-TGAACCCAGCCCGATCTTTC-3'	5'-ACGATCGGTCCTACCCAGAA-3'
mHopx	5'- CCAGCGGAAACAAGGATTTCAG-3'	5'-ATTTCTGCGTCTGCTCCTCC-3'
mFlt1	5'-TTCATCAGTGTGAAACATGC-3'	5'-CGAGCCATCTTTTAACCATAC-3'

Table 4: List of both human and murine primers.

3.3.2 Protein extraction

3.3.2.1 Samples Preparation

For cellular protein analysis, single cell suspension was obtained, following the first passage described on 2.1.2 of this section, without performing negative selections. After digestion cells were filtered and the protein lysates were prepared in RIPA buffer (40 mM Tris-HCl pH 7.5, 2 mM EDTA, 300 mM NaCl, 2% NP40, 1% Sodium desoxycholate) supplemented with protease inhibitors (Roche, Complete Mini #11836153001) and 20% SDS in H_2O. The cells were centrifuged at 14.000 RPM for 30 minutes at +4°C and the supernatant was transferred in another tube. The lysate fraction was quantified through the Bradford method using a Biorad reagent (Bio-Rad Laboratories GmbH) at final concentration 1X in ddH_2O. The calibration is carried out by putting 1 ul of RIPA in 999 µl of Biorad reagent 1X. To do this, 1 µl of each sample is mixed in 999 µl of Biorad 1X. The measure of optic density (OD) of each sample is carried out at 595 nm using a spectrophotometer. For protein analysis 20 µg of lysate was run in acrylamide gel.

3.3.2.2 SDS-PAGE Electrophoresis

The protein samples were mixed with 6X Laemmli buffer and denaturated at 95°C for 10 minutes. Protein samples were separated in 10% polyacrylamide gel, prepared with Protogel (PolyMed, #EC890), 357 mM Bis-Tris pH 6.8, APS and TEMED (Sigma). Chloroform was also added to the gel solution (0.5% v/v), to allow protein visualization (stain-free gel). MOPS/SDS running buffer was composed by 1M MOPS, 1M Tris Base, 69.3 mM SDS and 20.5 mM free acid EDTA. The gels were run at 100V for 1:30 hours.

3.3.2.3 Western-Blot analysis

Transfer buffer was prepared with 25mM Tris, 192 mM glycine and 20% MtOH. Proteins were transferred to a PVDF membrane (GE Healthcare, #10600015) at 350 mA for 1:30 hours. After the transfer, membranes were incubated with 5% milk in 1X TBST (20 mM Tris pH 7.5, 150 mM NaCl, 0.1% Tween-20) for 1 hour at RT. Membranes were then incubated with anti-Pro-Spc (1:500; Abcam, #ab90716), anti-CD31 (1:500; R&D systems, AF3628), anti-Rage (1:500; AF1145), anti-Aquaporin 5 (1:200; Millipore, ab15858), anti-CD45 (1:500; abcam, ab154885) antibodies overnight at 4°C or anti-GAPDH (1:7000; Sigma, G9295) for 1 hour at RT, followed by 1 hour incubation at RT

with secondary antibodies, polyclonal goat anti-mouse IgG (H+L) horseradish peroxidase (HRP) (1:2000; Dako #P0447), or polyclonal goat anti-rabbit IgG (H+L) HRP (1:2000; Invitrogen, #31460). Western blots were developed using SuperSignal West Dura kit (Thermoscientific, #34577). Images were acquired using Biorad Chemidoc Touch and quantified with the Biorad software.

3.3.3 Immunostaining

The harvested samples were fixed with PFA 4% overnight at +4°C. The day after sample were refreshed with Sucrose 20% in PBS. Tissues were cut at 5µm thickness for staining. Frozen slides were permeabilized by incubating with 0.1% Triton in PBS at RT for 20 minutes and were then blocked with 5% BSA in PBS containing 0.1% Triton at RT for 1 hour. Then, the slides were incubated with the primary antibodies in blocking solution overnight +4°C. After washing in PBS, the slides were incubated with the secondary antibodies diluted 1:500 in blocking solution at RT for 2 hours. The primary and secondary antibodies that were used are listed in Table 5. Finally, the slides were incubated for 30 minutes at RT with Hoechst solution (Invitrogen, #33342) diluted 1:5000 in PBS, and then mounted with Moviol solution

PRIMARY ANTIBODIES (target)	**COMPANY AND CODE**
Pro-Spc	Abcam, #ab90716
Podoplanin	Hybridoma bank, #ab531893
Aqp5	Millipore, #ab15858
Erg	Abcam, #ab92513
CD31	R&D, #af3628
CD45	Abcam, #ab10558
Rage	R&D, #af1145
SECONDARY ANTIBODIES	**COMPANY AND CODE**
Alexa Fluor™ 568 Donkey anti goat IgG	Invitrogen, #A-11057
Alexa Fluor™ 488 Donkey anti rabbit IgG	Invitrogen, #A-21206
Alexa Fluor™ 647 Donkey anti rabbit IgG	Invitrogen, #A-31576
Goat Anti-Syrian Hamster IgG H&L (Alexa Fluor 488)	Abcam, #ab180063

Table 5. Antibodies used for immunostaining.

3.3.4 Immunohistochemistry

Masson Trichrome staining was performed using reagents from BioOptica. Briefly, paraffin sections were deparaffinized incubating them overnight at 56°C and the 30 minutes in xylene. Then slides were put in X-free solvent (#21-A1305) for 5 minutes and then a scale of ethanol dilutions was applied (100%, 90%, 75% and 50%). After 5 minutes of washing in tap water, slides were incubated in Mayer's hematoxylin (#21-a06002) for 20 minutes, then rinsed in tap water. The sections were then incubated with reagent C for 4 minutes. After washing in tap water, slides were incubated with Reagent D for 4 minutes. After washing, sections were incubated with Reagent E for 10 minutes and then without washing, they were incubated with the Reagent F for 10 minutes and washed with tap water for 5 minutes. Finally, slides were subjected to 1 minute of incubation with 50%, followed by 1 minute in 70%, following by 1 minutes in 100% of ethanol, 3 minutes in X-free solvent and then mounted with Moviol.

3.4 Mass Spectrometry

3.4.1 Sample preparation

Conditioned medium (CM) was centrifuged at 2000× g at 4 °C for 10 min and passed through a 0.2 μm filter to remove cellular debris. CM was then concentrated using a 3 kDa cut-off concentrator and precipitated with four volumes of pre-chilled acetone at –20˚C overnight. Protein pellets were washed with 80% acetone, suspended in 6M Urea and 100 mM ammonium bicarbonate pH 8, and protein concentration was quantified using bicinchoninic acid assay.

Proteins (20μg) were reduced using 10 mM dithiothreitol (DTT)for 45 min at room temperature followed by alkylation with 20mM iodoacetamide (IAA) for 30 min in the dark. Proteins were then digested with 0.5 μg Lys-C (Promega, #VA1170) for 4 h at room temperature. Subsequently, the samples were diluted to 1:5 with 100 mM ammonium bicarbonate and digested with 1 μg of trypsin (Promega, #V5111) overnight. The following morning, digestion was stopped with 1% trifluoroacetic acid. Samples were then desalted on in-house–packed StageTips (doi: 10.1038/nprot.2007.261), lyophilized in a Speed-vac and resuspended in 20 μL of 0.1% formic acid for LC-MS/MS analysis.

3.4.2 LCMS Method

Digested samples were separated on an Easy-nLC 1200 system (Thermo Fisher Scientific) by a 85 minutes gradients with a 400 nl/min flow rate on a 28cm column with an inner diameter of 75 µm packed in-house with ReproSil-Pur C18-AQ material (3µm particle size, Dr. Maisch, GmbH), heated at 40°C. The gradient was set as follows: from 5% to 25% over 52 minutes, from 25% to 40% over 8 minutes and from 40% to 98% over 10 minutes at a flow rate of 400 nL/min. Buffers were 0.1% formic acid in water (A) and 0.1% formic acid in acetonitrile (B). Samples were analyzed in an Orbitrap Fusion Tribrid mass spectrometer (Thermo Fisher Scientific, San Jose, CA, USA) and data acquired in data-dependent mode (2100 V). Full scans were acquired in the Orbitrap performed at 120.000 FWHM resolving power (at 200m/z) and an AGC target of 1x106, followed by a set of (higher-energy collision dissociation) MS/MS scans over 3 sec cycle time. A mass range of 350-1100 m/z was surveyed for precursors, with a maximum injection time of 50 ms and the first mass set at 140 m/z for fragments. The MS/MS scans were performed at a collision energy of 30%, 150 ms of maximum injection time (ion trap) and a target of 5x103 ions.

Peptide searches were performed in Proteome Discoverer 2.2 software (Thermo Fisher Scientific) against the Mus musculus FASTA file (uniprot, downloaded April 2021) and a database containing major common contaminants. Proteins were identified using MASCOT search engine with a mass tolerance of 10 ppm for precursors 0.6 Da for products. Trypsin was chosen as the enzyme with 5 missed cleavages, and static modification of carbamidomethyl (C) with variable modification of oxidation (M) and acetyl (protein N-term) were incorporated in the search. False discovery rate was filtered for <0.01 at PSM, peptide and protein level. A minimum number of two peptides for protein was set and results were filters to exclude potential contaminants.

3.5 Image acquisition and analysis

Images were aquired using 3 different microscopes and respective software:

- Nikon A1 Plus Microscope equipped with DC-152Q-C00-FI using NIS 4.30 software (Nikon).
- Zeiss LSM 880 Airyscan
- Operetta high content screening microscope (Perkin Elmer).

3.6 Statistical analysis

GraphPad Prism software was used to calculate the statistical significance of the presented data. The reported results are expressed as mean value +/- standard error mean (SEM) and the number of experiments was performed 3 times with 3 biological replicates. One-way ANOVA statistics followed by Dunnet multiple comparison test was used for multiple datasets whereas the unpaired Student's t-test was used to compare 2 groups of data. Only significant values are indicated by the asterisks above the graphs (*p<0.05, ** p<0,01, ***p<0,001, ****p<0,0001).

4. Results

4.1 Characterization of the trans-differentiation ability of primary human ATII cells

4.1.1 Human ATII cells harvested from IPF patients show a critical phenotype

IPF is characterized by abnormal type II alveolar epithelial cells, which become unable to activate, proliferate and trans-differentiate in ATI cells (Sakai et al., 2013). To discover the mechanisms implicated in ATII cell dysfunction in IPF, we started a collaboration with the Temple University in Philadelphia, where we could isolate primary human ATII cells from both IPF patients and healthy donors. Human ATII cells were isolated using EpCam magnetic beads (Kosmider et al., 2018). To determine the purity of these cells, we performed immunofluorescence staining, using Pro-Surfactant Protein C (Pro-Spc) to specifically label ATII from cells and flow cytometry using EpCam and Pro-Spc antibodies, which label lung epithelial cells (i.e bronchial epithelial cells) and ATII cells, respectively (Fig. 1A; 1B). Both analyses showed that the purity of primary human ATII cells, obtained after the isolation, was around 70%. To better characterize the phenotype of human ATII IPF cells, we performed a qPCR analysis to evaluate the expression of ATI makers, such as *Aquaporin 5 (AQP5)* and *Homeobox (HOPX)* (Fig. 1C;1F) as well as of ATII markers, including *Surfactant protein C* (*SFTPC) and Surfactant protein A1 (SFTPA1)* (Fig. 1E; 1F). As shown in figure 1C-1F, ATII cells isolated from IPF patients expressed reduced levels of ATII markers (*SFTPA1 and SFTPC*) compared to control cells. Several studies reported that multiple insults to the lung tissue, followed by inadequate repair due to abnormal response of ATII cells, may initiate IPF (Uhal, Joshi et al., 1998) (Jablonski, Kin et al., 2017). Furthermore, it has been shown that aging can induce replicative arrest and aberrant secretion of profibrotic senescence-associated factors, which in turn promote ATII cells senescence. All these pathways could contribute to EMT in the alveolar epithelium, with subsequent pneumocytes loss, myofibroblast accumulation and lung fibrosis (Moimas et al., 2019). To investigate this aspect, we analyzed the expression of the EMT markers *Zinc Finger E-Box Binding Homeobox 1 and 2* (*ZEB1-ZEB2*) (Fig. 1G; 1H). We found that EMT markers (*ZEB1and ZEB2*) were increased in IPF ATII cells compared to controls, suggesting that EMT is ongoing in IPF cells.

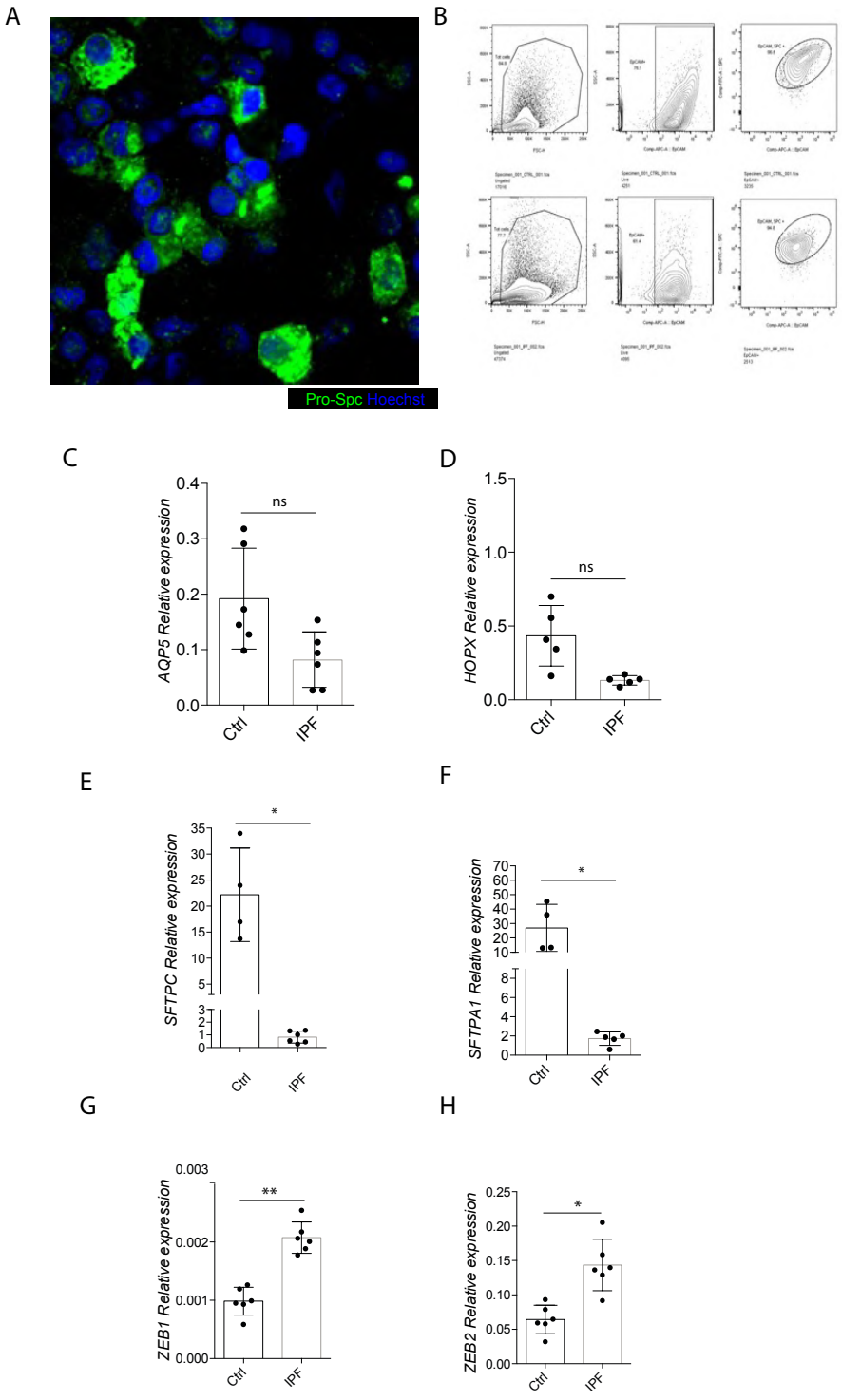

Figure 11: ***Characterization of Human ATII cells.*** *1A) Representative immunofluorescence image of freshly isolated human alveolar cells stained for Pro-Spc marker (green) and with the nuclear dye Hoechst (blue). B) Flow cytometry analysis showing the expression of EpCAM. 1C-H: Real-time PCR quantification of the expression levels of the following genes in ATII cells harvested from control and IPF patients: C) Aquaporin5 (AQP5), D) HOP homeobox (HOPX), 1E) surfactant protein C (SFTPC), F) surfactant protein A1 (SFTPA1), G) zinc finger E-box binding homeobox 1 (ZEB1), H) zinc finger E-box homeobox 2 (ZEB2). Data are presented as relative expression normalized to glyceraldehyde-3-phosphate dehydrogenase (GAPDH). All data are shown as mean ± S.E.M. Statistical significance was determined using a one-way ANOVA followed by Dunnett's multiple comparison test, *P < 0.05, **P < 0.01.*

4.1.2 Human ATII cells, harvested from IPF patients, fail to trans-differentiate into ATI cells.

To check the trans-differentiation capacity of ATII into ATI cells, both IPF and control ATII cells were isolated. To promote their trans-differentiation into ATI cells *in vitro,* cells were cultured on rat tail collagen-coated plates. Both IPF and control ATII cells were cultured for 2, 4 and 6-days. qPCR analysis showed that the expression of *AQP5* and *HOPX* increased over time in control ATII cells but not in ATII cells from IPF patients (Fig. 2A; 2B). Conversely, the expression levels of *SFTPC* and *SFTPA1* progressively decreased over time, with very low expression at day 6 in control cells, while they remained low at all time points in IPF (Fig. 2C; 2D). To understand if the expression of EMT and senescence markers (such as *Cyclin Dependent Kinase 1A* and *2A*, respectively *CDKN1A* and *CDKN2A*) changed over time, we evaluated their expression levels by qPCR (Fig. 2E; 2H). Our results showed that in control ATII cells the expression of both *ZEB1* and *ZEB2* remained constant over time, while in IPF cells, these markers progressively increased, suggesting the acquisition of a senescent phenotype in these cells. Immunofluorescence analysis was performed to visualize protein expression and cellular localization of Pro-Spc (ATII) and AQP5 (ATI). Consistent with the mRNA results, after 2 days in culture, control ATII cells expressed higher Pro-Spc signals compared to ATII isolated from IPF patients and in both cases, they progressively downregulated expression of Pro-Spc overtime (Fig. 2I; 2J). In contrast, AQP5 expression was almost undetectable, in both control and IPF ATII cells, at day 2 and it progressively increased over time (Fig. 2K; 2L).

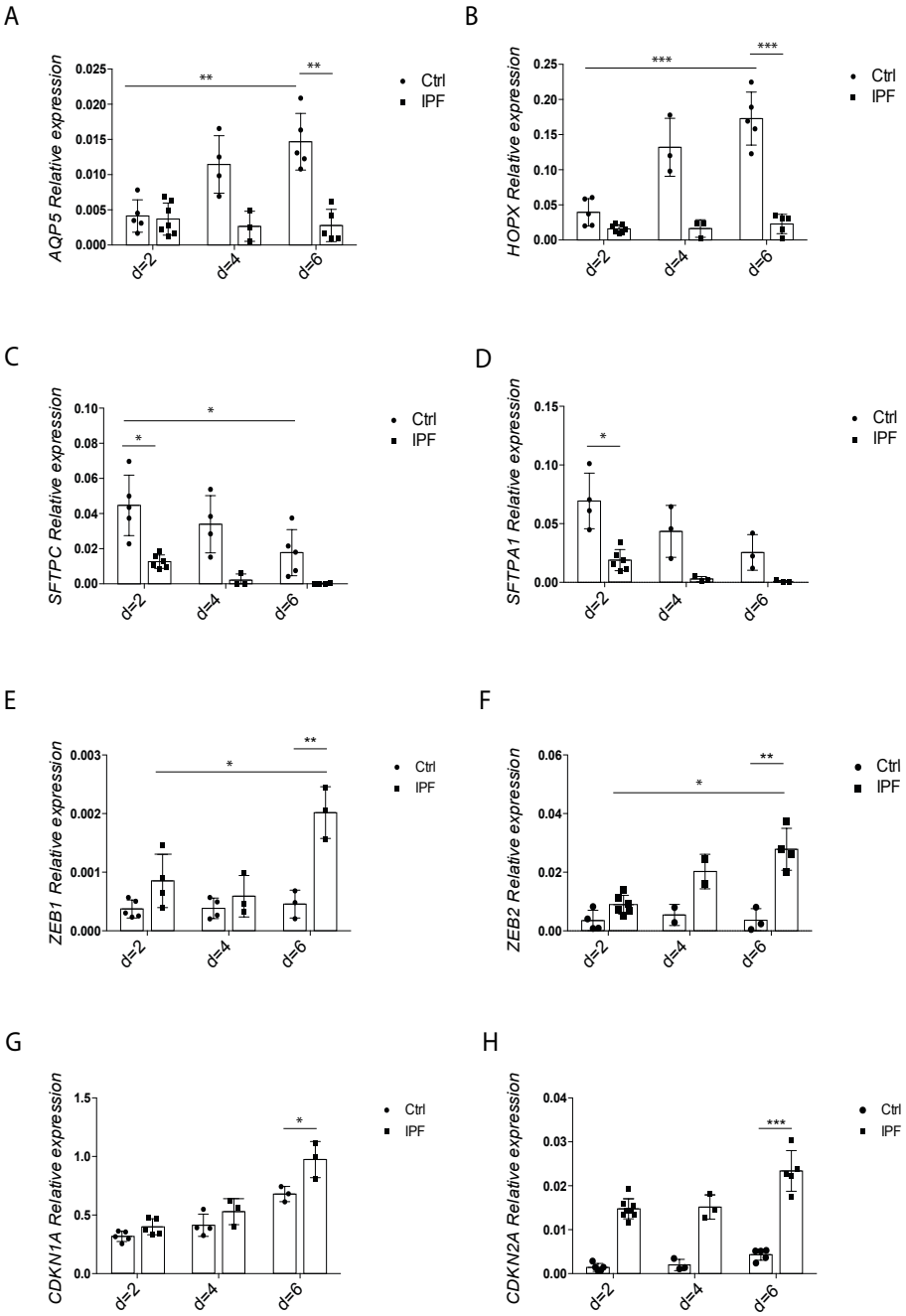
A
AQP5 Relative expression
0.025
0.020
0.015
0.010
0.005
0.000
**
**
d=2
d=4
d=6
Ctrl
IPF
B
HOPX Relative expression
0.25
0.20
0.15
0.10
0.05
0.00
***
***
d=2
d=4
d=6
Ctrl
IPF
C
SFTPC Relative expression
0.10
0.08
0.06
0.04
0.02
0.00
*
*
d=2
d=4
d=6
Ctrl
IPF
D
SFTPA1 Relative expression
0.15
0.10
0.05
0.00
*
d=2
d=4
d=6
Ctrl
IPF
E
ZEB1 Relative expression
0.003
0.002
0.001
0.000
*
**
d=2
d=4
d=6
Ctrl
IPF
F
ZEB2 Relative expression
0.06
0.04
0.02
0.00
*
**
d=2
d=4
d=6
Ctrl
IPF
G
CDKN1A Relative expression
1.5
1.0
0.5
0.0
*
d=2
d=4
d=6
Ctrl
IPF
H
CDKN2A Relative expression
0.04
0.03
0.02
0.01
0.00
***
d=2
d=4
d=6
Ctrl
IPF

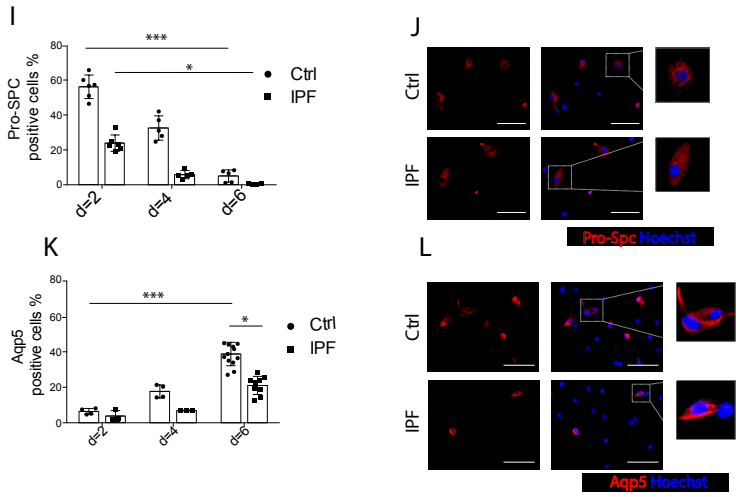

Figure 12: ***Time-course analysis of differentiation markers in ATII cells****. Real-time quantification of the expression levels of the following genes in ATII cells harvested from control and IPF patients and kept in culture for 2, 4 and 6 days: 2A) AQP5, 2B) HOPX, 2C) SFTPC, 2D) SFTPA1, 2E) ZEB1, 1F) ZEB2, 1G) cyclin-dependent kinase inhibitor 1A (CDKN1A) and 1H) cyclin-dependent kinase inhibitor 2A (CDKN2A). Trans-differentiation was validated by immunofluorescence for the expression of the same markers. 2I) Quantification of the number of cells expressing Pro-Spc at the indicated time points in control and IPF patients. 2J) Representative images of cells expressing Pro-Spc (red) after 2 days of culture. 2K) Quantification of cells expressing AQP5 at days 2, 4 and 6 as in image 2I. 2L) Representative images of cells expressing AQP5 (red) after 2 days of culture. All data are shown as mean ± S.E.M. Statistical significance was determined using a one-way ANOVA followed by Dunnett's multiple comparison test, *P < 0.05, **P < 0.01.*

4.2 An animal model of lung fibrosis induced by bleomycin

4.2.1 The optimization of the bleomycin model

To characterize ATII cells *in vivo*, we used a mouse model of lung fibrosis induced by bleomycin. We instilled bleomycin intratracheally in wild-type C57BL/6 mice. We used 2 months old male mice, as they are more susceptible to fibrosis compared to females. To optimize dose and timing of bleomycin administration, we compared 3 concentrations (0.5, 1 and 1.5 U/Kg) and multiple time points (14, 21, 28 and 60 days after bleomycin administration) for lung tissue harvesting (Fig. 3A;3F). Masson trichrome staining showed that after 28 days, a single bleomycin injection of 0.5 U/Kg efficiently increased collagen content in the sub-pleural portion of the lung (Fig. 3C). This fibrotic phenotype was still visible at day 60 (Fig. 3E). At a higher concentration (1U/Kg, Fig.3F), mice developed a more severe phenotype, with sparse areas of lung fibrosis visible at day 30 after bleomycin administration. Animals treated with the highest dose (1,5 U/Kg), died after 15 days from bleomycin administration. Thus, the most effective dose in inducing fibrosis was 1 U/Kg and animal sacrifice was set at 30 days post-administration. The extent of fibrosis was quantified using the Ashcroft score and was about 5-fold higher in animals treated with 1 U/Kg of bleomycin compared to 0,5 U/Kg (Fig. 3G) (Ashcroft et al., 1988).

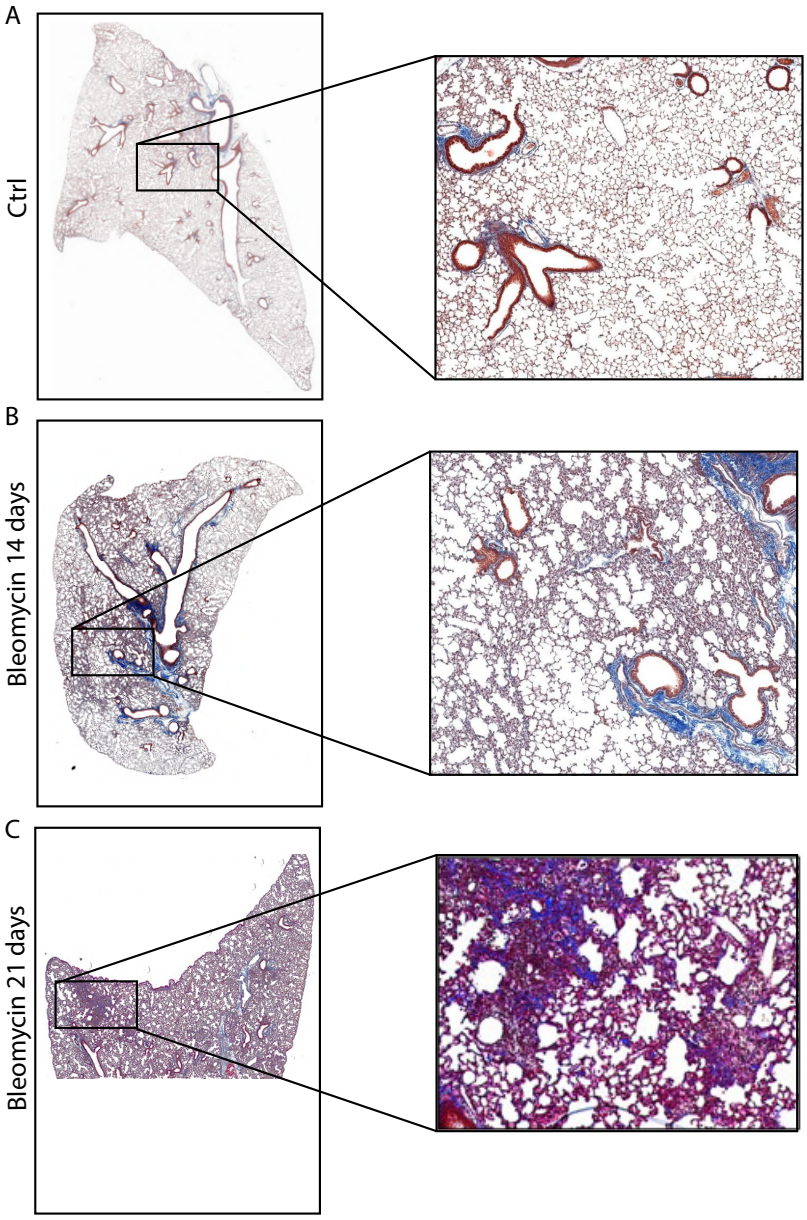
A
Ctrl
B
Bleomycin 14 days
C
Bleomycin 21 days

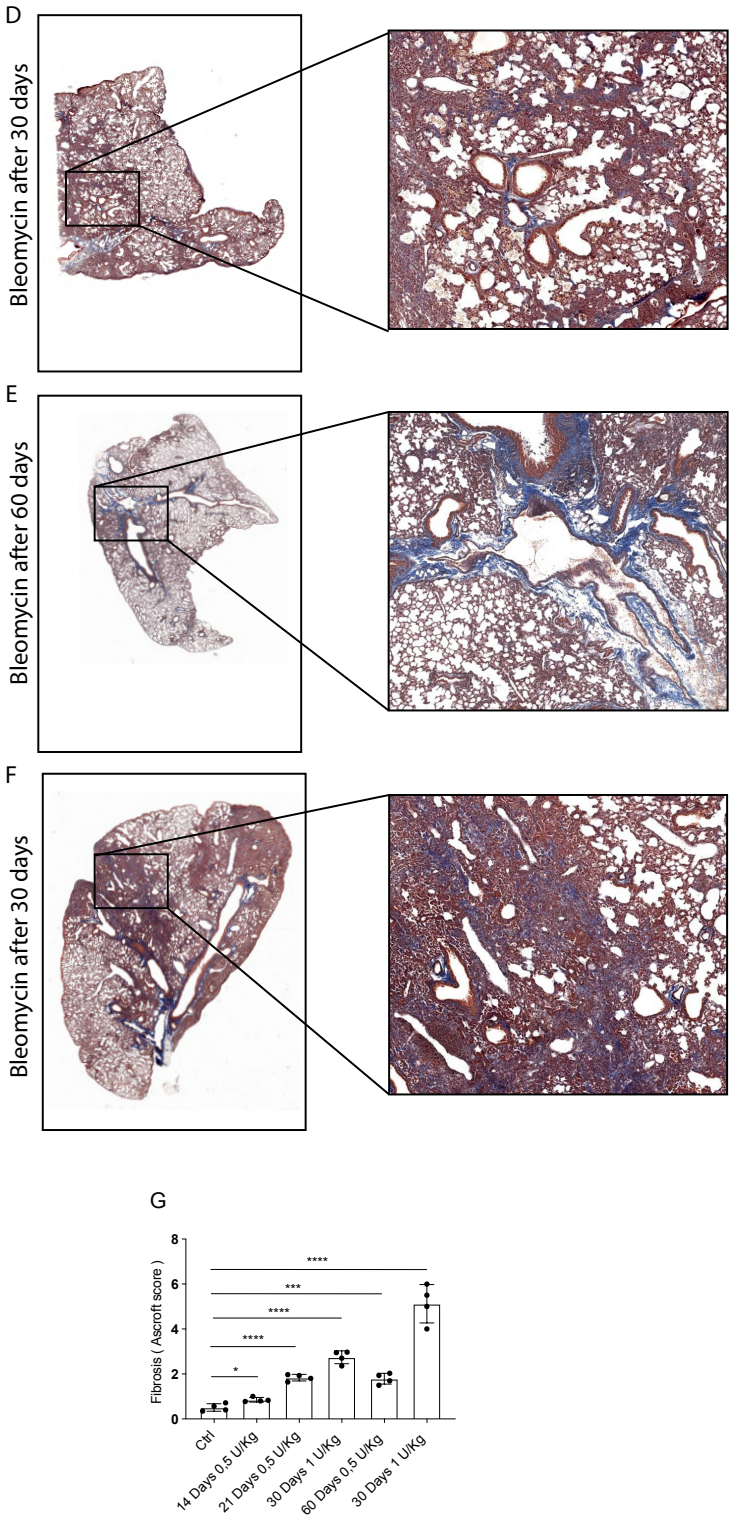

*Figure 13: **Lung fibrosis after bleomycin treatment**. Representative images of Masson Trichrome staining of lungs harvested from control mice (3A) and bleomycin mice, sacrificed after 14 days (3B), 21 days (3C), 30 days (3B), and 60 days (3E) treated with a low dose of bleomycin (0,5 U/Kg). 3F) Masson Trichome staining of lung harvested from bleomycin treated mice at a higher dose (1 U/Kg) and sacrificed at 1 month. High magnifications are shown for each image. Quantification of the fibrotic area was performed using the Ashcroft score. All data are shown as mean ± S.E.M. Statistical significance was determined using a one-way ANOVA followed by Dunnett's multiple comparison test, *P < 0.05, ****P < 0.0001.*

.

4.3 Characterization of murine ATII cells

To characterize murine ATII cells, we isolated cells from the right and left distal lobes of adult mice lungs. After enzymatic and mechanical digestion, cells were filtered with two different cell strainers. The first cell strainer (100 μm) was used to remove the majority of the cells, while the second one (40 μm) allowed to obtain a single cell suspension.

We used western blot to analyze cell purity at different stages of the isolation. An anti-GAPDH antibody was used as a loading control. Cells in the upper and lower portion of 100 μm cell strainer were composed of Cd45 (inflammatory cells), Cd31 (endothelial cells), Rage (ATI cells), Pro-Spc (ATII cells) and Aqp5 (ATI cells) positive cells (Fig. 4A, first lane and middle lane). However, ATI cells were reduced in the lower portion of 100 μm cell strainer and completely disappeared in the 40 μm cell strainer (Fig. 4A last lane). On the other hand, ATII and inflammatory cells were enriched in the lower portion of 40 μm cell strainer (Fig. 4A last lane).

Cell filtering was followed by three pre-plating steps to remove macrophages and fibroblasts. The supernatant was collected and centrifuged for subsequent removal of Cd45 cells by negative selection. In this way, we purified ATII cells, which were seeded on Matrigel-coated plates and fixed the day after. Quantification was performed using Image Lab software (Fig. 4B). To ulterior confirm these results, we performed an immunofluorescence analysis using the cytospin centrifugation to apply cell suspension onto a slide. The analysis confirmed the results obtained with western blot. Cells filtered with 100 μm cell strainer were mostly ATI (positive in green for Rage or Podoplanin) and inflammatory cells (positive in red for Cd45) (Fig. 4C), while cells strained afterward with 40 μm filters were positive only for Pro-Spc (positive cells in red) and Cd45 antibodies. In conclusion, to check the purity of ATII cells, we performed immunofluorescence analysis after 1 day in culture. Results showed that most of the cells are positive for Pro-Spc, which suggests that the protocol was efficient in isolating ATII cells (Fig.4D).

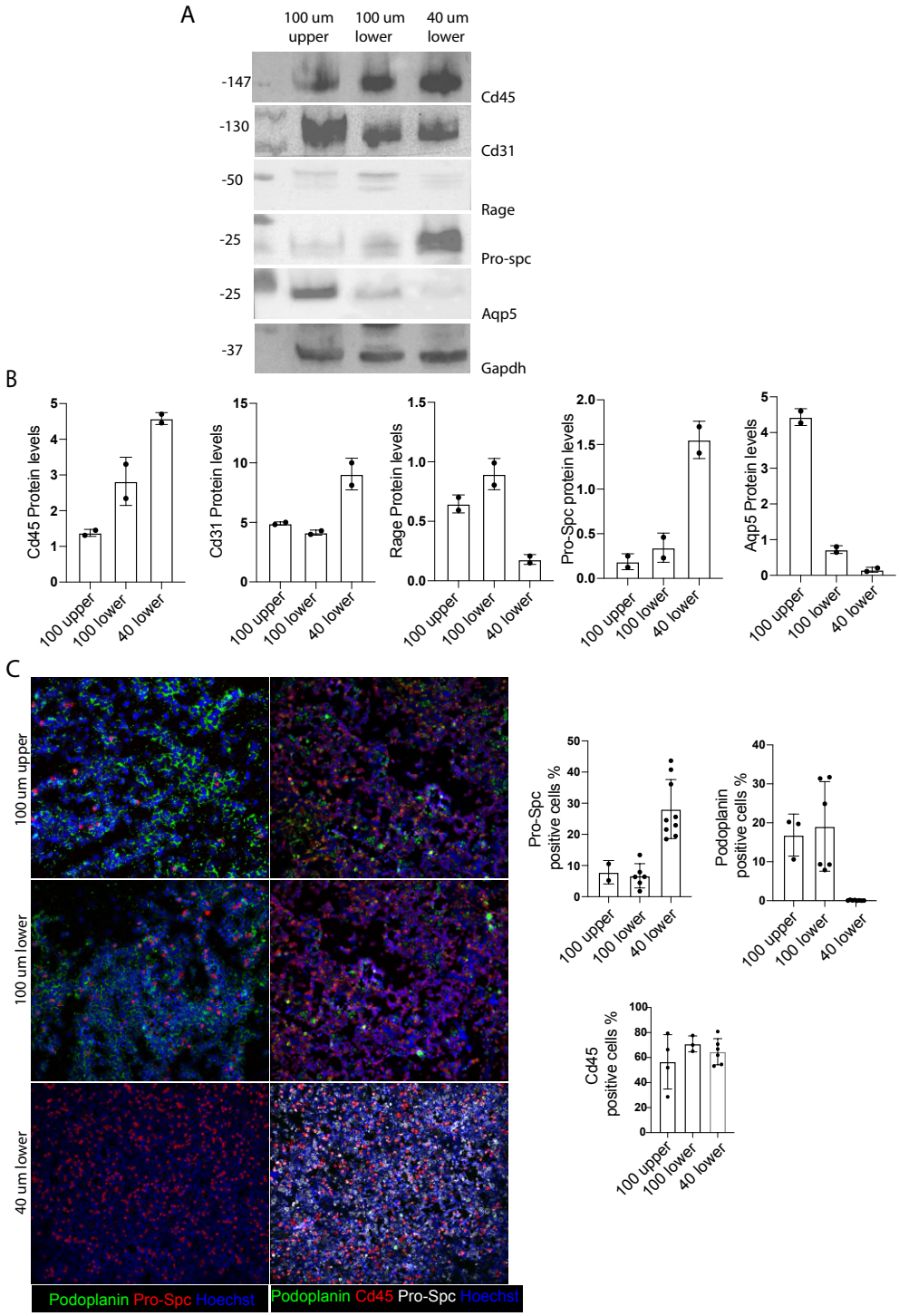
A
100 um upper
100 um lower
40 um lower
-147
Cd45
-130
Cd31
-50
Rage
-25
Pro-spc
-25
Aqp5
-37
Gapdh
B
Cd45 Protein levels
Cd31 Protein levels
Rage Protein levels
Pro-Spc protein levels
Aqp5 Protein levels
100 upper
100 lower
40 lower
C
100 um upper
100 um lower
40 um lower
Podoplanin Pro-Spc Hoechst
Podoplanin Cd45 Pro-Spc Hoechst
Pro-Spc positive cells %
Podoplanin positive cells %
Cd45 positive cells %

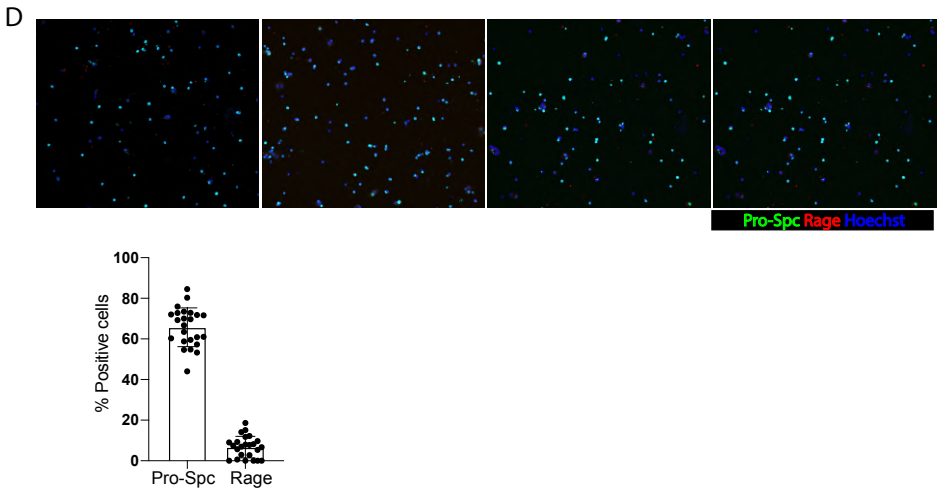

Figure 14: ***Characterization of ATII cells****. 4A) Western blot analysis of cells suspension after digestion for Cd45, Cd31, Rage, Pro-Spc and Aqp5 and Gapdh. 4B) Quantification of detected bands was performed using Bio-Rad Chemidoc imager and Image Lab software. Data are presented as relative expression normalized to Gapdh. 4C) Representative immunofluorescence images of freshly lung cells stained for Podoplanin (green), Pro-Spc (red) in the left panel and Podoplanin (green), Cd45 (red) and Pro-Spc (white)in the right panel. Nuclei were stained with Hoechst (blue). Quantification of expressing Pro-Spc, Podoplanin and Cd45 after indicated cell strainers. 4D) Representative immunofluorescence of murine ATII cells stained for Pro-Spc (green), Rage (red) and with the nuclear dye Hoechst (blue). Quantification of expressing Pro-Spc and Rage was assessed.*

4.4 Primary ATII cells isolated from bleomycin-treated mice show a similar phenotype as human ATII cells isolated from patients with IPF.

Human ATII cells isolated from IPF patients fail to trans-differentiate into ATI cells over time (Fig. 2A; 2B). In order to characterize ATII cells isolated from the bleomycin model, we cultured ATII cells on rat tail collagen-coated plates to promote their trans-differentiation. We isolated mice ATII cells at 14, 30 and 60 days after bleomycin injection. Immunofluorescence analysis at 14 days post-bleomycin showed that most of the cells were Pro-Spc positive (green signal), in both control and bleomycin groups (Fig. 5A first lane) after two days in culture. Pro-Spc-positive cells were about 60 % in controls and 40 % in bleomycin mice-derived ATII cells (Fig. 5B). No signal was detected for Rage, a marker of ATI cells. On day 4, control cells showed an intermediate phenotype, resulting positive for both Pro-Spc and Rage. After 8 days in culture, control cells trans-differentiate into ATI cells (Fig. 5A last lane), while ATII cells isolated from bleomycin-treated mice were not able to trans-differentiate (Fig. 5A).

Next, ATII cells were isolated from mice sacrificed at day 30 after bleomycin injection and analyzed by both immunofluorescence and qPCR. After 2 days in culture, both controls and bleomycin cells were positive for the ATII marker Pro-Spc, and negative for the ATI marker Rage (Fig. 5C first lane). After 4 days, ATII control cells became positive for Rage, indicating their trans-differentiation into ATI cells, while ATII cells from bleomycin-treated mice were still positive for Pro-Spc (Fig. 5C second lane). Finally, after 8 days in culture, control cells were completely trans-differentiated into ATI cells, while cells from bleomycin-treated mice were unable to trans-differentiate into ATI (Fig. 5C last lane). The immunofluorescence results were confirmed by qPCR analysis (Fig. 5G), in which we evaluated the expression of *SFTPC* and *SFTPA1*, as ATII markers, and *AQP5* and *HOPX* as ATI markers. Also in this case, bleomycin ATII cells did not fully acquire an ATI phenotype after 8 days (Fig. 5G). Finally, we isolated ATII cells 60 days after bleomycin injection. As showed in Fig. 5E (last lane) and 5F, ATII cells isolated from bleomycin-treated mice completely trans-differentiated into ATI cells after 8 days in culture, confirming the results shown in Fig. 3 and consistent with the resolution of bleomycin-induced damage at this late time point. These results indicate that bleomycin-treated ATII cells, showed an impairment of trans-differentiation at 30 days, similar to what observed in ATII cells isolated from IPF patients.

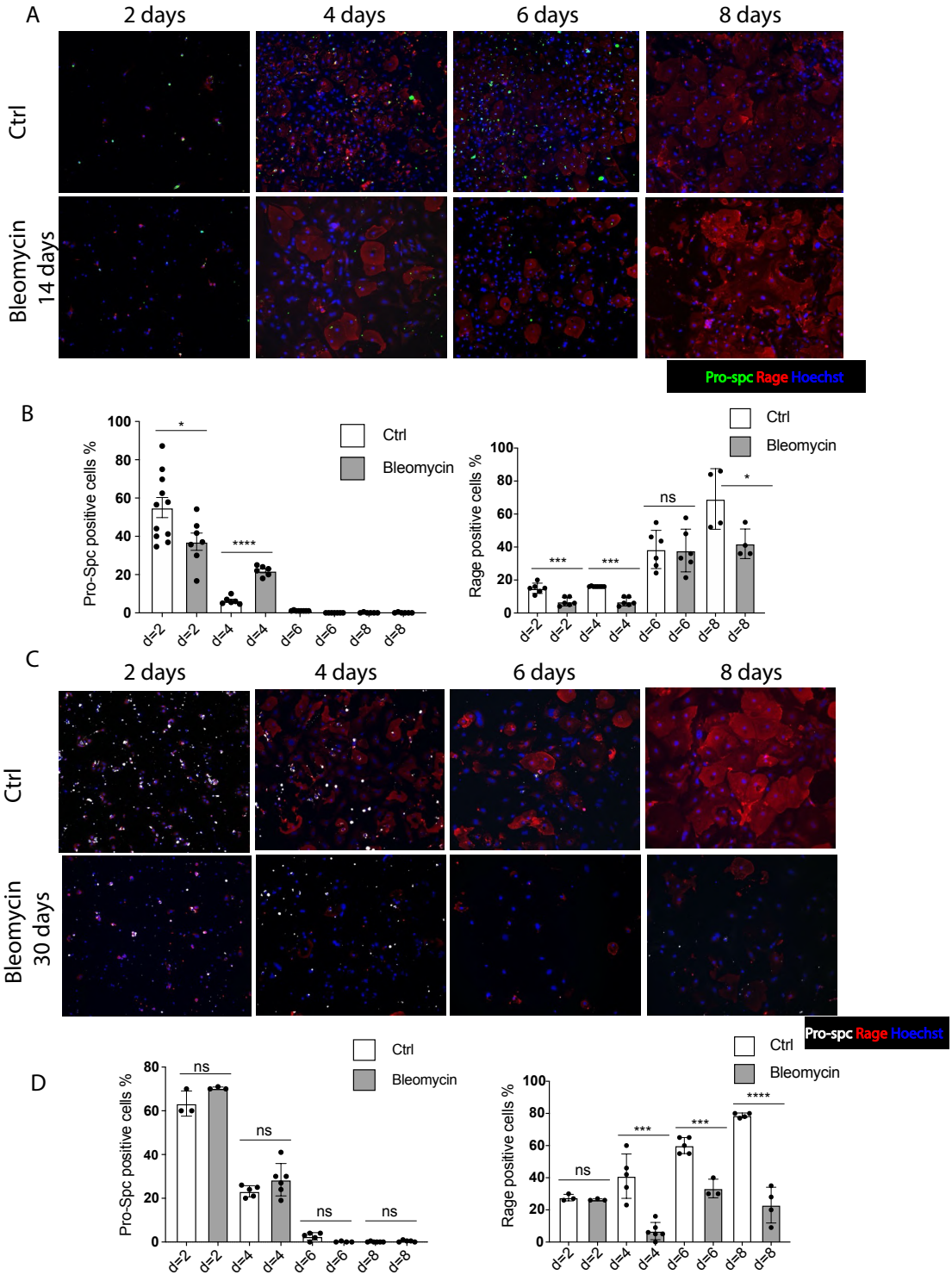
A
2 days
4 days
6 days
8 days
Ctrl
Bleomycin 14 days
Pro-spc Rage Hoechst
B
Pro-Spc positive cells %
Ctrl
Bleomycin
Rage positive cells %
d=2
d=4
d=6
d=8
C
2 days
4 days
6 days
8 days
Ctrl
Bleomycin 30 days
Pro-spc Rage Hoechst
D
Pro-Spc positive cells %
Rage positive cells %
ns

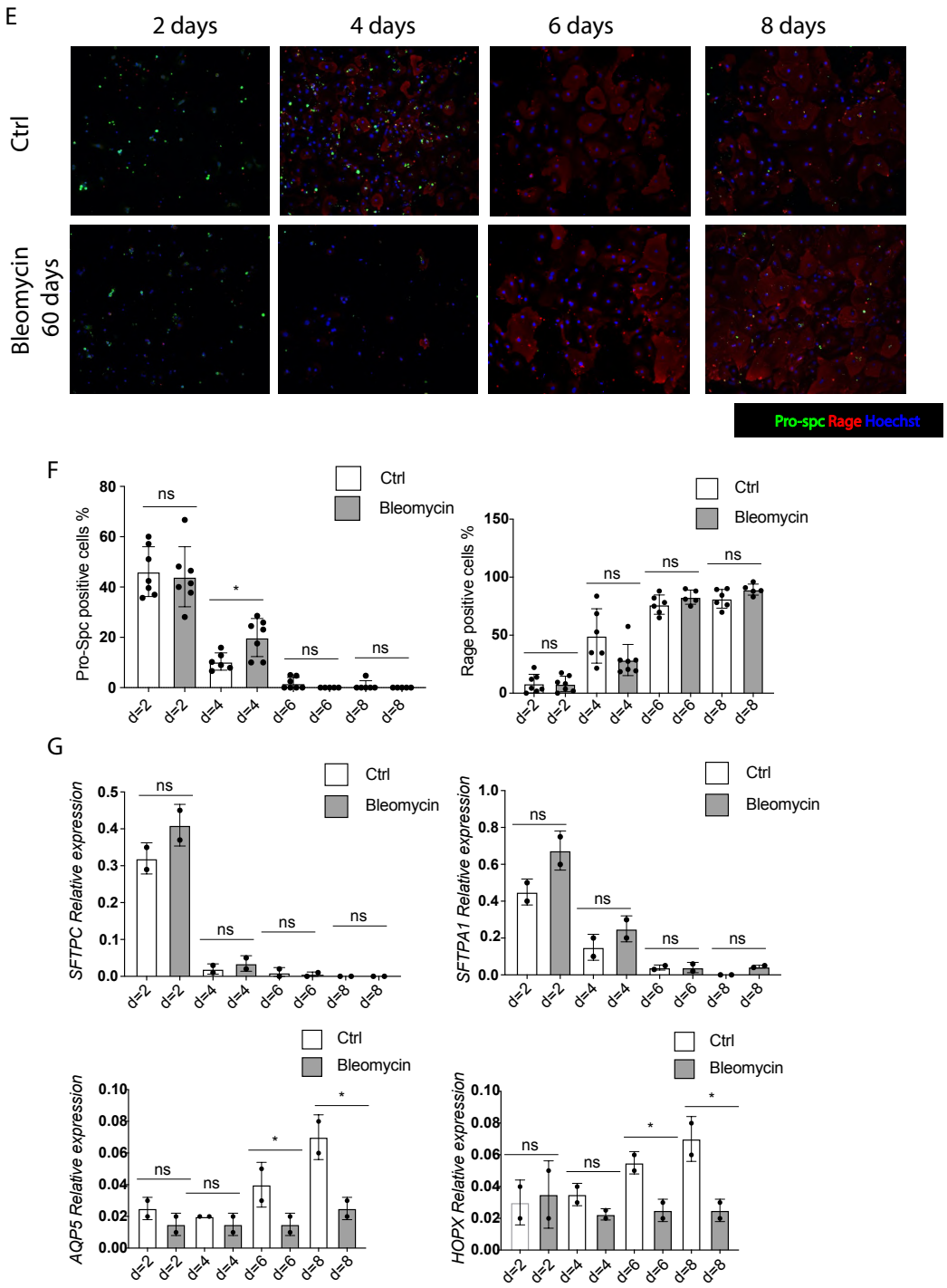

Figure 15: ***ATII cells from bleomycin treated mice showed the same impairment of ATII cells from IPF patients****. Representative immunofluorescence analysis of ATII cells harvested from ctrl and bleomycin mice and kept in culture for 2,4,6 and 8 days and stained for Pro-Spc (green), Rage (red) and with the nuclear dye Hoechst (blue): 5A) 14 days after bleomycin administration. 5C) 30 days after bleomycin administration. 5E) 60 days after bleomycin administration. 5B;5D and 5F) Quantification of cells expressing Pro-Spc and Rage after 2,4,6 and 8 days in culture. 5G) Real-time quantification of the expression levels of the following genes in ATII cells harvested from control and bleomycin mice after 30 days and kept in culture for 2, 4 and 6 days: Sftpc, Sftpa1, Aqp5 and Hopx. Data are presented as relative expression normalized to glyceraldehyde-3-phosphate dehydrogenase (GAPDH). All data are shown as mean ± S.E.M. Statistical significance was determined using a one-way ANOVA followed by Dunnett's multiple comparison test, *P < 0.05, **P < 0.01.*

4.5 MicroRNA-200 family members enhanced IPF ATII cell trans-differentiation into ATI cells and prevent their senescence

Several miRNA networks have been implicated in the complex IPF pathogenesis (Miao et al., 2018). Our laboratory has shown that miR-200 family members are dysregulated in lungs affected by IPF (Moimas et al., 2019). To evaluate the involvement of the miR-200 family in the trans-differentiation process we used primary human IPF ATII cells. At day 2 after isolation, we transfected different miRNAs and assessed the expression of trans-differentiation and senescence-associated genes at day 8. We tested 4 different miRNAs: miR-200a-3p, miR-141-3p, miR-200b-3p, miR-200c-3p. These selected miRNAs contained very similar seed sequences, as the seed sequence of miR-200b/c-3p (AAUACU) differs from the seed sequence of miR-200a/141-3p (AACACU) by only one nucleotide (Fig. 6A). After 8 days in culture, we performed qPCR analysis to assess transfection efficiency and to evaluate the expression of the validated direct targets of the miR-200 family *ZEB1* and *ZEB2* (Fig. 6B). All four miRNAs were able to downregulate the expression of these targets. Furthermore, we analyzed the expression of the ATI marker *Aqp5* (Fig. 6C). Interestingly, miR-200b-3p and miR-200c-3p, which share the same seed sequence, promoted the expression of *AQP5*. This was further validated by immunofluorescence analysis, confirming the capacity of these miRNAs to foster ATII trans-differentiation into ATI cells (Fig. 6C ;6D). Next, we evaluated the effect of this miRNAs family on cell senescence and evaluated the expression levels of the *CDKN1A* and *CDKN2A*. Only miR-200a-3p and miR-141-3p reduce the expression of these senescence markers (Fig. 6E).

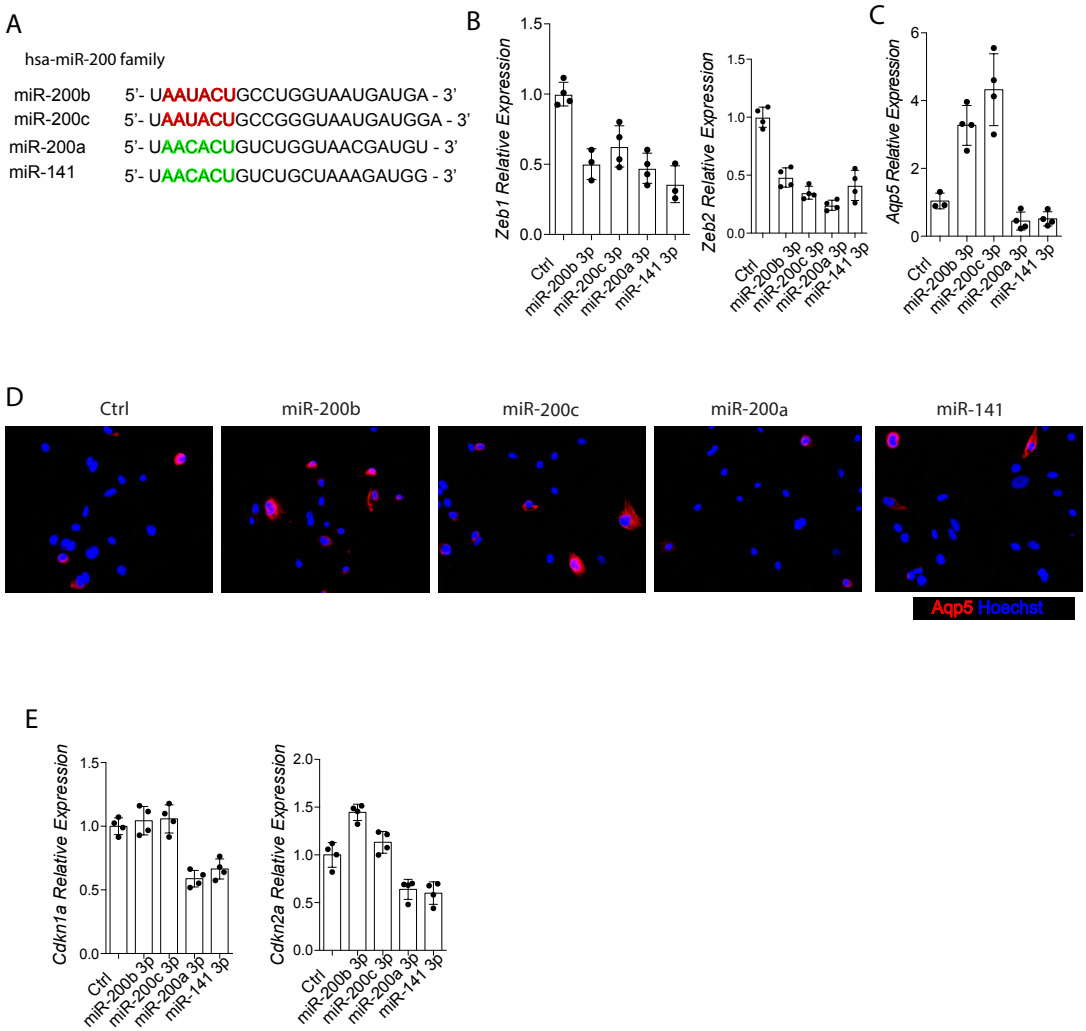

Figure 16: ***Effect of miR-200 family members on the differentiation and senescence of ATII cells from IPF patients****. 6A) Sequences of the selected miR-200 family, with an indication of the seed sequence and the unique single nucleotide difference between miR-200b/c-3p and miR-200a/141-3p, highlighted in red and green respectively. 6B) Real-time quantification of the expression levels of the following genes in ATII cells harvested from control and IPF patients: ZEB1, ZEB2 and 6C) AQP5. 6D) Representative immunofluorescence images of ATII cells from IPF patients stained for Aqp5 and with the nuclear dye Hoechst (blue). 6E) Real-time quantification of the expression levels of the following genes in ATII cells harvested from control and IPF patients: CDKN1A and CDKN2A. Data are presented as relative expression normalized to GAPDH.*

4.6 Delivery of miR-200c-3p *in vivo*

4.6.1 Aerosol administration efficiently deliver miRNAs to the lung

Nucleic acid delivery to the lung is challenging, as the respiratory tract has evolved defense mechanisms to expel and destroy any inhaled particle (Newman., 2017). First, we used a fluorescent-miRNA, to be delivered by aerosol in healthy mice (Fig. 7A), to visualize its internalization by lung cells. Mice, that received fluorescent-miRNA, were sacrificed after 7 days, and lung sections were stained for Pro-Spc and Podoplanin. Immunofluorescence staining (Fig. 7A;7B) showed that the fluorescent miRNA entered both ATI and ATII cells, confirming that aerosol efficiently delivers small molecules, such as miRNAs, to the lungs.

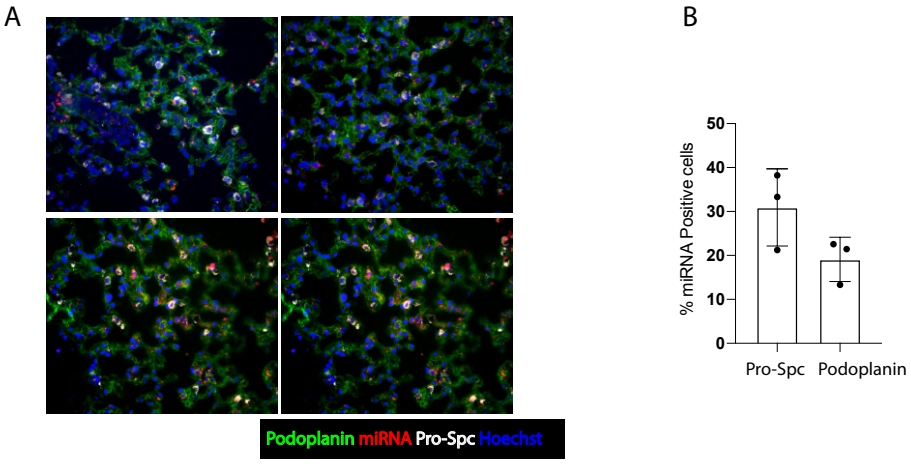

Figure 17: ***Delivery of fluorescent miRNA in vivo****. 7A) Representative immunofluorescence analysis of lung tissue sections stained for Pro-Spc (white), Podoplanin (green) and the fluorescent miRNA (red). Nuclei were stained with nuclear dye, Hoechst (blue). 7B) Quantification of the expression of miRNA in ATII cells and miRNA in ATI cells after the delivery of the fluorescent miRNA.*

4.6.2 miR-200c-3p ameliorated lung fibrosis *in vivo*

We then assessed the antifibrotic effect of miR-200c-3p in the experimental model of pulmonary fibrosis. Either a 30 ug/Kg control miRNA or 30 ug/Kg miR-200c-3p (Yang et al., 2012) were administered by aerosol way, together with bleomycin (1 U/Kg). Masson trichrome staining showed increased collagen deposition in the lungs of both bleomycin-instilled mice and in those treated with the control miRNA mimics (Fig. 8B; 8C). In contrast, bleomycin-instilled mice that received miR-200c-3p have an attenuated collagen deposition in the lungs (Fig. 8D; 8E). The extent of fibrosis was quantified using the Ashcroft score and showed 3-fold reduction of fibrotic tissue in miRNA-treated animals compared to controls (Fig. 8F) (Ashcroft et al., 1988). To better characterize the therapeutic effect exerted by miR-200c-3p, lung sections of controls, bleomycin and miR-200c-3p were stained for Podoplanin and Pro-Spc markers by immunofluorescence. The lung parenchyma of bleomycin mice showed massive inflammation (Fig. 8G), with loss of alveolar structure. Mice treated with miR-200c-3p showed preservation of lung structure and parenchymal cells.

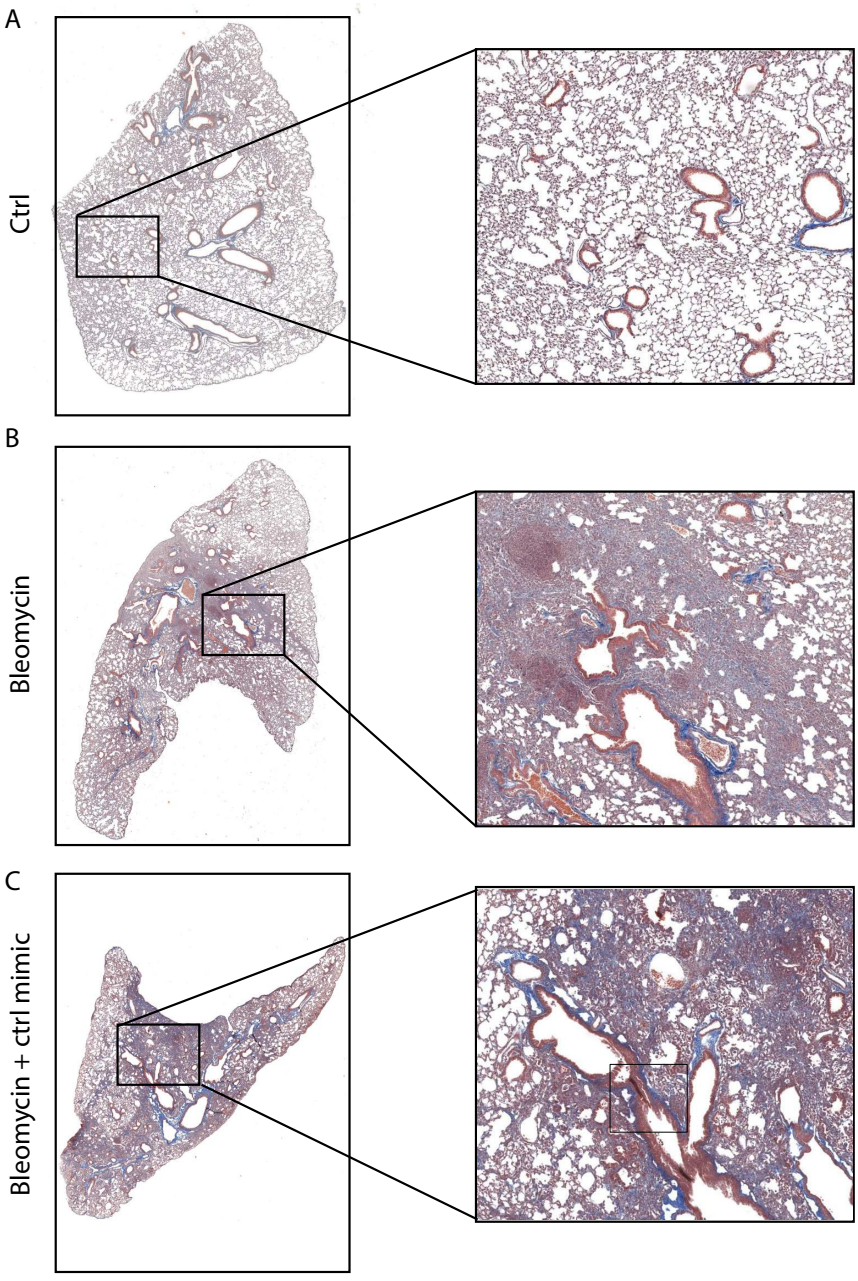
A
Ctrl
B
Bleomycin
C
Bleomycin + ctrl mimic

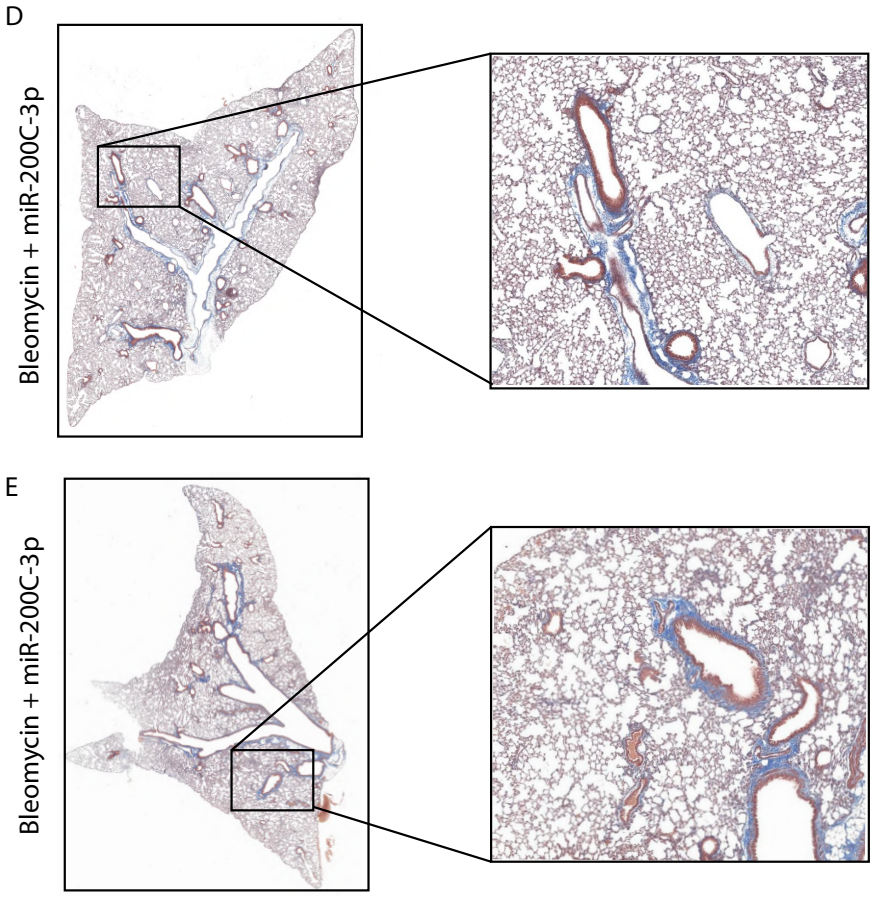
D
Bleomycin + miR-200C-3p
E
Bleomycin + miR-200C-3p

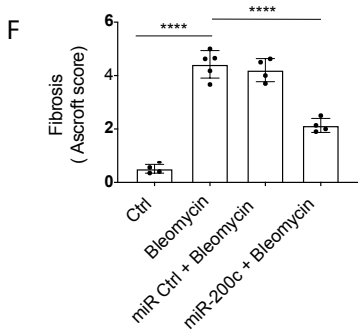
F
Fibrosis
(Ascroft score)
6
4
2
0
****
****
Ctrl
Bleomycin
miR Ctrl + Bleomycin
miR-200c + Bleomycin

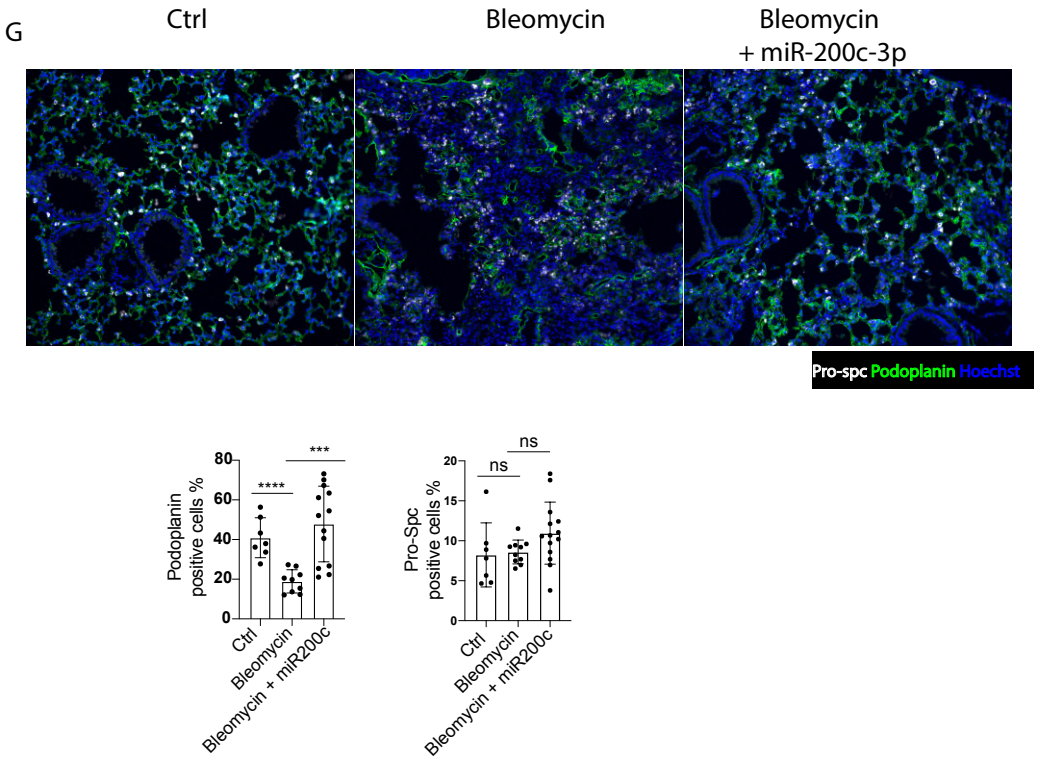

Figure 18: ***miR-200C-3p prevented lung fibrosis in vivo****. Representative images of Masson Trichrome staining lungs harvested from ctrl 8A) bleomycin mice 8B), miR ctrl and bleomycin 8C) bleomycin and miR-200c 8D and 8E). High magnifications are shown for each image. 8F) Quantification of the fibrotic area was performed using the Ashcroft score. 8G) Representative immunofluorescence images of tissue sections from ctrl, bleomycin and bleomycin + miR-200c-3p stained for Pro-Spc (white) and Podoplanin (green). Nuclei were stained with nuclear marker Hoechst (blue). Quantification of cells expressing Podoplanin and Pro-Spc was performed. All data are shown as mean ± S.E.M. Statistical significance was determined using a one-way ANOVA followed by Dunnett's multiple comparison test, *P < 0.05, ****P < 0.0001.*

Next, we assessed the therapeutic effect of miR-200c-3p in reverting established fibrosis. We treated mice with bleomycin and administered miR-200c-3p after two weeks, when fibrosis is already evident. In control mice, Masson trichrome staining showed a normal lung parenchyma structure (Fig.9A). After bleomycin administration, lung parenchyma was completely replaced by fibrotic and inflammatory tissue (Fig. 9B). In mice treated with miR-200c-3p the lung showed reduced fibrosis and preserved alveolar structure (Fig. 9C). Ashcroft score was 2.5-fold lower in miR-200c-3p-treated lungs than in bleomycin-treated mice (Fig. 9D). These results confirm that miR-200c-3p can revert collagen deposition even when fibrosis is established.

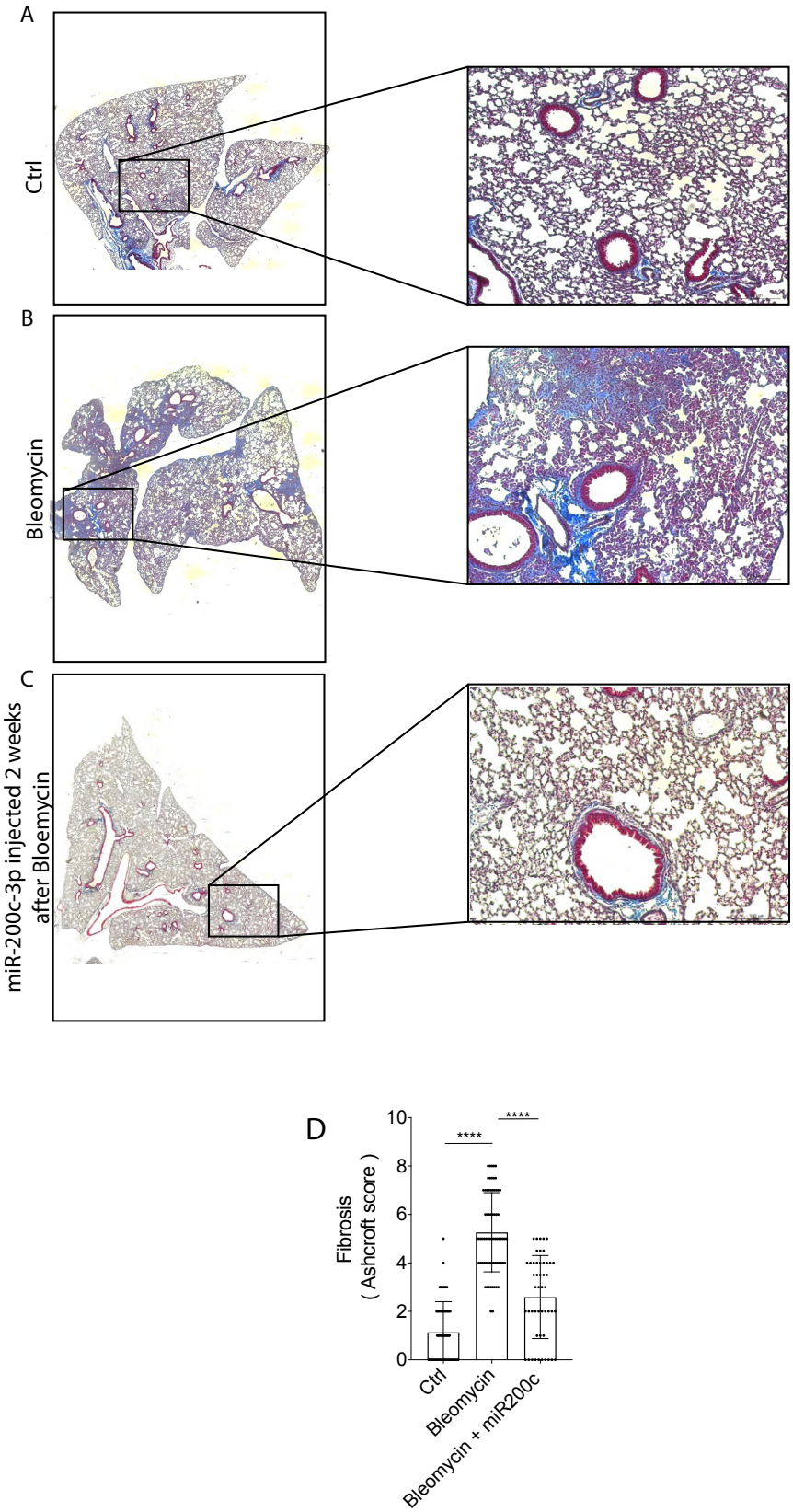

Figure 19: ***miR-200C-3p reverted lung fibrosis in vivo****. Representative images of Masson Trichrome stained lungs harvested from control mice 9A), bleomycin treated mice (9B) miR-200c injected 2 weeks after bleomycin administration (9C). High magnifications are shown for each image. 9D) Quantification of the fibrotic area was performed using the Ashcroft score. All data are shown as mean ± S.E.M. Statistical significance was determined using a one-way ANOVA followed by Dunnett's multiple comparison test, *P < 0.05, ****P < 0.0001.*

4.7 Identification of relevant miR-200c targets

miR-200c has been shown to inhibit EMT by downregulating ZEB1/2 and up-regulating E-cadherin, a known epithelial marker (Moimas et al., 2019). In this work we have demonstrated that miR-200c acts directly on ATII cells, downregulating the expression of ZEB1/2 and increasing their trans-differentiation. To identify additional targets that could mediate the trans-differentiation of ATII cells in ATI cells, we used two miRNA target prediction software (www.microRNA.org and www.mirtabase.org) that scan the genome for putative miR-200 binding sites in both humans and mice. We selected targets that were experimentally validated by luciferase 3'UTR reporter assay and focused on those that could control cell growth and proliferation based on literature data. Among these, we further studied the receptor tyrosine kinase VEGFR1, also known as *Flt1*. *Flt1* is expressed mainly in endothelial cells, where it inhibits proliferation, acting as a decoy receptor that sequesters VEGF-A and thereby competes for its binding to VEGFR2 (Rajasekaran et al., 2015). To validate *Flt1* as a target of miR-200c-3p, we isolated lung endothelial cells from wild-type (WT) mice and transfected them with miR-200c-3p, a control miRNA and siUBC (to check and normalize for transfection efficiency). After 2 days, we performed qPCR (Fig. 10A) and detected a significantly decreased *Flt1* expression in miR-200c-3p-transfected primary lung endothelial cells compared to non-transfected cells and cells transfected with control miRNA.

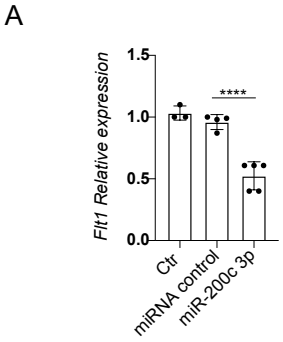

*Figure 20: **Flt1 is a target of miR200c**. 10A) Real-time quantification of the expression levels of the following gene in endothelial cells Flt1 upon miR-200c overexpression. Data are presented as relative expression normalized to GAPDH. All data are shown as mean ± S.E.M. Statistical significance was determined using a one-way ANOVA followed by Dunnett's multiple comparison test, *P < 0.05, ****P < 0.0001.*

4.8 The crosstalk between endothelial and epithelial cells during lung fibrosis

4.8.1 Inactivation of *Flt1* enhances ATII trans-differentiation

To evaluate the crosstalk between alveolar endothelial and epithelial cells, we co-cultured epithelial cells from either control or bleomycin treated mice, and endothelial cells isolated from either WT or Cdh5-ERT2-Flt1$^{flox/flox}$ (*Flt1* KO) mice. In this latter model, a Tamoxifen-inducible inducible CRE is under the control of the endothelial-scoeific Cdh5 promoter. After tamoxifen injections for five consecutive days, CRE-mediated recombination results in the excision of a portion of the *Flt1* gene and thus in the depletion of *Flt1* specifically in endothelial cells (Fig. 11A). After one additional week (washout period), expression of *Flt1* was evaluated by qPCR in purified endothelial cells. Results confirmed a significant decrease in *Flt1* expression in lung endothelial cells (Fig. 11B). Thus, we proceeded with the transfection of endothelial cells from WT and *Flt1* KO mice with miR-200c-3p or a control miRNA. The day after, ATII cells were isolated from either control or bleomycin mice and seeded on top of endothelial cells. After 2 days in culture, EdU was added in the medium, assuming that the only epithelial cell type able to proliferate were ATII cells. Therefore, we used EdU to track and visualize any ATII-derived cell. Cells were fixed after two additional days, as schematically represented in Fig. 11 C. Cells were stained for Rage to label ATI cells (red), ERG to label endothelial cells (white) and EdU (green) to label ATII-derived cells. These results demonstrate that control ATII cells trans-differentiate more efficiently when cultured with *Flt1* KO than with WT endothelial cells (Fig. 11D; 11E). ATII cells isolated from bleomycin treated mice were not able to trans-differentiate to ATI cells in co-culture with WT endothelial cells (Erg positive cells), but their trans-differentiation potential was rescued by endothelial cells isolated from *Flt1* KO (Fig.11F; 11G). These data implicate that *Flt1* inhibits the trans-differentiation of AII cells.

Thus, we propose a new mechanism by which miR-200c exerts its anti-fibrotic effect, namely its capacity to down-regulate *Flt1* in endothelial cells and in this way to control epithelial cell activation. We hypothesized that endothelial cells might release angiocrine factors and promoting epithelial cell activation through a paracrine mechanism.

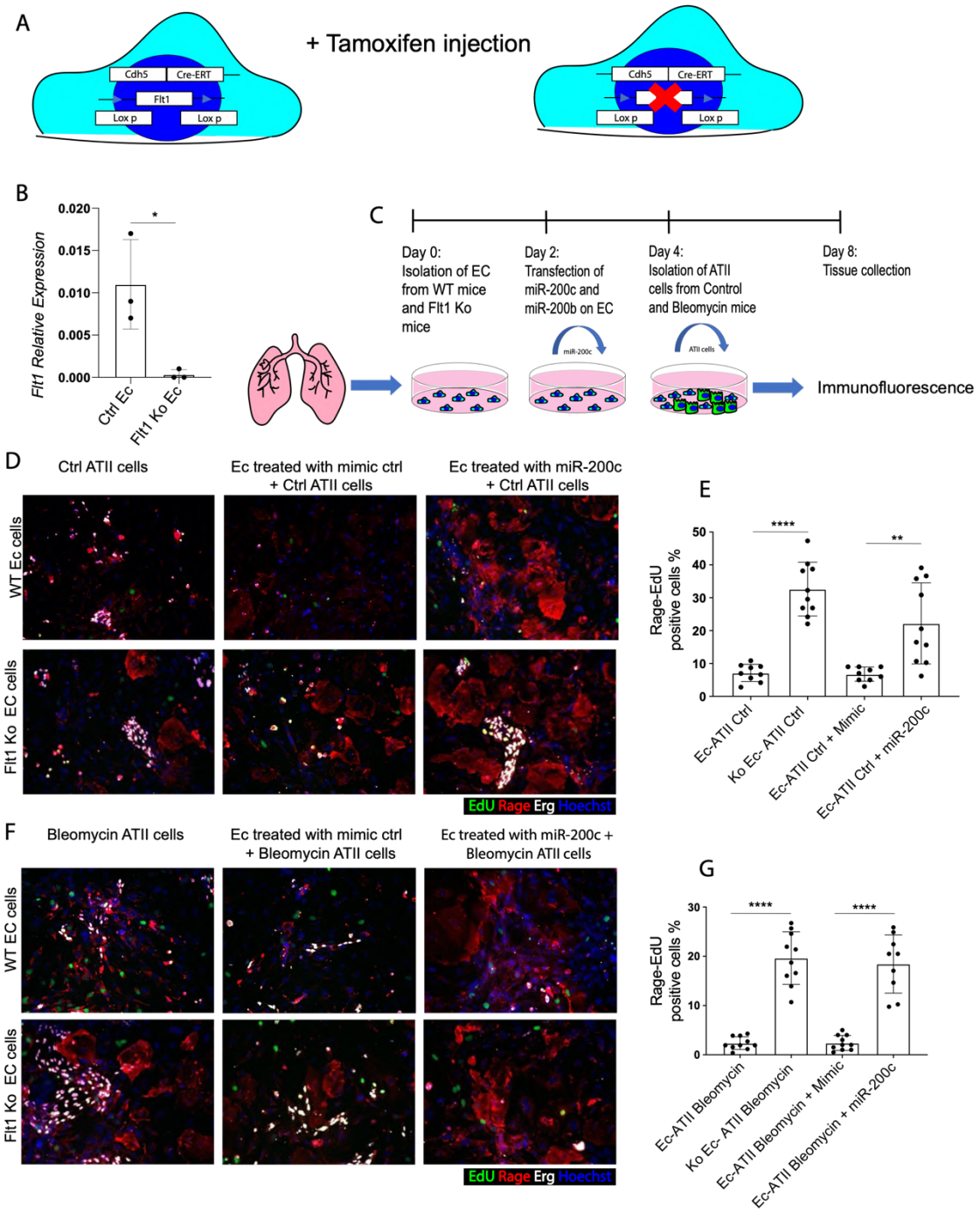

*Figure 21: **Flt1 endothelial cells improve ATII trans-differentiation**. 11A) Schematic mouse model of endothelium specific Flt1 ablation using Cdh5 ERT2 Flt1$^{flox/flox}$ knock out mouse system. 11B) Real-time quantification of the expression levels of the following gene in endothelial cells (Ec): Flt1. Data are presented as relative expression normalized to GAPDH. 11C) Schematic representation of physical co-culture assay between alveolar endothelial and ATII cells. Representative immunofluorescence images of WT and Flt1 Ko endothelial cells with control ATII cells (11D) and bleomycin ATII cells (11F) stained for EdU (green), Rage (red), Erg (white) and with nuclear marker dye Hoechst (blue). Quantification of cells expressing Rage-EdU cells in control (11E) and in bleomycin (11G) ATII cells. All data are shown as mean ± S.E.M. Statistical significance was determined using a one-way ANOVA followed by Dunnett's multiple comparison test, *P < 0.05, ****P < 0.0001.*

4.8.2 *Flt1* KO endothelial cells promote ATII activation through the secretion of angiocrine factors

To determine whether the observed increased in ATII cells activation and trans-differentiation depends on proteins secreted by *Flt1* KO endothelial cells, we collected the medium conditioned by alveolar lung endothelial cells purified from WT and Cdh5 ERT2 Flt1$^{flox/flox}$ mice. On the same day, we purified ATII cells from controls and bleomycin-treated mice, on which we added the endothelial cell supernatant, as schematically shown in Fig. 12A. We observed that control ATII cells trans-differentiated into ATI cells in all conditions, but trans-differentiation increased by 40% when the supernatant from *Flt1* KO endothelial cells was added (Fig. 12B). As expected, ATII cells isolated from bleomycin-treated mice were not able to efficiently trans-differentiate into ATI cells (Fig. 12C) with their own culture medium or in the presence of WT endothelial cell supernatant, while trans-differentiation was rescued by the addition of supernatant from Cdh5 ERT2 Flt1$^{flox/flox}$ endothelial cells. In conclusion, the supernatant obtained from Cdh5 ERT2 Flt1$^{flox/flox}$ promoted trans-differentiation to ATI cells (Fig. 12B; 12C), supporting our initial hypothesis that *Flt1* in endothelial cells suppresses the production of angiocrine factors able promote the trans-differentiation to ATI cells.

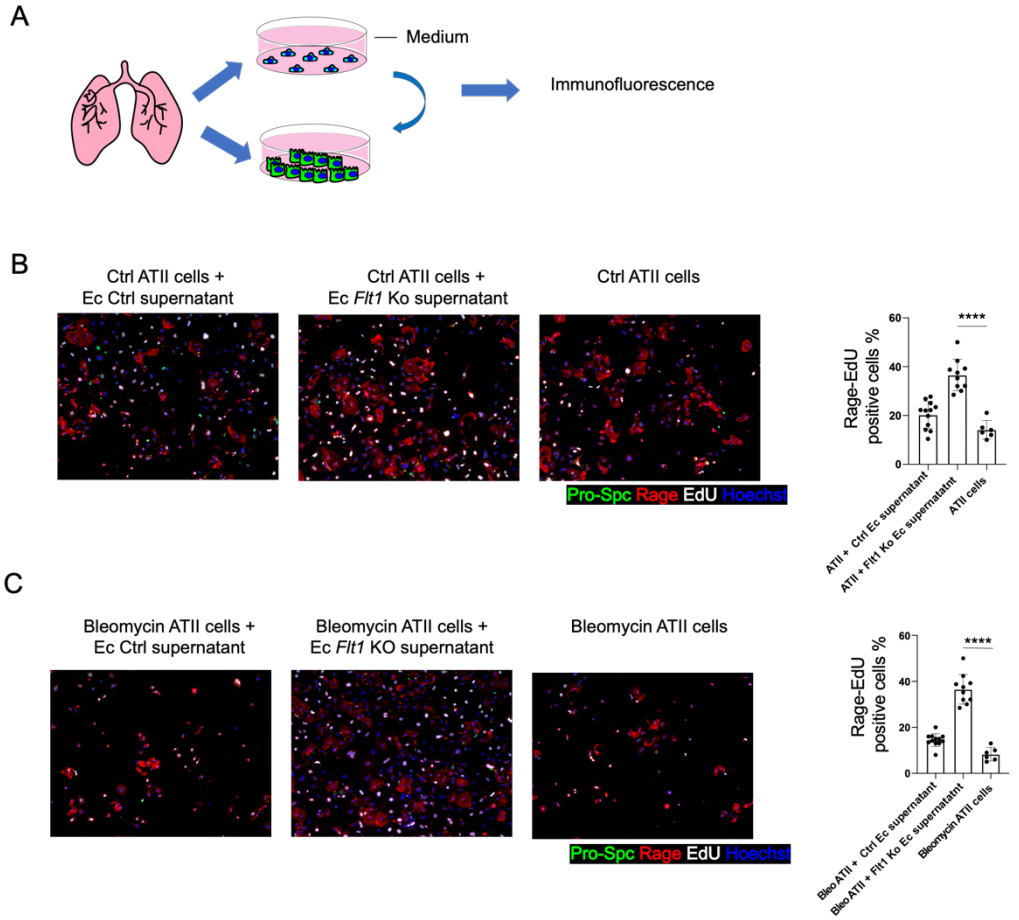

*Figure 22: **Alveolar endothelial cells improve ATII trans-differentiation through releasing of secreted proteins**. 12A) Schematic representation of supernatant experiment. Representative immunofluorescence images of WT and Flt1 Ko supernatants in control ATII cells (12B) and in bleomycin ATII cells (12C) stained for Pro-Spc (green), Rage (red), EdU (white) and nuclear marker dye Hoechst (blue). Quantification of cells expressing Rage-EdU was performed. All data are shown as mean ± S.E.M. Statistical significance was determined using a one-way ANOVA followed by Dunnett's multiple comparison test, *P < 0.05, ****P < 0.0001.*

4.8.3 ATII cells in Cdh5 ERT2 Flt $^{flox/flox}$ mice are able to trans-differentiation into ATI cells upon bleomycin injection

To assess whether the negative role of *Flt1* on ATII cell trans-differentiation is also exerted in vivo, Cdh5 ERT2 Flt $^{flox/flox}$ mice were treated with Tamoxifen and then injected intratracheally with bleomycin (1 U/Kg). After 30 days, ATII cells were harvested and cultured for different times (2, 4, 6 and 8 days) to evaluate their trans-differentiation capacity. Immunofluorescence analysis showed that cells were positive for both the ATII markers Pro-Spc (green) and the ATI marker Rage (red). On day 4 and day 6, expression of the ATI marker RAGE was observed both in control cells and ATII cells obtained from bleomycin-treated mice, but the latter exhibited a trans-differentiation impairment, that indicates impaired trans-differentiation (Fig. 13A). At the last time-point (day 8), control cells and cells obtained from CRE- positive mice but not treated with bleomycin completely trans-differentiated into ATI cells, whereas cells isolated from bleomycin-treated mice were not able to do so. In contrast, ATII cells isolated from CRE-positive, bleomycin-treated mice acquired the normal phenotype of ATI cells, consistent with restored trans-differentiation capacity (13A). Trans-differentiation capacity was quantified by counting the number of cells that were both Rage and EdU positive (Fig. 13B). Thus, ATII cells isolated from Cdh5 ERT2 Flt $^{flox/flox}$ mice rescued their capacity to trans-differentiate into ATI cells, even upon bleomycin injection.

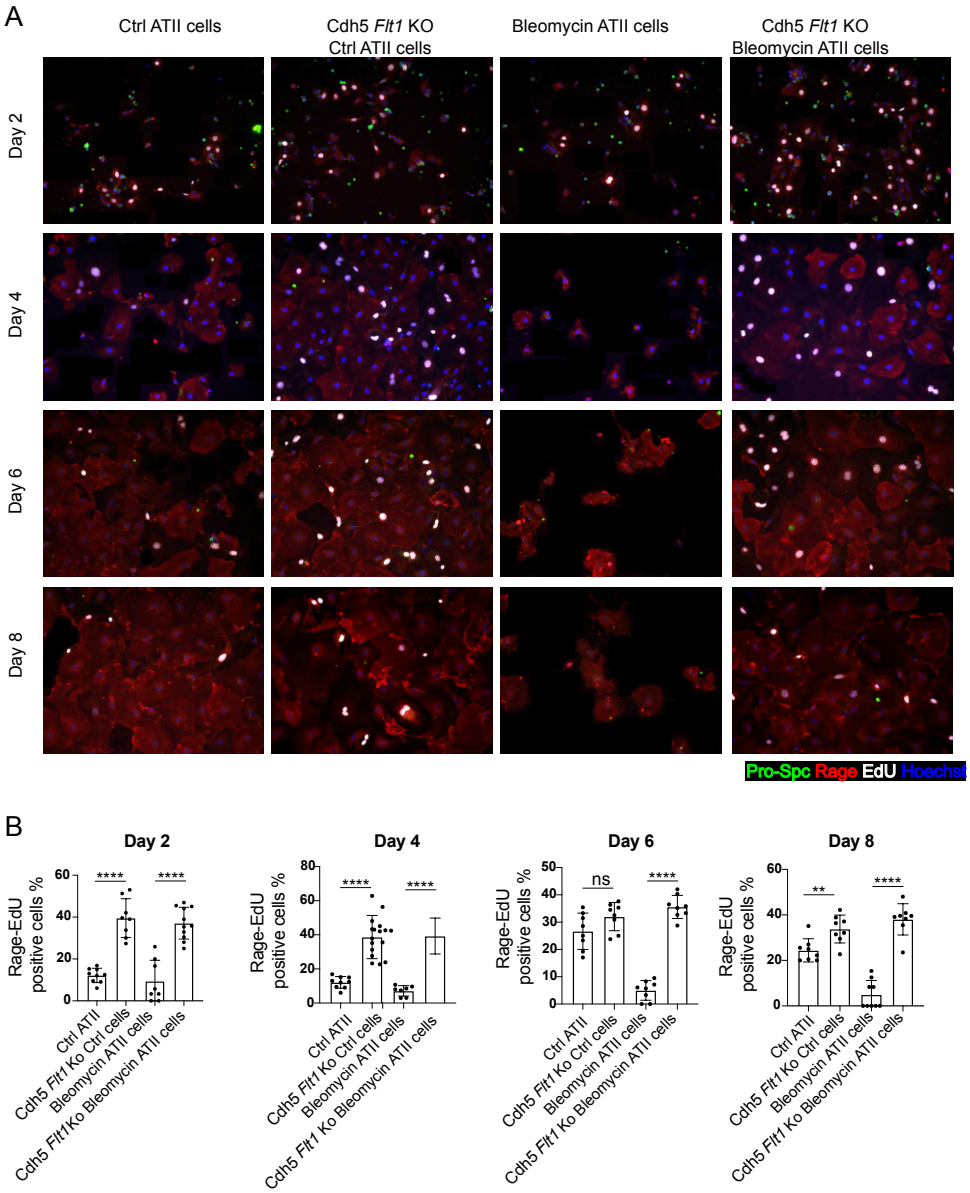

Figure 23: ***ATII cells from Cdh5 ERT2 Flt1$^{flox/flox}$ mice exhibited an enhanced capacity of trans-differentiation into ATI cells.*** *13A) Representative immunofluorescence analysis of ATII cells harvested from Cdh5 ERT2 Flt1$^{flox/flox}$ mice treated with bleomycin and kept in culture for 2,4,6 and 8 days and stained for Pro-Spc (green), Rage (red), EdU (white) and with the nuclear dye Hoechst (blue). 13B) Quantification of cells expressing Rage-EdU was performed at indicated time points. All data are shown as mean ± S.E.M. Statistical significance was determined using a one-way ANOVA followed by Dunnett's multiple comparison test, *P < 0.05, ****P < 0.0001.*

4.8.4 Co-culture assay confirms the capacity of *Flt1* KO endothelial cells to rescue in trans-differentiation

We set up a co-culture assay, mimicking the interaction between epithelial and endothelial cells that happens in the lung, where they are separated by the basal membrane. Endothelial cells from WT and Cdh5 ERT2 $Flt1^{flox/flox}$ mice were harvested and seeded on the lower side of the membrane of a transwell. The next day, ATII cells, from control and bleomycin-treated mice, were seeded on the upper side of the same membrane (Fig. 14A). We set three experimental conditions, in which ATII cells were always seeded in the upper compartment, whereas the lower surface was either left empty or seeded with WT and *Flt1* KO endothelial cells. Immunofluorescence staining revealed that control ATII cells trans-differentiate into ATI cells at 4 days. Importantly, when control ATII cells are in contact with WT endothelial cells their trans-differentiation does not increase, and a higher trans-differentiation is achieved when ATII cells are in culture with endothelial cells from *Flt1* KO mice (Fig. 14B). No differences were observed in the trans-differentiation potential of control ATII in the presence or absence of endothelial cells (Fig. 14C). In agreement with previous experiments, ATII cells harvested from bleomycin mice did not trans-differentiate either spontaneously or in contact with WT endothelial cells, keeping an elongated shape. Interestingly, when bleomycin ATII cells were in contact with endothelial cells from *Flt1* KO mice, they completely rescued their capacity to differentiate (Fig. 14D), as shown by their increased area (Fig. 14E). Thus, we added additional evidence in support of our hypothesis that secreted proteins from *Flt1* KO endothelial cells are induce epithelial trans-differentiation.

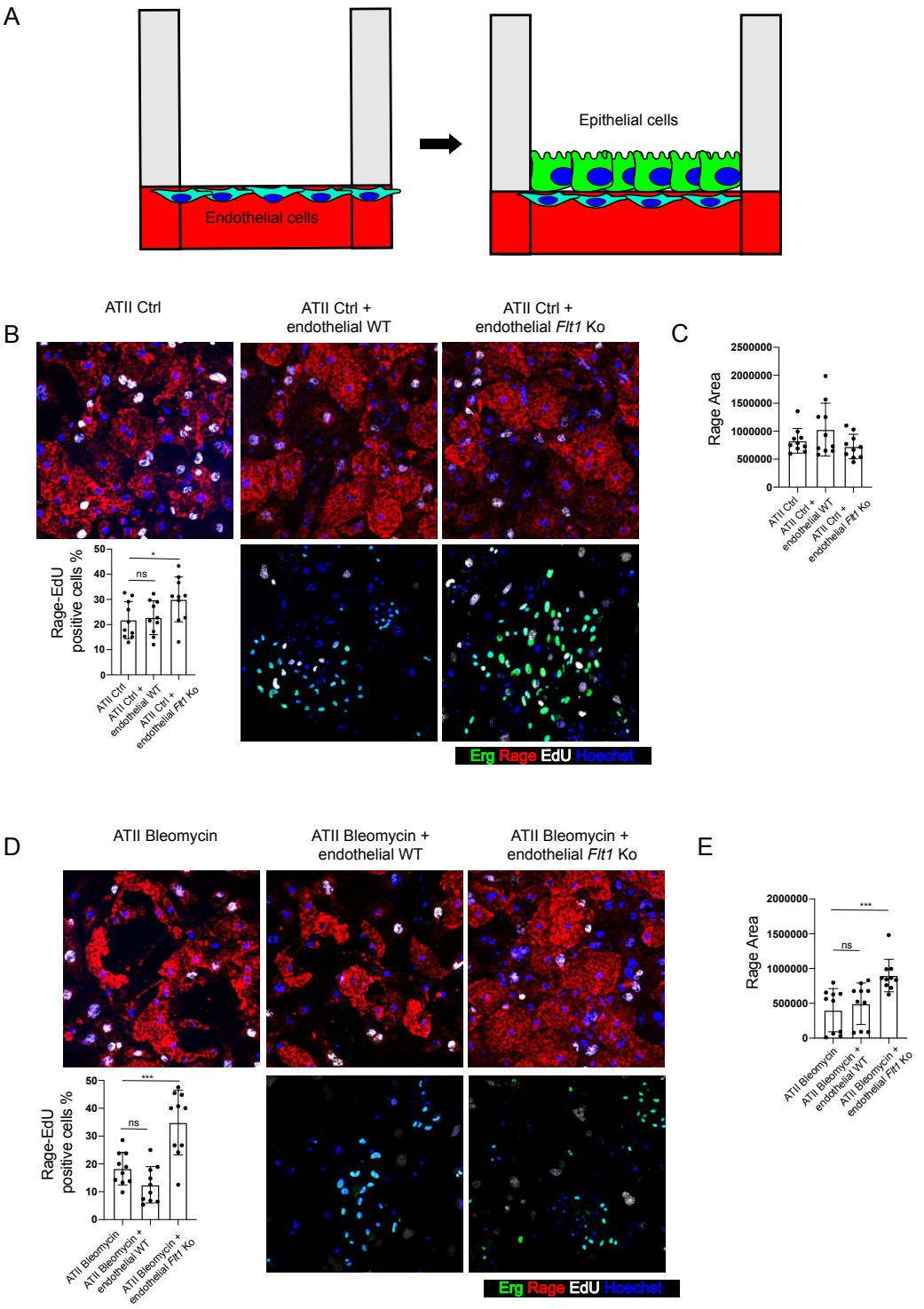

Figure 24: ***Flt1 KO Endothelial cells secreted factors rescued the ATII trans-differentiation in pathological conditions****. 14A) Schematic representation of co-culture experiment. Representative immunofluorescence images of WT and Flt1 Ko endothelial cells with control ATII cells (14B) and bleomycin ATII cells (14D) stained for Erg (green), Rage (red), EdU (white) and with nuclear marker dye Hoechst (blue). Quantification of cells expressing Rage-EdU was performed. Quantification of area of cells expressing Rage in control (14C) and in bleomycin (14E) ATII cells. All data are shown as mean ± S.E.M. Statistical significance was determined using a one-way ANOVA followed by Dunnett's multiple comparison test, *P < 0.05, ****P < 0.0001.*

4.8.5 Endothelial *Flt1* depletion prevents bleomycin-induced fibrosis *in vivo*

We then assessed the role of endothelial *Flt1* in lung fibrosis. Cdh5 ERT2 Flt $^{flox/flox}$ mice were treated with tamoxifen to obtain *Flt1* depletion in endothelial cells, as described After 1 week, mice were treated intratracheally with bleomycin (1 U/Kg). Masson trichrome staining at 30 days demonstrated a normal alveolar structure in control mice (Fig. 15A), whereas the lung parenchyma was completely replaced by fibrotic tissue upon bleomycin treatment (Fig. 15B). Interestingly, endothelial *Flt1* depletion prevented the formation of fibrosis (Fig. 15C-D), resulting in a 2,5-fold decrease in Ashcroft score. (Fig. 15E). Finally, to confirm whether the depletion of *Flt1* in endothelial cells promotes the activation and trans-differentiation of ATII cells *in vivo,* we analyzed the lung tissue by immunofluorescence analysis. Tissue sections were stained for the ATII cell marker Pro-Spc (white), for the ATI cell marker Podoplanin (green), and proliferating cells were labeled by EdU incorporation (red). We observed that in bleomycin-treated mice, the lung parenchyma was extensively infiltrated by inflammatory cells, with few surviving ATI cells (shown in green) (Fig. 15G). On the contrary, upon *Flt1* depletion, the inflammatory response was reduced (Fig. 15G) and the structure of the alveoli was preserved. The trans-differentiation rate was increased (Fig. 15F), paralleled by a decrease in proliferating ATII cells (Pro-Spc-EdU/Pro-Spc), indicating that ATII cells are activated and differentiate into ATI cells in endothelial *Flt1* KO mice

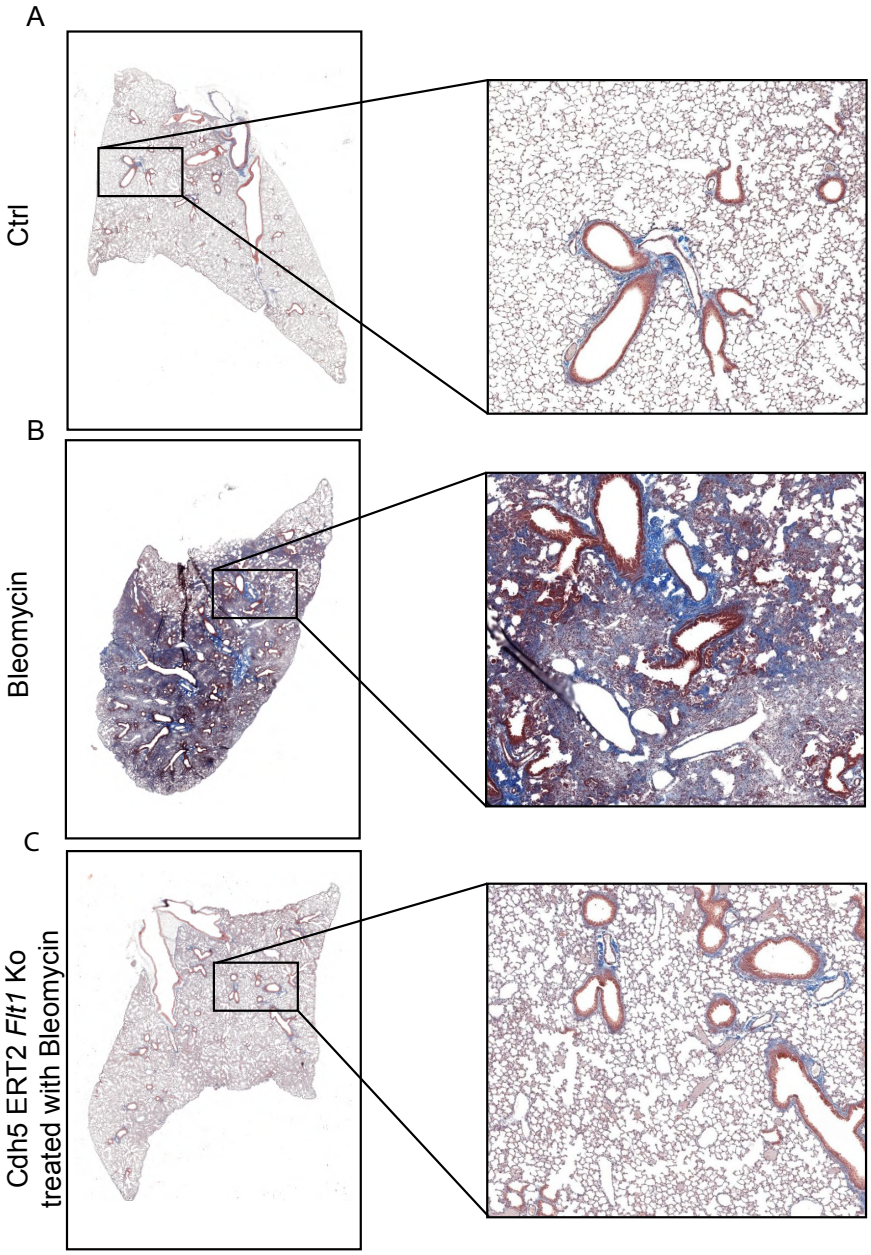
A
Ctrl
B
Bleomycin
C
Cdh5 ERT2 Flt1 Ko
treated with Bleomycin

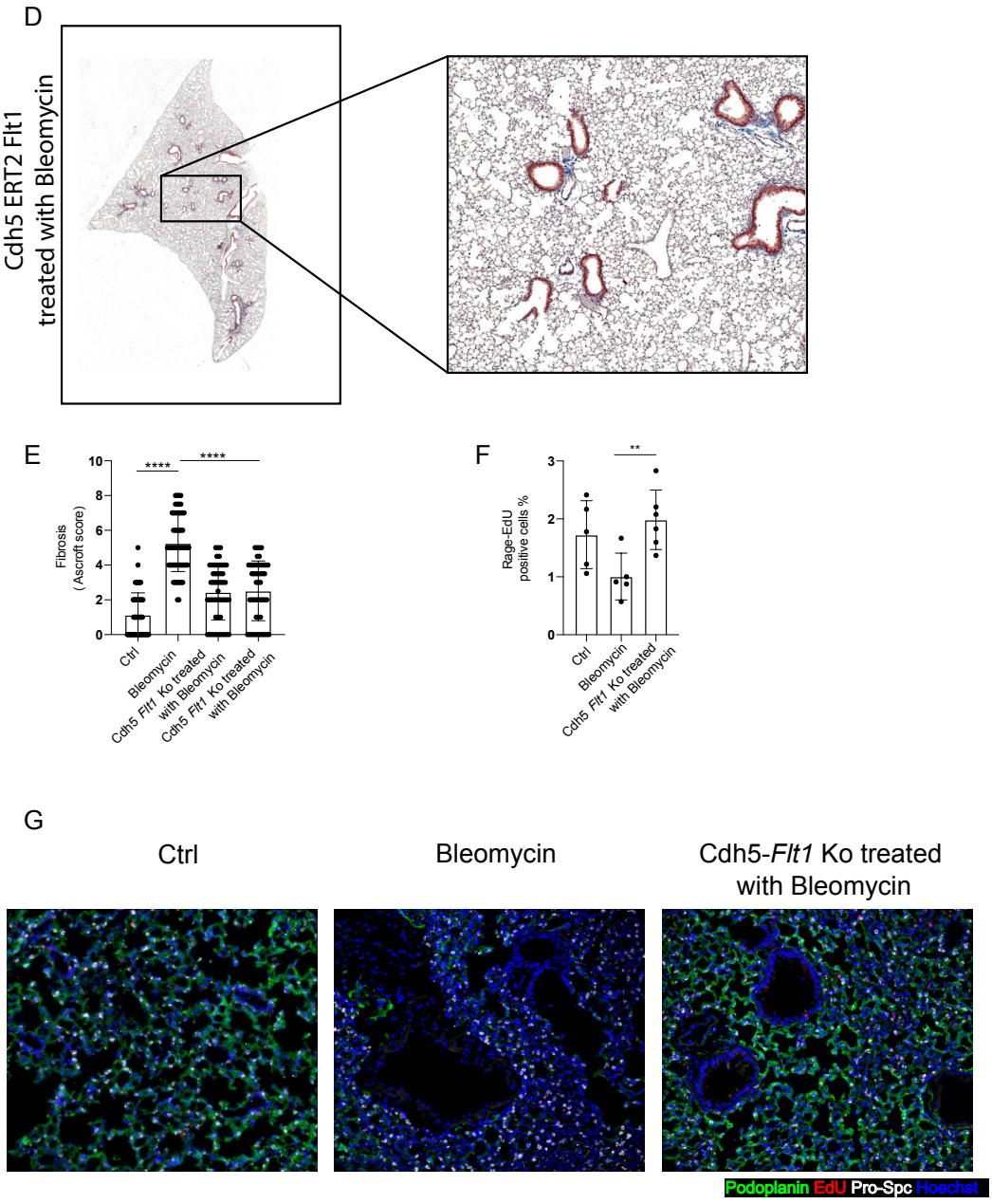

Figure 25: ***Endothelial Flt1 depletion rescued bleomycin-induced fibrosis in vivo.*** *Representative images of Masson Trichrome stained lungs harvested from control mice (15A), bleomycin treated mice (15B) and Cdh5 ERT2 Flt* $^{flox/flox}$ *mice treated with bleomycin (15C; 15D). High magnifications are shown for each image. 15E) Quantification of the fibrotic area was performed using the Ashcroft score. 15F) Quantification of cells expressing Rage-EdU was performed. 15G) Representative immunofluorescence images of lung section from ctrl, bleomycin and Cdh5 ERT2 Flt* $^{flox/flox}$ *mice treated with bleomycin stained for Podoplanin (green), EdU (red), Pro-Spc (white) and with nuclear marker dye Hoechst (blue). All data are shown as mean ± S.E.M. Statistical significance was determined using a one-way ANOVA followed by Dunnett's multiple comparison test, *P < 0.05, ****P < 0.0001.*

4.9 Proteomic analysis revealed that the depletion of *Flt1* leads to matrix remodelling

To better study the molecular mechanism behind the antifibrotic effect of *Flt1* KO in endothelial cells and to identify differentially secreted factors that could modulate trans-differentiation of ATII cells, we performed a mass spectrometry analysis on the secretome of Cdh5 ERT2 Flt1$^{flox/flox}$ and WT endothelial cells. They were harvested from Cdh5 ERT2 Flt1$^{flox/flox}$ and seeded without FBS supplement for 3 days. Thereafter, supernatant of WT and Cdh5 ERT2 Flt1$^{flox/flox}$ endothelial cells were filtered and purified, and mass spectrometry (LC-MS/MS) was performed. Peptides were analyzed using the Mus musculus FASTA file. Proteins were identified using MASCOT search engine with a mass tolerance of 10 ppm for precursor 0.6 Da for products. A total of 819 proteins were identified in the endothelial cells from *Flt1* Ko compared to controls. Among the 819 proteins, we identified 772 downregulated and 47 upregulated. A volcano plot revealed differential expressed proteins between WT and *Flt1* Ko endothelial cells showing a strong decrease of protein expression in the *Flt1* Ko endothelial cells in comparison with the controls (Fig. 16A). As we hypothesized that *Flt1* expression is reducing the production and secretion of angiocrine factors, we focused our attention only on upregulated proteins. Next, we performed functional annotations to visualize the enrichment of biological function using the Ingenuity Pathway analysis that exploits gene set databases (Fig. 16B). Our results were filtered with absolute value of Z-score >1. Then, we performed a protein cell localization filtration of up-regulated proteins for selecting only secreted proteins (Fig.16C). Finally, the list of proteins was filtered using previous RNAseq dataset (Gillich et al., 2020) to exclude proteins lacking a corresponding receptor on ATII cells. We selected only proteins with fold change >1.5 (Fig. 16D). Our enrichment analysis showed that the upregulated proteins are mainly related to cell movement, CCR2, inflammatory response, wound healing signaling pathways and growth of epithelial cells. To further our understanding of the regulatory role of these pathways in ATII trans-differentiation, all upregulated proteins were used to build a regulatory network using String software. The result demonstrated that these screened upregulated proteins formed a complex regulatory network in which several interactions were found to be important hubs and were implicated in the activation of ATII cells, such as the upregulation of Serpinc1 and Haptoglobin, both proteins that are downregulated in IPF patients.

A

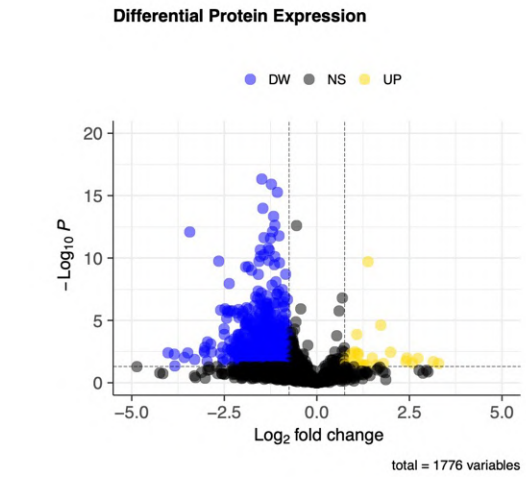
Differential Protein Expression
DW
NS
UP
20
15
10
5
0
−Log10 P
−5.0
−2.5
0.0
2.5
5.0
Log2 fold change
total = 1776 variables

B

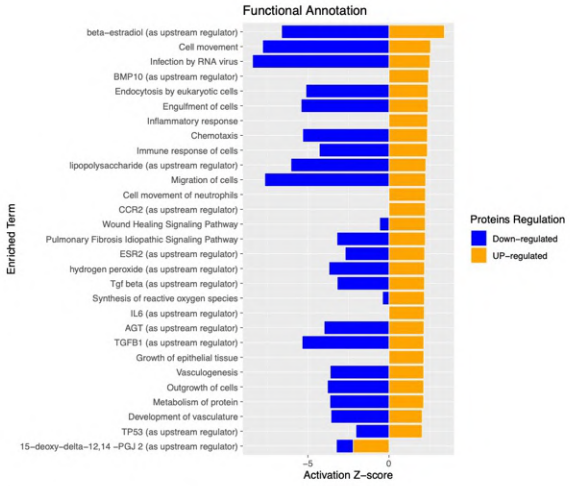
Functional Annotation
beta−estradiol (as upstream regulator)
Cell movement
Infection by RNA virus
BMP10 (as upstream regulator)
Endocytosis by eukaryotic cells
Engulfment of cells
Inflammatory response
Chemotaxis
Immune response of cells
lipopolysaccharide (as upstream regulator)
Migration of cells
Cell movement of neutrophils
CCR2 (as upstream regulator)
Wound Healing Signaling Pathway
Pulmonary Fibrosis Idiopathic Signaling Pathway
ESR2 (as upstream regulator)
hydrogen peroxide (as upstream regulator)
Tgf beta (as upstream regulator)
Synthesis of reactive oxygen species
IL6 (as upstream regulator)
AGT (as upstream regulator)
TGFB1 (as upstream regulator)
Growth of epithelial tissue
Vasculogenesis
Outgrowth of cells
Metabolism of protein
Development of vasculature
TP53 (as upstream regulator)
15−deoxy−delta−12,14 −PGJ 2 (as upstream regulator)
Enriched Term
−5
0
Activation Z−score
Proteins Regulation
Down−regulated
UP−regulated

C

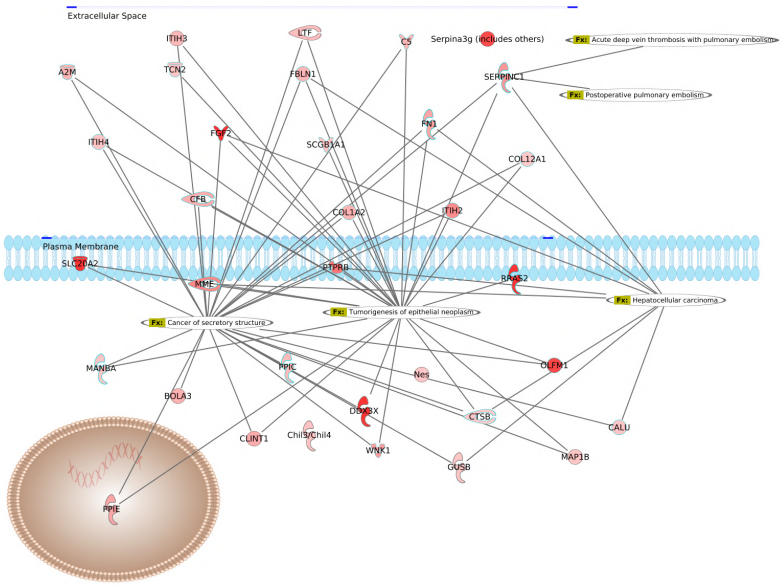

D

Col2A1
Vegf-A
Fgf2
Col3A1
Itih2
Mmp2
Haptoglobin
SerpinC1

*Figure 26**: Proteomic analysis of the Flt1 Ko endothelial cells**. 16A) Volcano plot displaying differential expressed proteins between control cells and treated cells. The vertical axis (y-axis) corresponds to the mean expression value of log 10 (q-value), and the horizontal axis (x-axis) displays the log 2-fold change value. The yellow dots and the blue dots represent the proteins whose expression is differential expressed. Positive x-values represent up-regulation log fold change >0.75 and negative x-values represent down-regulation (log fold change < -0.75). Grey/black dots represent the proteins whose expression is not differential expressed. 16B) Functional annotations graph represent the enrichment of the biological terms based on the activation Z-score (x axis), as calculated by the Ingenuity Pathway analysis; this tool provides a large collection of gene set databases. All the terms have multiple test correction adjusted $p < 0.05$. The orange bars and the blue bars represent the activation z-score of the specific term derived by the proteins whose expression is differential up-regulated and down-regulated, respectively. 16C) Cell localization of up-regulated proteins in terms of cellular compartments. 16D) List of upregulated proteins connected with ATII cells.*

4.9.1 Serpinc1, Haptoglobin and Itih2 could have a positive role in promoting trans-differentiation of ATII cells

To validate the findings from the proteomics study, 8 upregulated proteins (Col2a1, Vegf-a, Fgf2, Col3a1, Itih2, Mmp2, Hp and Serpinc1) were selected (Fig.16D). For the over-expression experiment, we transfected Hek-293T cells with specific plasmids. Transfection of GFP was performed as a positive control. After 48h, the supernatant was centrifuged and added to fresh isolated ATII cells harvested from bleomycin mice. The supernatant of GFP was added to ATII cells as negative control. The EdU was added into the medium in the same day in order to track the trans-differentiation. After 4 days, cells were fixed, and immunofluorescence staining was performed. Results revealed that only three proteins as SerpinC1, Itih2 and Haptoglobin can rescue the pathological trans-differentiation of ATII cells (Fig. 17A). Moreover, proteomics analysis showed the increase of Collagen2A1 and Collagen3A1. In order to validate these two proteins, we cultured and transfected 3T3-NIH cells for several days to secrete Col2a1 and Col3a1. When the matrix was decellularized, ATII cells from bleomycin mice were harvested and seeded on the top of the new matrix for 5 days. Results showed that both Col2a1 and Col3a1 failed in inducing trans-differentiation of ATII cells, resulting in an unfavorable matrix for ATII growth and activation (Fig.17B). However, these data are preliminary results, other experiments will be performed in order to validate the effect of these proteins in promoting ATII trans-differentiation.

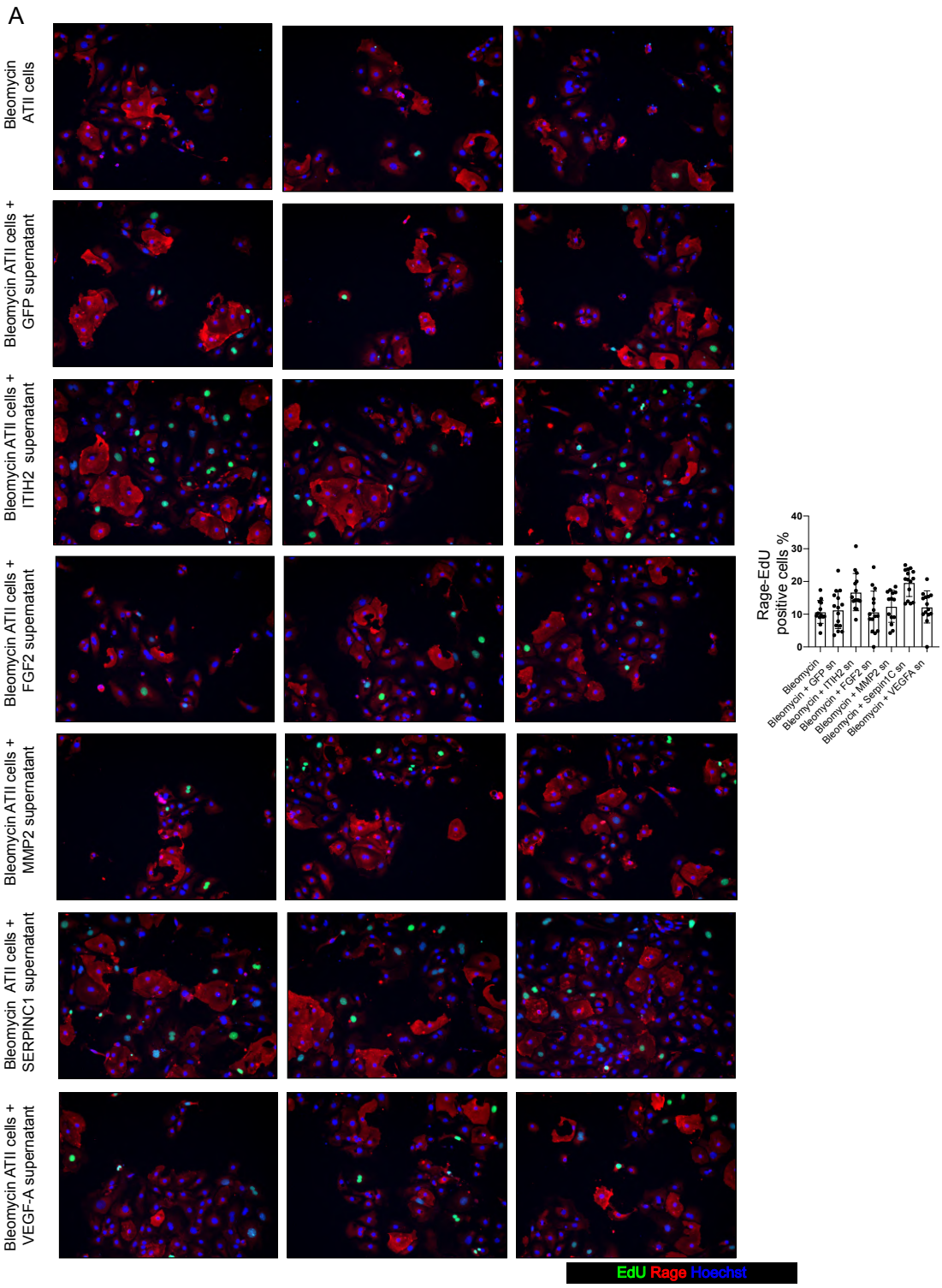
A
Bleomycin ATII cells
Bleomycin ATII cells + GFP supernatant
Bleomycin ATII cells + ITIH2 supernatant
Bleomycin ATII cells + FGF2 supernatant
Bleomycin ATII cells + MMP2 supernatant
Bleomycin ATII cells + SERPINC1 supernatant
Bleomycin ATII cells + VEGF-A supernatant
EdU Rage Hoechst
Rage-EdU positive cells %
40
30
20
10
0
Bleomycin
Bleomycin + GFP sn
Bleomycin + ITIH2 sn
Bleomycin + FGF2 sn
Bleomycin + MMP2 sn
Bleomycin + Serpin1C sn
Bleomycin + VEGFA sn

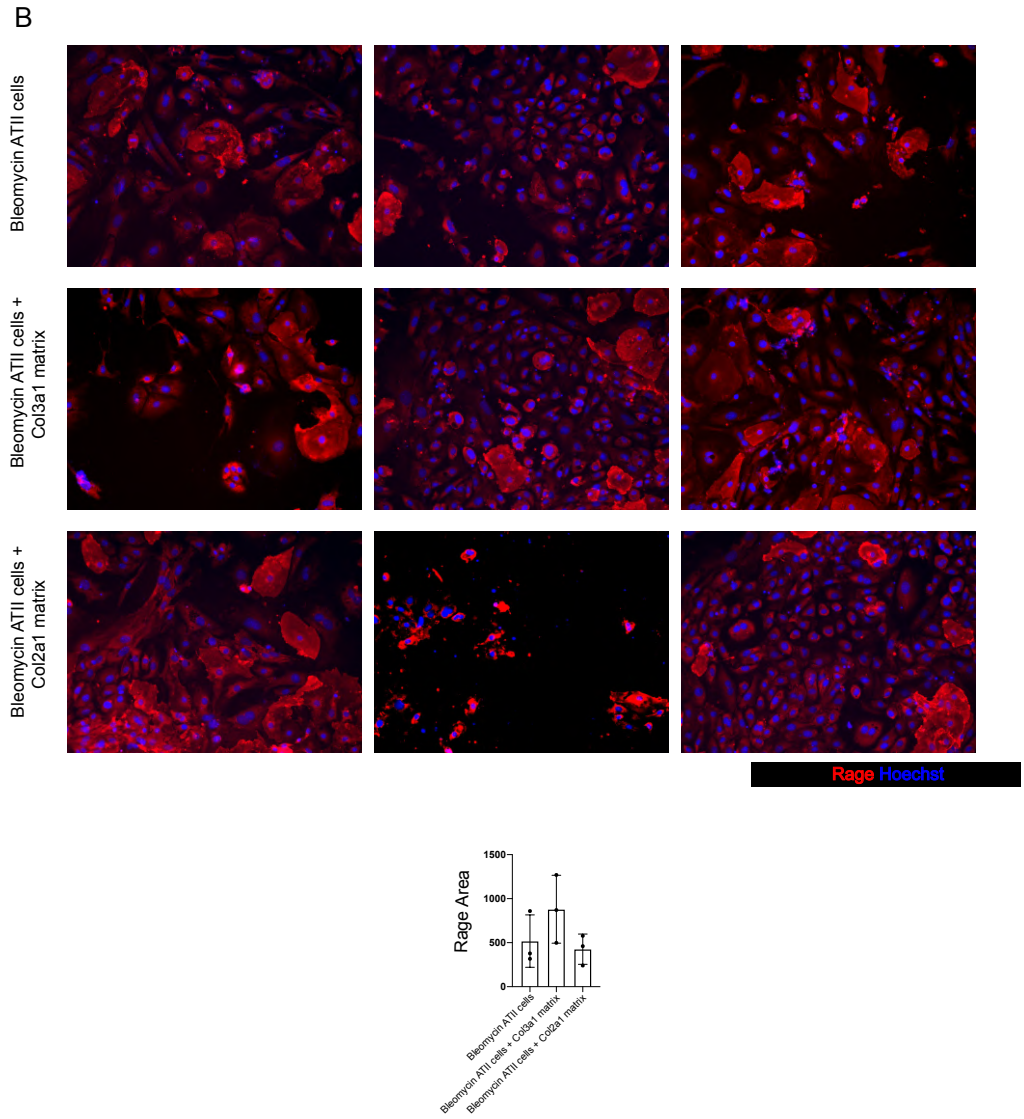

Figure 27: Validation of secreted proteins upregulated in Flt1 Ko endothelial cells. 17A) Representative immunofluorescence images of bleomycin ATII cells treated with supernatant overexpressing GFP, ITIH2, FGF2, MMP2, SERPINC1 and VEGF-A and stained for EdU (green), Rage (red) and with nuclear marker dye Hoechst (blue). Quantification of cells expressing Rage-EdU was performed. 17B) Representative immunofluorescence images of bleomycin ATII cells seeded on GFP, Col3a1 and Col2a1 matrix stained for Rage (red) and with nuclear marker dye Hoechst (blue). Quantification of area of Rage cells was performed.

4.10 Epithelial and endothelial crosstalk in lung regeneration

4.10.1 A mouse model of lung regeneration induced by pneumectomy

We adopted a mouse model of pneumonectomy (PNX) to study epithelial-endothelial crosstalk during lung regeneration. Mice underwent left PNX and EdU was injected intraperitoneally after 2 days to label proliferating cells (Fig. 18A). At day 8 post-PNX, right lobes were harvested, separated and stained for EdU and with nuclear marker Hoechst (Fig. 18B). Quantification of EdU positive cells showed that each lobe had a peculiar proliferation capacity, with the fourth lobe, known as the accessory lobe, being the most proliferative one.

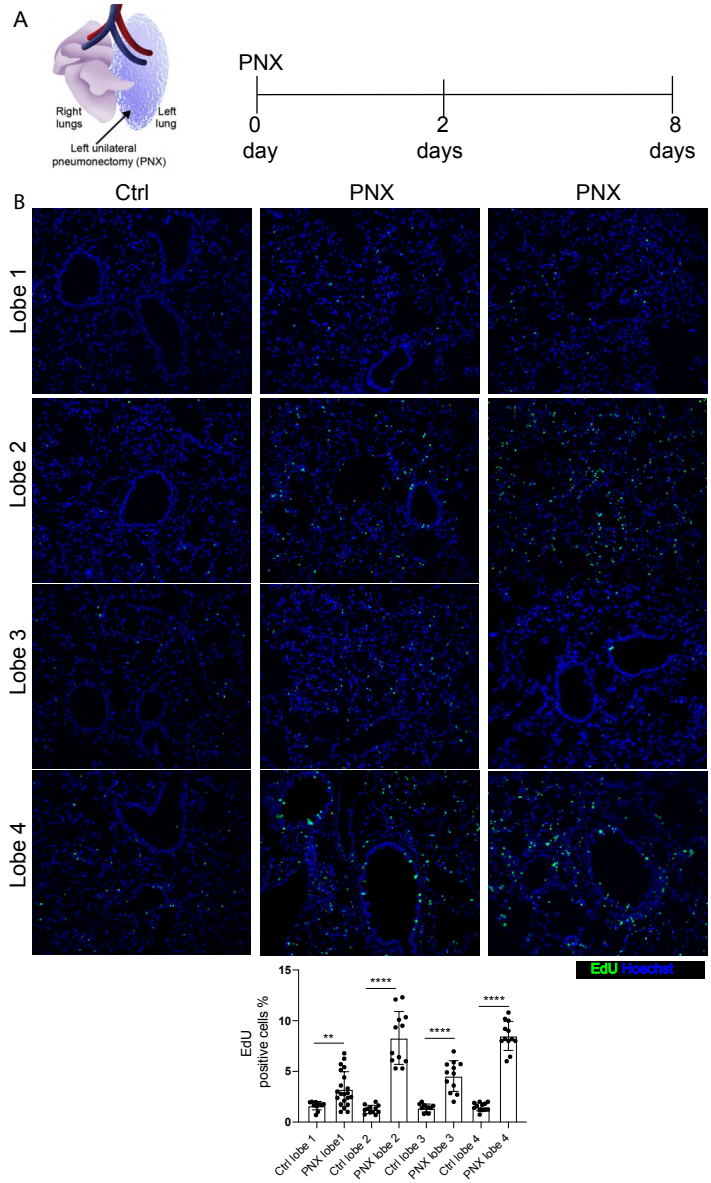

*Figure 28: **PNX surgery leads to lung regeneration**. 18A) Schematic representation of PNX experiment. 18B) Representative immunofluorescence images of tissue section harvested from control and PNX mice stained for EdU (green) and with nuclear marker dye Hoechst (blue). Quantification of cells expressing EdU was performed. All data are shown as mean ± S.E.M. Statistical significance was determined using a one-way ANOVA followed by Dunnett's multiple comparison test, *P < 0.05, ****P < 0.0001.*

To investigate which cells start proliferating early after PNX, mice were sacrificed 3 days after the surgical procedure (Fig 19A) and EdU was injected 24h before tissue collection. We stained both endothelial cells, marked in white, and epithelial cells, marked in green. The endothelial proliferating cells are highlighted by yellow circles (Fig 19B). Results indicated that 3 days after PNX, proliferating Erg-EdU positive cells were significantly increased, whereas we could not detect an increase in Podoplanin-EdU positive cells (Fig.19B).

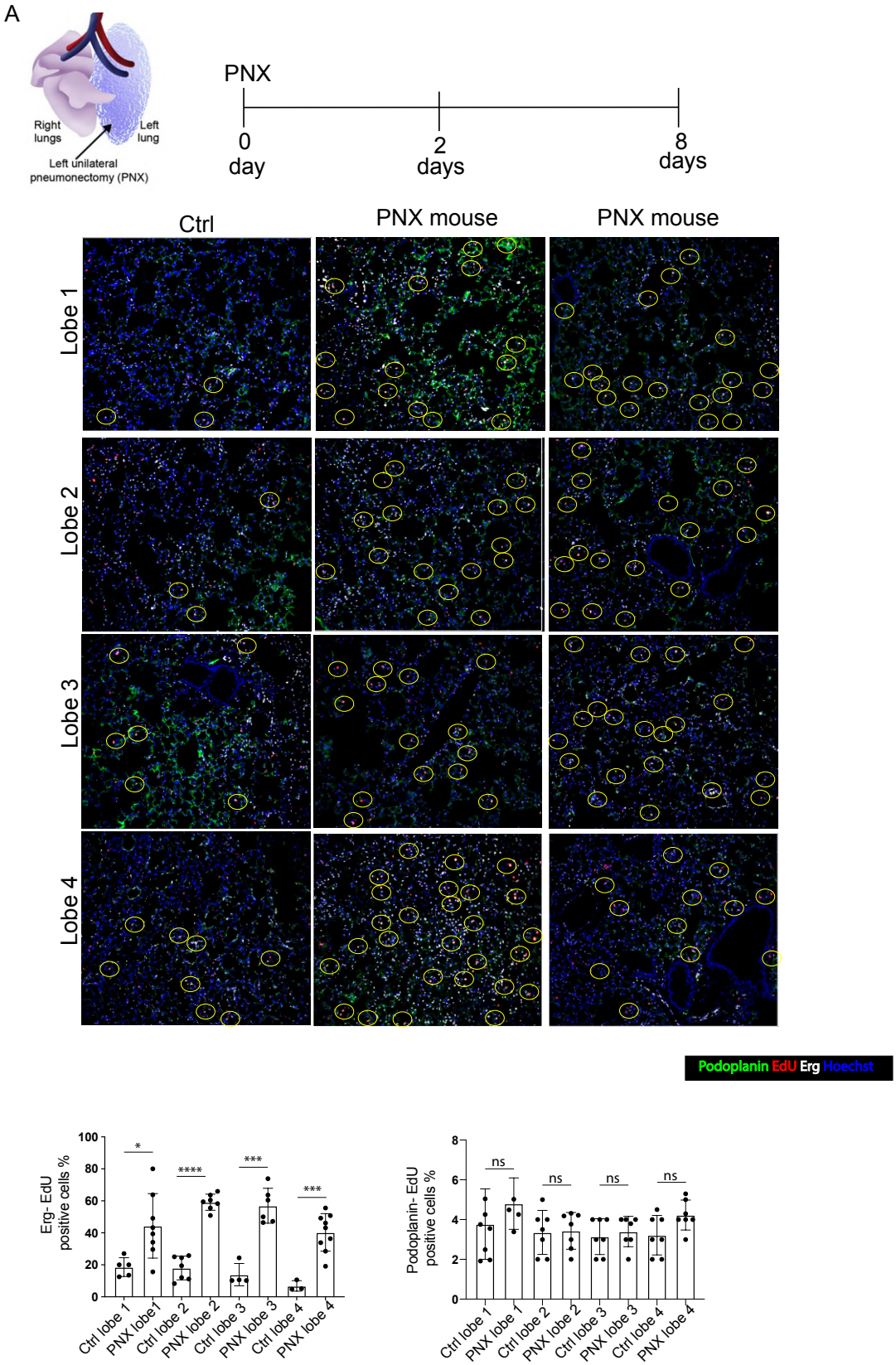

Figure 29: ***Endothelial cells drive the activation of Alveolar Epithelial Cells****. 19A) Schematic representation of the PNX experiment after 3 days. 19B) Representative immunofluorescence images of tissue section harvested from control and PNX mice stained for Podoplanin (green), EdU (red), Erg (white) and with nuclear marker dye Hoechst (blue). Erg-EdU positive cells were highlighted with yellow circles. Quantification of cells expressing Erg-Edu and Podoplanin-EdU was performed. All data are shown as mean ± S.E.M. Statistical significance was determined using a one-way ANOVA followed by Dunnett's multiple comparison test, *P < 0.05, ****P < 0.0001.*

Next, we evaluated mice that were sacrificed 8 days post-PNX, with EdU administration 24h before tissue collection (Fig.20A). Endothelial proliferating cells are again highlighted by yellow circles and epithelial cells by purple circles. Interestingly, at 8 days after PNX, also epithelial cells start to proliferate (Fig.20B).

In conclusion, these results suggest that during alveologenesis endothelial cells first sense the stimulus and start proliferating, while epithelial cells react later.

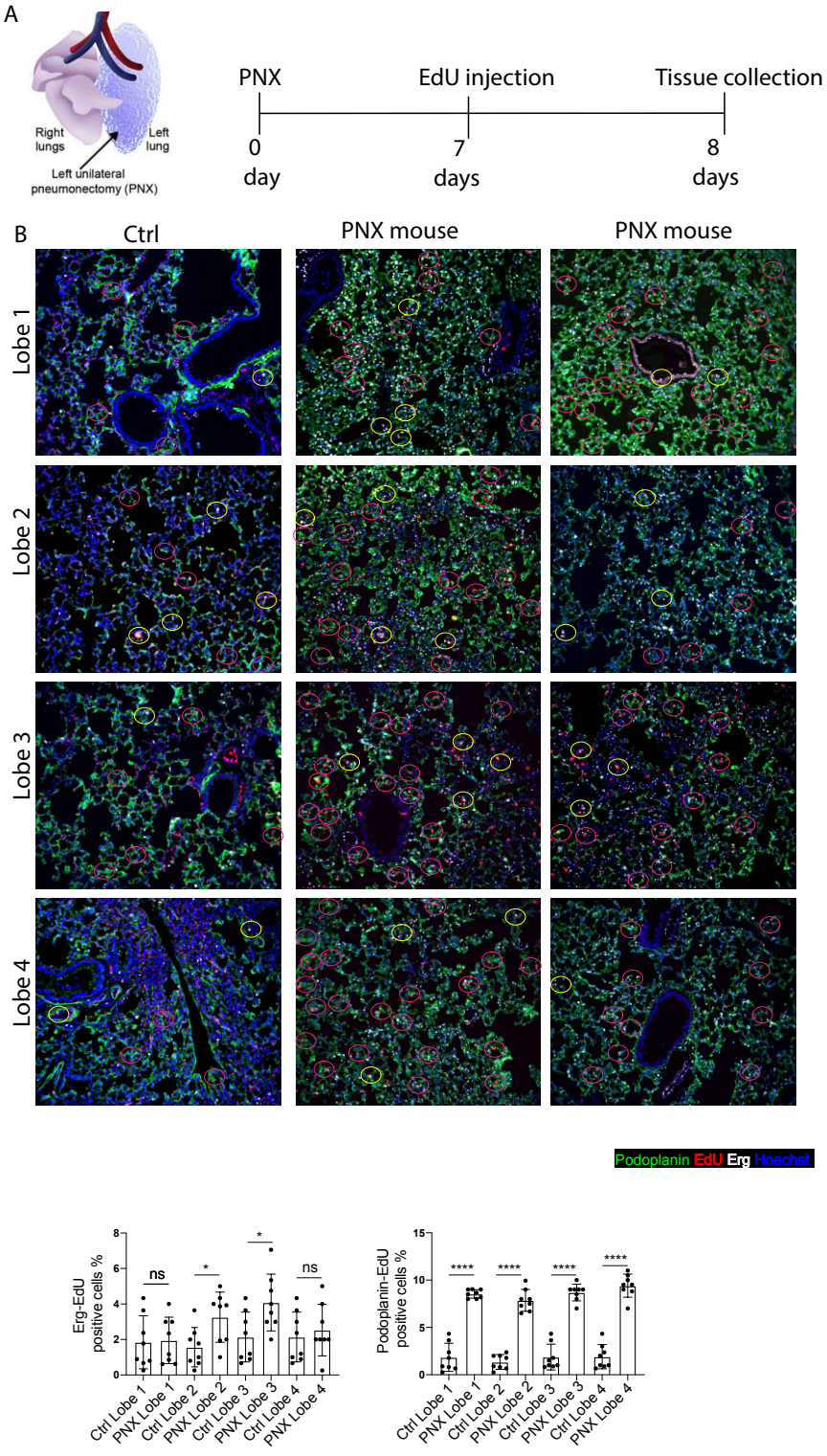

Figure 30: ***Endothelial cells drive the activation of Alveolar Epithelial Cells****. 20A) Schematic representation of the PNX experiment after 3 days. 20B) Representative immunofluorescence images of tissue section harvested from control and PNX mice stained for Podoplanin (green), EdU (red), Erg (white) and with nuclear marker dye Hoechst (blue). Erg-EdU positive cells were highlighted with yellow circles, whilst Podoplanin-EdU positive cells were highlighted in purple. Quantification of cells expressing Erg-Edu and Podoplanin-EdU was performed. All data are shown as mean ± S.E.M. Statistical significance was determined using a one-way ANOVA followed by Dunnett's multiple comparison test, *P < 0.05, ****P < 0.0001.*

4.10.2 Endothelial tip cells are required in the ATII cells activation

Activated endothelial cells express abundant levels of Apelin, which is a secreted peptide that acts as an endogenous ligand for the human G protein-coupled receptor APJ (Kocijan et al., 2021). Apelin is expressed during embryonic development, whilst in the adulthood, the levels of Apelin are reduced. However, in response to angiogenic stimuli, as it happens after PNX, Apelin expression is reactivated particularly by tip cells, which in turn induce stalk cell proliferation during sprouting angiogenesis (Kocijan et al., 2021). To experimentally confirm that endothelial cells drive alveolar epithelial cell activation, we used a genetic lineage tracing approach. In this model, the Tamoxifen-inducible form of the Cre recombinase (CreER) is expressed under the control of the Apelin (Apln) promoter (Fig. 21A). By crossing these mice with mTmG reporter mice, Cre activation results in a shift from red to green fluorescence specifically in sprouting endothelial cells. In these double transgenic mice, we performed PNX surgery, followed by intraperitoneal EdU administration. Lungs were harvested after 4 days (Fig. 21B). Immunofluorescence analysis showed a significant increase of Apln-EdU positive cells at early time points (Fig. 21C; 21D), indicating that endothelial cells are activated early after PNX and possibly drive the activation of alveolar epithelial cells during lung regeneration.

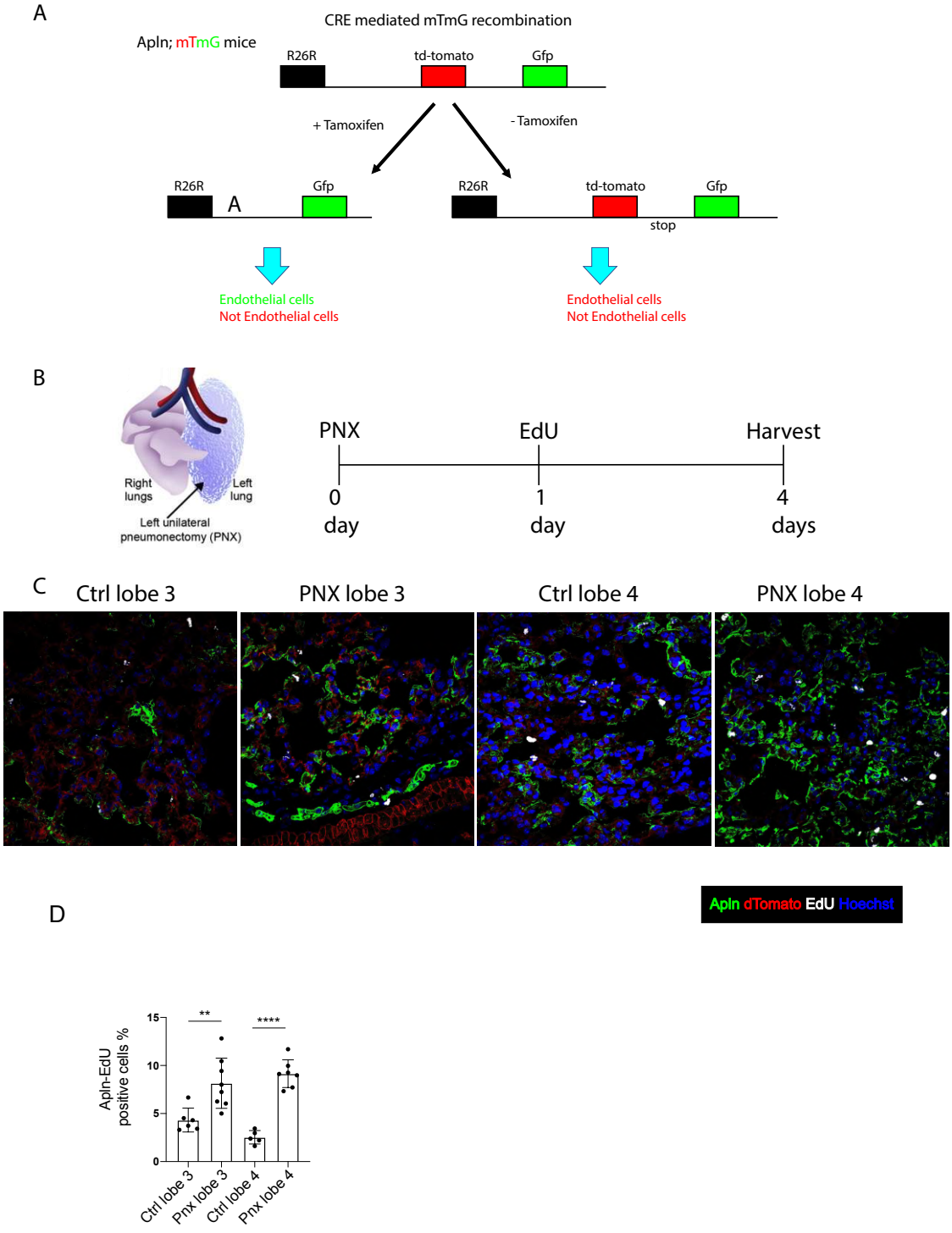

*Figure 31: **Endothelial tip cells are activated 3 days after PNX surgery**. 21A) Representative scheme of Apln genetic lineage tracing mouse model. 21B) Schematic representation of the PNX experimental plan after 4 days from PNX surgery. 21C) Representative immunofluorescence images of tissue section harvested from control and PNX mice showing Apln (green), dTomato (red), EdU (white) and nuclei were stained with nuclear marker dye Hoechst (blue). 21D) Quantification of cells expressing Apln-EdU was performed. All data are shown as mean ± S.E.M. Statistical significance was determined using a one-way ANOVA followed by Dunnett's multiple comparison test, *P < 0.05, ****P < 0.0001.*

4.10.3 Endothelial *Flt1* depletion induces lung regeneration *in vivo*

Finally, we investigated whether *Flt1* depletion in endothelial cells affected lung regeneration in vivo. Inducible *Flt* knockout Cdh5 ERT2 Flt $^{flox/flox}$ mice were treated with tamoxifen and after 1 week they underwent PNX. After six additional days, when an expansion of proliferating alveolar epithelial cells was expected, mice received EdU intraperitoneally (Fig. 22A). Lobes were collected separately after 2 additional days and processed for immunofluorescence staining. *Flt1* knockout mice showed a significant increase in both Pro-Spc-EdU positive and Podoplanin-EdU positive cells after PNX, compared to controls (Fig. 22B). Furthermore, to assess whether depletion of *Flt1* in endothelial cells affected ATII cell trans-differentiation, we analyzed the ratio between ATII and ATI cells. Cdh5 ERT2 Flt $^{flox/flox}$ mice showed an increased number of ATI cells compared to ATII cells, suggesting that the depletion of *Flt1* in endothelial cells has driven the activation and the trans-differentiation of alveolar epithelial cells.

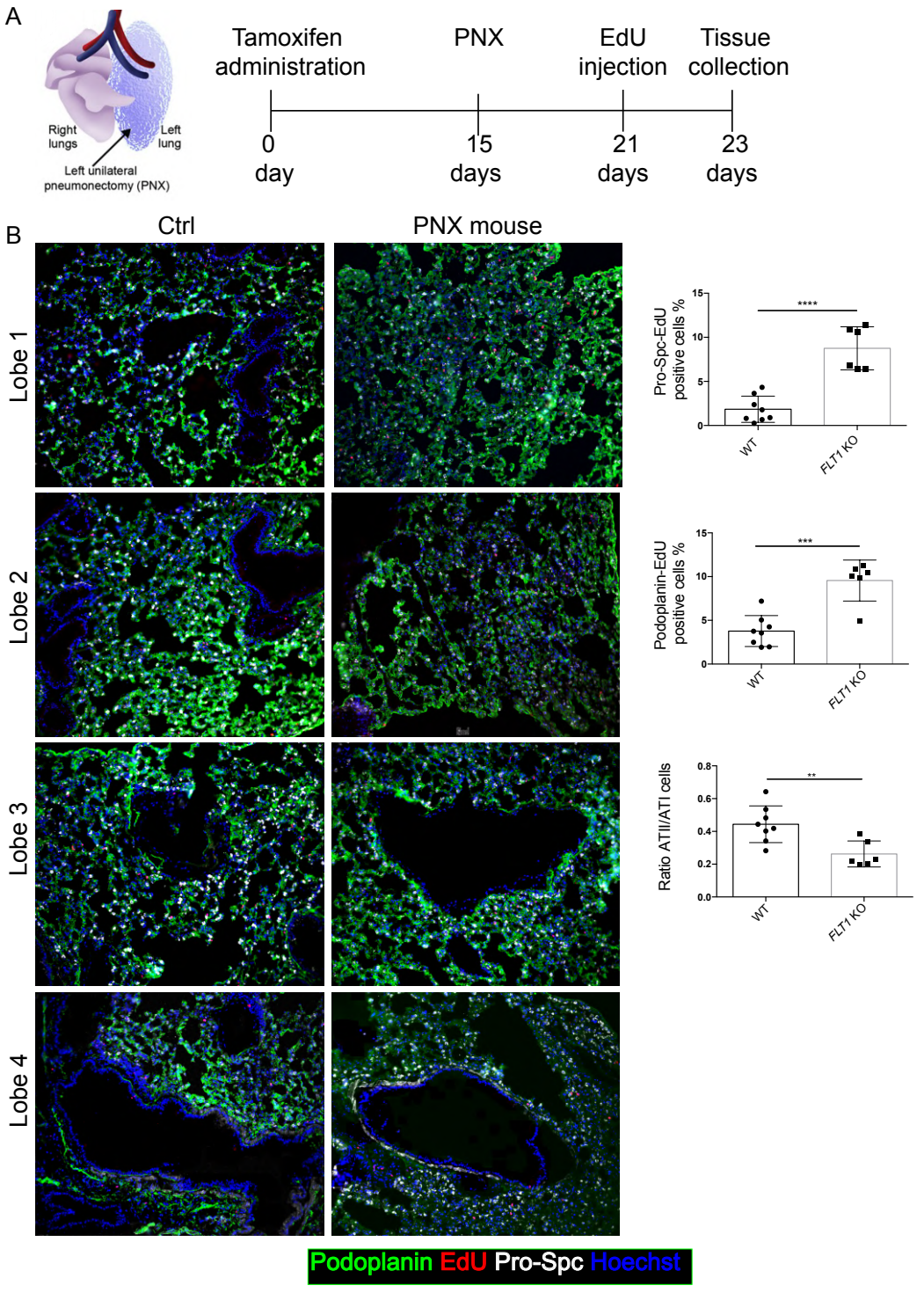

Figure 32: ***Endothelial Flt1 depletion induces lung regeneration in vivo.*** *22A) Schematic representation of the PNX experiment after 8 days PNX surgery for Cdh5 ERT2 Flt* $^{flox/flox}$ *mice. 22B) Representative immunofluorescence images of tissue section harvested from control and PNX mice stained for Podoplanin (green), EdU (red), Pro-Spc (white) and with nuclear marker dye Hoechst (blue). Quantification of Pro-Spc-EdU, Podoplanin-EdU and the ratio between ATI and ATII cells was performed. All data are shown as mean ± S.E.M. Statistical significance was determined using a one-way ANOVA followed by Dunnett's multiple comparison test, *P < 0.05, ****P < 0.0001.*

5. DISCUSSIONS

5.1 Characterization of primary human and murine ATII cells

Idiopathic pulmonary fibrosis (IPF) is a devastating progressive fibrotic lung disease characterized by a decline in lung function and early mortality. The pathogenesis of fibrosis development is very complex and includes repetitive damages, disequilibrium of pro-fibrotic mediators and loss of alveolar type II (ATII) cells (Wolters et al., 2014; Ahluwalia et al., 2014; Parimon et al., 2020; Salton et al., 2020). Moreover, there are no major data about the critical drivers of disease onset and its progression (Lehmann et al., 2018; Nemeth et al., 2020). It is known that lung fibrosis starts from the distal portion of the lung, spreading in the center and leading to a loss of the alveolar structures. However, the origin of this dysfunction in the distal lung epithelium remains unclear due to the absence of relevant human and murine model systems (Schruf et al., 2020).

Recent studies suggest that ATII cells may play a central role in the pathogenesis of IPF due to the loss of regenerative potential (Naikawadi et al., 2016; Barkauskas and Noble., 2014; Camelo et al., 2014). During lung injury, ATI cells die, resulting in increased epithelial permeability, and ATII cells re-epithelialize the alveolar surface via proliferation and trans-differentiation into ATI cells (Barkauskas et al., 2013). Conversely, in IPF lungs, ATII cells cannot trans-differentiate to ATI cells, which leads to the parenchyma destruction and lung fibrosis (Salton et al., 2020).

In this PhD thesis we characterized human and murine ATII cells harvested both from explanted lungs of patients with IPF and from bleomycin-induced lung fibrosis in mice. Our results showed that ATII cells, harvested from both IPF and bleomycin-treated lungs, displayed reduced expression levels of ATI cell markers. Indeed, several studies support the evidence that multiple insults to the lung tissue followed by inadequate repair due to abnormal response of ATII cells may trigger IPF onset (Uhal et al., 2017; Jablonski et al., 2017).

The main trigger for the pathological activation of ATII cells remain unclear, nevertheless aging processes have been shown to induce a specific phenotype that is characterized by replicative arrest and the aberrant secretion of pro-fibrotic and pro-inflammatory senescence-associated factors. All these pathways lead to the aberrant activation of EMT pathways in the alveolar epithelium, which leads to pneumocyte loss,

myofibroblast accumulation and therefore lung fibrosis (Moimas et al., 2019). Our data, in line with the literature, showed that ATII cells from both human and murine models displayed higher levels of senescence and EMT markers, confirming the hypothesis that ATII cells in IPF are exhausted and inactivated (Parimon et al., 2020; Reyfman et al., 2019; Parimon et al., 2019; Raredon et al., 2019).

Furthermore, we cultured ATII cells derived from IPF and bleomycin-treated lungs in trans-differentiating conditions. Our results revealed that ATII cells from both IPF and bleomycin-treated lungs cultured in trans-differentiating conditions displayed reduced expression levels of ATI cell markers, consistent with impaired trans-differentiation capacity in either case. Our observation is supported by published data where single-cell RNA sequencing was used to demonstrate that human epithelial cells from IPF lungs have an impaired trans-differentiation program that leads to a lack of lung renewal and regeneration (Xu et al., 2016).

5.2 The anti-fibrotic effect of miR-200c

Since the molecular and cellular mechanism of alveolar repair in IPF remain enigmatic, in this work we aimed to identify mechanisms that drive lung regeneration by using a lung injury IPF mouse model. Recent studies have shown that the expression of certain miRNAs correlate with the pathological mechanisms of lung fibrosis, including lung epithelial repair, epithelial-mesenchymal transition, alveolar epithelial cells and collagen production (Pandit et al., 2015; Takagi et al., 2019; Miao et al., 2018). Indeed, the downregulation of multiple miRNAs is associated with initiation and progression of IPF (Pandit et al., 2018), making miRNAs an interesting therapeutic tool for IPF. In particular, the miR-200 family members are known to be downregulated in IPF and in bleomycin-induced lung fibrosis, especially in fibrotic alveolar epithelial cells (Yang et al., 2013). Pecot and colleagues showed that miR-200 family members could stop the progression of experimental fibrosis (Pecot et al., 2013). Indeed, in a previous publication, we showed that the transfection of specific family members (miR-200c and miR-200b) is able to restore trans-differentiation impairment of human IPF ATII cells to ATI cells (Moimas et al., 2019).

One proposed mechanism for this effect was linked to the finding that the overexpression of miR-200b and miR-200c in human fetal lung activates trans-differentiation of epithelial alveolar cells by targeting ZEB1 and ZEB2, the main markers of the EMT

process (Benlhabib et al., 2015). Indeed, ZEB proteins are part of a double-negative feedback loop with miR-200 family members, which prevent EMT during repair and promote tissue regeneration after injuries (Kolesnikoff et al., 2014). In contrast, the work performed for this thesis shows that while miR-200c and miR-200b block EMT and increase trans-differentiation, miR-200a blocks EMT but does not increase trans-differentiation. This novel finding suggests that the inhibition of the EMT process is not sufficient to activate ATII cells and thereby promote lung regeneration.

Despite the mechanism being unclear, miR-200 family members represent an intriguing biotherapeutic. However, a potential drug delivery system to administer miRNAs effectively to patients is not yet optimized (Dua et al., 2017). Moreover, there are some limitations associated with miRNA delivery, including poor intracellular delivery, insufficient gene silencing and various off-target effects, degradation and elimination of miRNAs by nuclease, renal clearance and phagocytosis by immune cells. Despite that, several pre-clinical and clinical trials have been up and running to validate the capacity of miRNAs in improving respiratory diseases (Dua et al., 2017).

To address the issue of therapeutic miRNA delivery, we assessed an *in vivo* aerosol-mediated method to deliver naked miRNAs (not complexed with lipids) to ATII cells, by using a fluorescent miRNA as a proof of concept for therapeutic delivery. To attempt this technique in a therapeutic approach, we moved to miR-200c, which has been shown to regulate ATII cell physiology during IPF (Yang et al., 2013). We successfully administered naked miR-200c and were able to prevent, as well as reverse lung fibrosis in mice. We observed that miR-200c, delivered both prior to the induction of fibrosis and when it is well established, was able to significantly attenuate bleomycin-induced pulmonary fibrosis. These findings clearly demonstrate that aerosol-delivery of not complexed naked small RNAs is a feasible therapeutic strategy.

5.3 *Flt1*, a known target of miR-200c.

The main and most-studied targets of miR-200c are *ZEB1* and *ZEB2* genes, known markers of the EMT process. We showed that miR-200c can act directly on ATII cells, downregulating the expression of *ZEB1* and *ZEB2* and increasing the trans-differentiation. However, afterwards EMT, miR-200c is also involved in inhibiting cell proliferation, cell cycle control, apoptosis, as well as cancer invasion and metastasis. Moreover, as discussed above, the activation of ATII cells is independent of the

suppression of EMT. This indicates the involvement of further targets beyond *ZEB1* and *ZEB2*. In fact, another well described target of miR-200c which is involved in cell growth and proliferation is *Flt1*. This is a tyrosine kinase receptor, which is mainly expressed in endothelial cells. It acts as a decoy soluble receptor that sequesters VEGF-A ligand from VEGFR2, thereby inhibiting endothelial proliferation (Rajasekaran et al., 2015). In addition, *Flt1* is important for endothelial cell maintenance and vascular organization (Amano et al., 2019). We hypothesized that miR-200c rescues trans-differentiation of ATII cells indirectly by downregulating *Flt1* in endothelial cells and increasing the activation of VEGFR2. As consequence, this event could lead to a production of secreted proteins that could help the activation of pathological ATII cells.

While a role of *Flt1* in lung fibrosis has been shown previously, to our knowledge the importance of *Flt1* in the impact of miR-200c has never been explored. However, recent studies have shown a role of miR-200c in angiogenesis, especially in cancer studies (Pecot et al., 2013; Li et al., 2015). In human embryonic stem cells, miR-200c was shown to be essential for the activation of endothelial cells and for *in vivo* vasculogenesis and matrix remodeling, reducing endothelial cell migration and tube formation (Luo et al., 2013). Since miR-200c plays an essential role in modulating EMT, angiogenesis and matrix remodeling, we next explored whether the effect of down-regulation of *Flt1* in endothelial cells could be relevant in reducing the onset of lung fibrosis.

5.4 The crosstalk between alveolar type II cells and alveolar endothelial cells

ATI cells and alveolar endothelial cells are essential for performing gas exchange in the alveoli structure (Gillich et al., 2020). Upon injury in rodents, it has been demonstrated that there is rapid proliferation in the microvasculature, with expansion of resident alveolar endothelial cells (Alvarez et al., 2008). However, the role of alveolar endothelial cells in promoting alveolar regeneration after damage is incompletely understood. We showed that the expression of *Flt1* in endothelial cells could be a negative regulator of self-renewal in a model of induced-lung fibrosis in mice. Moreover, the preventative depletion of *Flt1* in endothelial cells was able to reduce the onset and progression of lung fibrosis in mice in our hands. To our knowledge the importance played by *Flt1* in the dysfunction of ATI cells in fibrosis is a novel finding of this thesis.

A recent study showed that the development of lung fibrosis is dependent on endogenous *Flt1* signaling (Amano et al., 2019). This study demonstrated that the *Flt1* pathway drives

the up-regulation of SDF-1 and CXCR4 in the lung, resulting in an aberrant angiogenesis and fibrosis formation (Amano et al., 2019). Other studies showed that the expression of *Flt1* was significantly increased in the early phase of bleomycin-induced fibrosis (Barratt et al., 2019). In our study, we indicated that the endothelial cell specific depletion of *Flt1*, as well as the therapeutic administration of miR-200c, can both reduce the formation of fibrosis *in vivo*. We showed increased fibrotic areas, fibrosis percentage and disruption of alveolar structure and loss of ATII cells in bleomycin-treated wild-type mice compared with *Flt1* KO mice that received bleomycin. All these data, that are in line with the literature, suggest that *Flt1* promotes lung fibrosis.

In addition, our co-culture assays showed that secreted factors from *Flt1* KO endothelial cells are able to rescue the pathological phenotype of ATII cells harvested from bleomycin mice, inducing trans-differentiation of ATII cells into ATI cells *in vitro*. Since the role of *Flt1* as an inhibitor of trans-differentiation process is a novel concept, we performed a pilot experiment in which ATII cells were harvested from bleomycin treated *Flt1* KO mice. In fact, ATII cells harvested from bleomycin mice displayed a pathological phenotype with a disrupted cellular shape, and an impairment of trans-differentiation process. In contrast, ATII cells isolated from *Flt1* KO mice treated with bleomycin demonstrated a restored trans-differentiation capacity.

To confirm that the crosstalk between epithelial and endothelial cells was responsible for the improved trans-differentiation, we performed a series of co-culture experiments. To mimic the basal membrane that separate *in vivo* the ATII cells from the endothelial cells, we performed a contacting co-culture. Results showed that when control ATII cells are in contact with endothelial cells WT the trans-differentiation rate does not increase, while a higher trans-differentiation is achieved when ATII cells are in culture with endothelial cells from *Flt1* KO mice. All these data led suggested that secreted proteins released from *Flt1* KO endothelial cells are involved in the trans-differentiation process. Moreover, our data are in line with results obtained from others, in which it has been demonstrated that a disruption of balance between the angiogenic factors modulating blood vessel homeostasis is a crucial factor contributing to the poorly characterized disease IPF (Kalluri and Sukhatme., 2000; Hanumegowda et al., 2012).

5.5 Secretome analysis of *Flt1* KO endothelial cells

The discovery of a pathological molecular mechanism is important for finding a therapy for IPF patients. In order to accurately study the pathological changes occurring during IPF, a proteomics study with a detailed bioinformatic analysis was used. This was able to elucidate dysregulated proteins, pointing us in the direction of possible treatment targets and therapies to cure IPF patients. We applied a LC-MS/MS analysis on the secretome of endothelial cells from *Flt1* KO and WT to identify differentially secreted proteins that could modulate the trans-differentiation of ATII cells. Interestingly, of the significantly differentially expressed proteins, there were 16-fold as many downregulated proteins as there were upregulated proteins. Following our hypothesis that a higher secretion of a specific protein was responsible for improved ATII functionality, we focused our efforts on 8 upregulated factors with corresponding receptors present on ATII cells: Haptoglobin (Hp), Metalloproteinase II (MMP2), SerpinC1, VEGF-A, Fibroblasts Growth Factor II (FGF2), ITIH2, Collagen IIA1 (Col2A1) and Collagen IIIA1 (Col3a1).

Next, we performed an experiment by which we incubated those protein with ATII cells derived from bleomycin-treated and wild-type mice. Importantly, we observed a higher trans-differentiation rate when cells were in contact with Haptoglobin (Hp), SerpinC1 and Itih2. Haptoglobin is an a_2-acid glycoprotein associated to hemoglobin catabolism. It is produced mainly by the liver and secreted into the circulation. Hp increases in plasma during inflammation, infection, trauma and tissue damage (Yang et al., 2003). Hp gene expression can be detected in airway epithelial cells in mice and in alveolar macrophages and endothelial cells (Yang et al., 2003). *Hp* expression in the lung increases several folds upon exposure to inflammatory stimuli and during disease states, suggesting its protective role of the lung tissue (Yang et al., 2003). Moreover, a recent study demonstrated that the Hp expression is reduced in the serum of IPF patients, and it increases after 1-year of Nintedanib treatment (Landi et al., 2020).

Another protein that was efficient in promoting trans-differentiation is SerpinC1. This protein is a regulator of the coagulation cascade, and it is one of the most important serine protease inhibitors in plasma, due its function to inhibit thrombin and other clotting factors (Landi et al., 2020). During acute and chronic lung injury, especially in IPF, it has been shown an abnormal alveolar coagulation, resulting in a pro-clotting state (Collard et al., 2015; Bargagli et al., 2014). In our SerpinC1 protein network analysis, we observed

a predicted connection with Syndecan 1, which is a receptor on the ATII membrane, and it is upregulated in IPF (Parimon et al., 2019). However, other studies need to be performed in order to discover the role of this factor in the rescue of pathological trans-differentiation process.

ITIH2 was the last protein to induce trans-differentiation. It is as serum-derived HA-associated protein (SHAP) and its main function is to regulate the localization, synthesis and degradation of hyaluronan in serum (Lord et al., 2021). Its role in IPF is less characterized, but a study demonstrated that the levels of ITIH2 increased soon after bleomycin administration and decreased during the next 14 days, when the fibrosis was well established (Garantziotis et al., 2008). On the contrary, in proteomic data sets obtained from IPF patients, ITIH2 was found upregulated (Tian et al., 2019; Ahrman et al., 2018). In this study, the interaction networks generated need to be further analyzed using *in vivo* validation measures. However, other experiments needed to performed other experiments to ascertain interactions between our potential treatment, the miR-200c, with Hp, Serpinc1 and ITIH2.

5.6 Endothelial cells drive the activation of ATII cells

To better characterize the cellular crosstalk, we used the PNX mouse model, as it is a robust model that has been widely used to understand lung regeneration (Paisley et al., 2014; Voswinckel et al., 2004). The compensatory lung growth can recapitulate the postnatal lung growth, characterized by the proliferation of multiple mature endogenous differentiated cell types. This work shows a first attempt to characterize whether the remaining right lobes could suffer the mechanical stretch after PNX surgery. What was observed was that mainly the fourth (also known as the accessory lobe) and the second lobe are sensing the mechanical stretch and therefore, start proliferating more compared to the other two lobes.

Next, we investigated PNX-induced alveolar regeneration to establish whether endothelial cells could drive the activation of ATII cells using a lineage tracing mouse model. With this model we observed that the expansion of endothelial cells is higher 3 days after PNX, while at later (day 6 and day 8), ATII cells expand and promote lung regeneration through trans-differentiation. Our results are in line with a publication in which after PNX the endothelial cells drive ATII cells activation. However, this activation was observed after 6 days, where in our case we are detecting already ATII proliferation. Ding and collogues showed that the activation is mediated by MMP14, a

metallo-proteinase, that is required for the expansion of ATII cells and the restoration of alveolar structure and pulmonary function (Ding et al., 2011). Moreover, we performed PNX surgery on *Flt1* KO transgenic mouse model to confirm our previous results suggesting the involvement of *Flt1* in the alveolar regeneration through ATII trans-differentiation. The analysis showed that in absence of *Flt1,* the ratio between ATI and ATII cells was increased compared to controls mice*,* 8 days after, further confirming that regeneration is increased when *Flt1* is not present. Another study, using a systemic *Flt1* KO model instead of an endothelial *Flt1* KO model, confirmed that *Flt1* signaling is a key mediator of compensatory lung growth (Matsui et al., 2015).

5.7 Advantages, limitations and future directions

In this work, we demonstrated that the trans-differentiation process is a valuable model for studying the pathogenesis of IPF, which was evaluated by the isolation and culture of both human and murine ATII cells.

Moreover, we proved that the administration of miR-200c not only can rescue the pathological trans-differentiation of ATII into ATI cells, but it can also reverse the bleomycin induced-lung fibrosis when fibrosis is well established opening the doors for a possible therapeutic approach. With this in mind, we delivered miR-200c through aerosol, which is a non-invasive approach that targets specifically the lung, and therefore, avoids other organs.

We investigated miR-200c targets and discovered that miR-200c has a direct effect on its targets, such as ZEB1 and ZEB2, in human ATII cells harvested from IPF cells. Since ZEB1 and ZEB2, which regulate EMT, are not the only players in the development of fibrosis, we investigated the role of Flt1, another validated miR-200c target, and demonstrated for the first time its role as a negative modulator in IPF.

Previous studies exploited the correlation between endothelial and ATI cells since these two populations are essential for gas exchange (Ding et al., 2011; Basil et al., 2020). However, the crosstalk between alveolar endothelial cells and ATII cells in an IPF model was investigated for the first time in this study, showing the importance of this mechanism during the disease progression.

One of the limitations of using miR-200c as a potential IPF drug is the possibility of acting on multiple unwanted targets and therefore the generation of side effects. Another limitation of this study is the lack of a proper analysis to evaluate the miR-200c delivery efficiency in fibrotic human lungs. Finally, the bleomycin animal model is not a perfect

representation of the human IPF disease, since bleomycin induces a massive inflammation before fibrosis onset, while human IPF lacks the inflammatory response.
Further studies need to be performed in order to assure a safer treatment, as the molecular pathway by which the miR-200c is functioning is still not completely understood.
In the future, the expression of SerpinC1 and ITIH2 will need to be examined also in human IPF derived ATII cells and validated in bleomycin-induced lung fibrosis *in vivo.*

6. Conclusions

In this PhD work we have developed new experimental models for studying IPF. We broadly characterized ATII cells for their senescence and EMT features. Furthermore, miR-200c was evaluated for its therapeutic effect and capacity to normalize EMT markers and to reduce fibrosis *in vitro* and *in vivo*. *Flt1*, a miR-200c target, has emerged as a major pro-fibrotic regulator, as its depletion re-activates ATII cells and therefore promotes lung regeneration both *in vitro* and *in vivo* in mouse models of lung fibrosis and pneumectomy. We shed light on the mechanisms that mediates the increased trans-differentiation of ATII cells when *Flt1* is depleted and characterized a few endothelial-derived angiocrine factors, including SerpinC1, Haptoglobin and ITIH2. Moreover, our genetic tracing data point toward a critical role of tip endothelial cells in driving the activation of ATII cells. Altogether, our data contribute to the understanding of the molecular mechanisms controlling lung fibrosis and regeneration and pave the way to innovative diagnostic and therapeutic opportunities.

7. REFERENCES

- Abuserewa, Sherif T et al. “Treatment of Idiopathic Pulmonary Fibrosis.” Cureus vol. 13,5 e15360. 31 May. 2021, doi:10.7759/cureus.15360
- Acloque, Hervé et al. “Epithelial-mesenchymal transitions: the importance of changing cell state in development and disease.” The Journal of clinical investigation vol. 119,6 (2009): 1438-49. doi:10.1172/JCI38019
- Ahluwalia, Neil et al. “New therapeutic targets in idiopathic pulmonary fibrosis. Aiming to rein in runaway wound-healing responses.” American journal of respiratory and critical care medicine vol. 190,8 (2014): 867-78. doi:10.1164/rccm.201403-0509PP
- Åhrman, Emma et al. “Quantitative proteomic characterization of the lung extracellular matrix in chronic obstructive pulmonary disease and idiopathic pulmonary fibrosis.” Journal of proteomics vol. 189 (2018): 23-33. doi:10.1016/j.jprot.2018.02.027
- Aird, William C. “Phenotypic heterogeneity of the endothelium: I. Structure, function, and mechanisms.” Circulation research vol. 100,2 (2007): 158-73. doi:10.1161/01.RES.0000255691.76142.4a
- Alder, Jonathan K et al. “Short telomeres are a risk factor for idiopathic pulmonary fibrosis.” Proceedings of the National Academy of Sciences of the United States of America vol. 105,35 (2008): 13051-6. doi:10.1073/pnas.0804280105
- Alvarez, Diego F et al. “Lung microvascular endothelium is enriched with progenitor cells that exhibit vasculogenic capacity.” American journal of physiology. Lung cellular and molecular physiology vol. 294,3 (2008): L419-30. doi:10.1152/ajplung.00314.2007
- Amano, Hideki et al. “The role of vascular endothelial growth factor receptor 1 tyrosine kinase signaling in bleomycin-induced pulmonary fibrosis.” Biomedicine & pharmacotherapy = Biomedecine & pharmacotherapie vol. 117 (2019): 109067. doi:10.1016/j.biopha.2019.109067
- Amano, Hideki et al. “VEGFR1-tyrosine kinase signaling in pulmonary fibrosis.” Inflammation and regeneration vol. 41,1 16. 3 Jun. 2021, doi:10.1186/s41232-021-00166-7
- American Thoracic Society. and European Respiratory Society. “American Thoracic Society/European Respiratory Society International Multidisciplinary Consensus Classification of the Idiopathic Interstitial Pneumonias. This joint statement of the American Thoracic Society (ATS), and the European Respiratory Society (ERS) was

adopted by the ATS board of directors, June 2001 and by the ERS Executive Committee, June 2001." American journal of respiratory and critical care medicine vol. 165,2 (2002): 277-304. doi:10.1164/ajrccm.165.2.ats01

- Ando, Masaru et al. "Significance of serum vascular endothelial growth factor level in patients with idiopathic pulmonary fibrosis." Lung vol. 188,3 (2010): 247-52. doi:10.1007/s00408-009-9223-x
- Antoniou, Katerina M et al. "Interstitial lung disease." European respiratory review : an official journal of the European Respiratory Society vol. 23,131 (2014): 40-54. doi:10.1183/09059180.00009113
- Ashcroft, T et al. "Simple method of estimating severity of pulmonary fibrosis on a numerical scale." Journal of clinical pathologyvol. 41,4 (1988): 467-70. doi:10.1136/jcp.41.4.467
- Balberova, Olga V et al. "The "Angiogenic Switch" and Functional Resources in Cyclic Sports Athletes." International journal of molecular sciences vol. 22,12 6496. 17 Jun. 2021, doi:10.3390/ijms22126496
- Barbas-Filho, J V et al. "Evidence of type II pneumocyte apoptosis in the pathogenesis of idiopathic pulmonary fibrosis (IFP)/usual interstitial pneumonia (UIP)." Journal of clinical pathology vol. 54,2 (2001): 132-8. doi:10.1136/jcp.54.2.132
- Bargagli, E et al. "Serum analysis of coagulation factors in IPF and NSIP." Inflammation vol. 37,1 (2014): 10-6. doi:10.1007/s10753-013-9706-z
- Barkauskas, Christina E et al. "Type 2 alveolar cells are stem cells in adult lung." The Journal of clinical investigation vol. 123,7 (2013): 3025-36. doi:10.1172/JCI68782
- Barkauskas, Christina E, and Paul W Noble. "Cellular mechanisms of tissue fibrosis. 7. New insights into the cellular mechanisms of pulmonary fibrosis." American journal of physiology. Cell physiology vol. 306,11 (2014): C987-96. doi:10.1152/ajpcell.00321.2013
- Barratt, S, and A Millar. "Vascular remodelling in the pathogenesis of idiopathic pulmonary fibrosis." QJM : monthly journal of the Association of Physicians vol. 107,7 (2014): 515-9. doi:10.1093/qjmed/hcu012
- Barratt, Shaney L et al. "Effects of hypoxia and hyperoxia on the differential expression of VEGF-A isoforms and receptors in Idiopathic Pulmonary Fibrosis (IPF)." Respiratory research vol. 19,1 9. 15 Jan. 2018, doi:10.1186/s12931-017-0711-x

- Barrios, Juliana et al. “Pulmonary Neuroendocrine Cells Secrete γ-Aminobutyric Acid to Induce Goblet Cell Hyperplasia in Primate Models.” American journal of respiratory cell and molecular biology vol. 60,6 (2019): 687-694. doi:10.1165/rcmb.2018-0179OC
- Barros, Andrew et al. “Genetics of Idiopathic Pulmonary Fibrosis.” The American journal of the medical sciences vol. 357,5 (2019): 379-383. doi:10.1016/j.amjms.2019.02.009
- Been, Jasper V et al. “Bronchoalveolar lavage fluid from preterm infants with chorioamnionitis inhibits alveolar epithelial repair.” Respiratory research vol. 10,1 116. 23 Nov. 2009, doi:10.1186/1465-9921-10-116
- Bellaye, Pierre-Simon et al. “Synergistic role of HSP90α and HSP90β to promote myofibroblast persistence in lung fibrosis.” The European respiratory journal vol. 51,2 1700386. 31 Jan. 2018, doi:10.1183/13993003.00386-2017
- Benlhabib, Houda et al. “The miR-200 family and its targets regulate type II cell differentiation in human fetal lung.” The Journal of biological chemistry vol. 290,37 (2015): 22409-22. doi:10.1074/jbc.M114.636068
- Blackwell, Timothy S et al. “Future directions in idiopathic pulmonary fibrosis research. An NHLBI workshop report.” American journal of respiratory and critical care medicine vol. 189,2 (2014): 214-22. doi:10.1164/rccm.201306-1141WS
- Boateng, Eistine, and Susanne Krauss-Etschmann. “miRNAs in Lung Development and Diseases.” International journal of molecular sciences vol. 21,8 2765. 16 Apr. 2020, doi:10.3390/ijms21082765
- Brown, Derek et al. “MicroRNAs in respiratory disease. A clinician's overview.” Annals of the American Thoracic Society vol. 11,8 (2014): 1277-85. doi:10.1513/AnnalsATS.201404-179FR
- Bruick, Richard K. “Oxygen sensing in the hypoxic response pathway: regulation of the hypoxia-inducible transcription factor.” Genes & development vol. 17,21 (2003): 2614-23. doi:10.1101/gad.1145503
- Buendía-Roldán, Ivette et al. “Increased Expression of CC16 in Patients with Idiopathic Pulmonary Fibrosis.” PloS one vol. 11,12 e0168552. 15 Dec. 2016, doi:10.1371/journal.pone.0168552
- Burri, Peter H et al. “Intussusceptive angiogenesis: its emergence, its characteristics, and its significance.” Developmental dynamics : an official publication of the American Association of Anatomists vol. 231,3 (2004): 474-88. doi:10.1002/dvdy.20184

- Calvert, Ben A, and Amy L Ryan Firth. “Application of iPSC to Modelling of Respiratory Diseases.” *Advances in experimental medicine and biology* vol. 1237 (2020): 1-16. doi:10.1007/5584_2019_430
- Camelo, Ana et al. “The epithelium in idiopathic pulmonary fibrosis: breaking the barrier.” Frontiers in pharmacology vol. 4 173. 10 Jan. 2014, doi:10.3389/fphar.2013.00173
- Caporarello, Nunzia et al. “Vascular dysfunction in aged mice contributes to persistent lung fibrosis.” Aging cell vol. 19,8 (2020): e13196. doi:10.1111/acel.13196
- Carmeliet, P, and R K Jain. “Angiogenesis in cancer and other diseases.” Nature vol. 407,6801 (2000): 249-57. doi:10.1038/35025220
- Carmeliet, Peter, and Rakesh K Jain. “Molecular mechanisms and clinical applications of angiogenesis.” Nature vol. 473,7347 (2011): 298-307. doi:10.1038/nature10144
- Cébe-Suarez, S et al. “The role of VEGF receptors in angiogenesis; complex partnerships.” Cellular and molecular life sciences : CMLS vol. 63,5 (2006): 601-15. doi:10.1007/s00018-005-5426-3
- Chaudhary, Nveed I et al. “Pharmacologic differentiation of inflammation and fibrosis in the rat bleomycin model.” American journal of respiratory and critical care medicine vol. 173,7 (2006): 769-76. doi:10.1164/rccm.200505-717OC
- Chen, Xi et al. “A combination of Let-7d, Let-7g and Let-7i serves as a stable reference for normalization of serum microRNAs.” PloS onevol. 8,11 e79652. 5 Nov. 2013, doi:10.1371/journal.pone.0079652
- Cines, D B et al. “Endothelial cells in physiology and in the pathophysiology of vascular disorders.” Blood vol. 91,10 (1998): 3527-61.
- Collard, Harold R et al. “A new era in idiopathic pulmonary fibrosis: considerations for future clinical trials.” The European respiratory journal vol. 46,1 (2015): 243-9. doi:10.1183/09031936.00200614
- Condrat, Carmen Elena et al. “miRNAs as Biomarkers in Disease: Latest Findings Regarding Their Role in Diagnosis and Prognosis.” Cells vol. 9,2 276. 23 Jan. 2020, doi:10.3390/cells9020276
- Corrin, Bryan. and Andrew G. Nicholson. “Occupational, environmental and iatrogenic lung disease.” Pathology of the Lungs (2011): 327–399. doi:10.1016/B978-0-7020-3369-8.00007-0

- Cross, Troy James et al. “The interactions between respiratory and cardiovascular systems in systolic heart failure.” Journal of applied physiology (Bethesda, Md. : 1985) vol. 128,1 (2020): 214-224. doi:10.1152/japplphysiol.00113.2019
- Cushing, Leah et al. “Disruption of miR-29 Leads to Aberrant Differentiation of Smooth Muscle Cells Selectively Associated with Distal Lung Vasculature.” PLoS genetics vol. 11,5 e1005238. 28 May. 2015, doi:10.1371/journal.pgen.1005238
- Deng L, Baker AH, Bradshaw AC. MicroRNA Delivery Strategies to the Lung in a Model of Pulmonary Hypertension. Methods Mol Biol. 2017;1521:325-338. doi: 10.1007/978-1-4939-6588-5_23. PMID: 27910060.
- Di Gregorio, Jacopo et al. “The Epithelial-to-Mesenchymal Transition as a Possible Therapeutic Target in Fibrotic Disorders.” Frontiers in cell and developmental biologyvol. 8 607483. 21 Dec. 2020, doi:10.3389/fcell.2020.607483
- Ding, Bi-Sen et al. “Endothelial-derived angiocrine signals induce and sustain regenerative lung alveolarization.” Cell vol. 147,3 (2011): 539-53. doi:10.1016/j.cell.2011.10.003
- Dua, Kamal et al. “MicroRNAs as therapeutics for future drug delivery systems in treatment of lung diseases.” Drug delivery and translational research vol. 7,1 (2017): 168-178. doi:10.1007/s13346-016-0343-6
- Ebina, Masahito et al. “Heterogeneous increase in CD34-positive alveolar capillaries in idiopathic pulmonary fibrosis.” American journal of respiratory and critical care medicine vol. 169,11 (2004): 1203-8. doi:10.1164/rccm.200308-1111OC
- Eelen, Guy et al. “Endothelial Cell Metabolism.” Physiological reviews vol. 98,1 (2018): 3-58. doi:10.1152/physrev.00001.2017
- Eldridge, Lindsey, and Elizabeth M Wagner. “Angiogenesis in the lung.” The Journal of physiology vol. 597,4 (2019): 1023-1032. doi:10.1113/JP275860
- Fadini, Gian Paolo et al. “The emerging role of endothelial progenitor cells in pulmonary hypertension and diffuse lung diseases.” Sarcoidosis, vasculitis, and diffuse lung diseases : official journal of WASOG vol. 24,2 (2007): 85-93.
- Fallah, Asghar et al. “Therapeutic targeting of angiogenesis molecular pathways in angiogenesis-dependent diseases.” Biomedicine & pharmacotherapy = Biomedecine & pharmacotherapie vol. 110 (2019): 775-785. doi:10.1016/j.biopha.2018.12.022

- Fan, Lichao et al. “Analysis of Microarray-Identified Genes and MicroRNAs Associated with Idiopathic Pulmonary Fibrosis.” Mediators of inflammation vol. 2017 (2017): 1804240. doi:10.1155/2017/1804240
- Farkas, Laszlo et al. “VEGF ameliorates pulmonary hypertension through inhibition of endothelial apoptosis in experimental lung fibrosis in rats.” The Journal of clinical investigation vol. 119,5 (2009): 1298-311. doi:10.1172/JCI36136
- Fong, G H et al. “Role of the Flt-1 receptor tyrosine kinase in regulating the assembly of vascular endothelium.” Nature vol. 376,6535 (1995): 66-70. doi:10.1038/376066a0
- Franco-Barraza, Janusz et al. “Preparation of Extracellular Matrices Produced by Cultured and Primary Fibroblasts.” Current protocols in cell biology vol. 71 10.9.1-10.9.34. 1 Jun. 2016, doi:10.1002/cpcb.2
- Friedrich, Emily E et al. “Endothelial cell Piezo1 mediates pressure-induced lung vascular hyperpermeability via disruption of adherens junctions.” Proceedings of the National Academy of Sciences of the United States of America vol. 116,26 (2019): 12980-12985. doi:10.1073/pnas.1902165116
- Gao L, Li P, Tian H, Wu M, Yang J, Xu X. Screening of Biomarkers Involved in Idiopathic Pulmonary Fibrosis and Regulation of Upstream miRNAs. Am J Med Sci. 2021 Oct 16:S0002-9629(21)00360-8. doi: 10.1016/j.amjms.2021.06.027. Epub ahead of print. PMID: 34666057.
- Garantziotis, Stavros et al. “Serum inter-alpha-trypsin inhibitor and matrix hyaluronan promote angiogenesis in fibrotic lung injury.” American journal of respiratory and critical care medicine vol. 178,9 (2008): 939-47. doi:10.1164/rccm.200803-386OC
- Gebert, Luca F R, and Ian J MacRae. “Regulation of microRNA function in animals.” Nature reviews. Molecular cell biology vol. 20,1 (2019): 21-37. doi:10.1038/s41580-018-0045-7
- Gerhardt, Holger et al. “VEGF guides angiogenic sprouting utilizing endothelial tip cell filopodia.” The Journal of cell biology vol. 161,6 (2003): 1163-77. doi:10.1083/jcb.200302047
- Giacca, Mauro. “Non-redundant functions of the protein isoforms arising from alternative splicing of the VEGF-A pre-mRNA.” Transcription vol. 1,3 (2010): 149-153. doi:10.4161/trns.1.3.13229
- Gillich, Astrid et al. “Capillary cell-type specialization in the alveolus.” Nature vol. 586,7831 (2020): 785-789. doi:10.1038/s41586-020-2822-7

- Gillich, Astrid et al. “Capillary cell-type specialization in the alveolus.” Nature vol. 586,7831 (2020): 785-789. doi:10.1038/s41586-020-2822-7
- Grześk, Grzegorz et al. “The Interactions of Nintedanib and Oral Anticoagulants-Molecular Mechanisms and Clinical Implications.” International journal of molecular sciences vol. 22,1 282. 30 Dec. 2020, doi:10.3390/ijms22010282
- Gulati, Swati, and Tracy R Luckhardt. “Updated Evaluation of the Safety, Efficacy and Tolerability of Pirfenidone in the Treatment of Idiopathic Pulmonary Fibrosis.” Drug, healthcare and patient safety vol. 12 85-94. 7 May. 2020, doi:10.2147/DHPS.S224007
- Hagimoto, N et al. Nihon Kyobu Shikkan Gakkai zasshi vol. 34,1 (1996): 3-8.
- Hanumegowda, Chandru et al. “Angiogenesis in pulmonary fibrosis: too much or not enough?.” Chest vol. 142,1 (2012): 200-207. doi:10.1378/chest.11-1962
- Hecker, Louise et al. “Reversal of persistent fibrosis in aging by targeting Nox4-Nrf2 redox imbalance.” Science translational medicine vol. 6,231 (2014): 231ra47. doi:10.1126/scitranslmed.3008182
- Herrera, Jeremy et al. “Dicer1 Deficiency in the Idiopathic Pulmonary Fibrosis Fibroblastic Focus Promotes Fibrosis by Suppressing MicroRNA Biogenesis.” American journal of respiratory and critical care medicine vol. 198,4 (2018): 486-496. doi:10.1164/rccm.201709-1823OC
- Herrera, Jeremy et al. “Extracellular matrix as a driver of progressive fibrosis.” The Journal of clinical investigation vol. 128,1 (2018): 45-53. doi:10.1172/JCI93557
- Heyn, Gabriella Simões et al. “The Impact of Adipose Tissue-Derived miRNAs in Metabolic Syndrome, Obesity, and Cancer.” Frontiers in endocrinology vol. 11 563816. 6 Oct. 2020, doi:10.3389/fendo.2020.563816
- Hoefel, Gabriela et al. “MicroRNAs in Lung Diseases.” Chest vol. 156,5 (2019): 991-1000. doi:10.1016/j.chest.2019.06.008
- Hoffmann, Thomas Walter et al. “MicroRNAs and hepatitis C virus: toward the end of miR-122 supremacy.” Virology journalvol. 9 109. 12 Jun. 2012, doi:10.1186/1743-422X-9-109
- Hogan, Brigid L M et al. “Repair and regeneration of the respiratory system: complexity, plasticity, and mechanisms of lung stem cell function.” Cell stem cell vol. 15,2 (2014): 123-38. doi:10.1016/j.stem.2014.07.012

- Inui, Naoki et al. “Molecular Pathogenesis of Pulmonary Fibrosis, with Focus on Pathways Related to TGF-β and the Ubiquitin-Proteasome Pathway.” International journal of molecular sciences vol. 22,11 6107. 5 Jun. 2021, doi:10.3390/ijms22116107
- Jablonski, Renea P et al. “SIRT3 deficiency promotes lung fibrosis by augmenting alveolar epithelial cell mitochondrial DNA damage and apoptosis.” FASEB journal : official publication of the Federation of American Societies for Experimental Biology vol. 31,6 (2017): 2520-2532. doi:10.1096/fj.201601077R
- Jenkins, R Gisli et al. “An Official American Thoracic Society Workshop Report: Use of Animal Models for the Preclinical Assessment of Potential Therapies for Pulmonary Fibrosis.” American journal of respiratory cell and molecular biology vol. 56,5 (2017): 667-679. doi:10.1165/rcmb.2017-0096ST
- Jia, Haiyan et al. “Characterization of a bicyclic peptide neuropilin-1 (NP-1) antagonist (EG3287) reveals importance of vascular endothelial growth factor exon 8 for NP-1 binding and role of NP-1 in KDR signaling.” The Journal of biological chemistry vol. 281,19 (2006): 13493-13502. doi:10.1074/jbc.M512121200
- Joshi, Sachindra R et al. “MicroRNAs-control of essential genes: Implications for pulmonary vascular disease.” Pulmonary circulation vol. 1,3 (2011): 357-64. doi:10.4103/2045-8932.87301
- Kalluri, Raghu, and Eric G Neilson. “Epithelial-mesenchymal transition and its implications for fibrosis.” The Journal of clinical investigation vol. 112,12 (2003): 1776-84. doi:10.1172/JCI20530
- Kalluri, Raghu, and Robert A Weinberg. “The basics of epithelial-mesenchymal transition.” The Journal of clinical investigation vol. 119,6 (2009): 1420-8. doi:10.1172/JCI39104
- Kaner, R J et al. “Lung overexpression of the vascular endothelial growth factor gene induces pulmonary edema.” American journal of respiratory cell and molecular biology vol. 22,6 (2000): 657-64. doi:10.1165/ajrcmb.22.6.3779
- Kato, Shinpei et al. “Changes in pulmonary endothelial cell properties during bleomycin-induced pulmonary fibrosis.” Respiratory research vol. 19,1 127. 26 Jun. 2018, doi:10.1186/s12931-018-0831-y
- Katzenstein, A L, and J L Myers. “Idiopathic pulmonary fibrosis: clinical relevance of pathologic classification.” American journal of respiratory and critical care medicine vol. 157,4 Pt 1 (1998): 1301-15. doi:10.1164/ajrccm.157.4.9707039

- King, Talmadge E Jr et al. “A phase 3 trial of pirfenidone in patients with idiopathic pulmonary fibrosis.” The New England journal of medicine vol. 370,22 (2014): 2083-92. doi:10.1056/NEJMoa1402582
- Kivelä, Riikka et al. “Endothelial Cells Regulate Physiological Cardiomyocyte Growth via VEGFR2-Mediated Paracrine Signaling.” Circulation vol. 139,22 (2019): 2570-2584. doi:10.1161/CIRCULATIONAHA.118.036099
- Kocijan, Tea et al. “Genetic lineage tracing reveals poor angiogenic potential of cardiac endothelial cells.” Cardiovascular research vol. 117,1 (2021): 256-270. doi:10.1093/cvr/cvaa012
- Kolesnikoff, Natasha et al. “Specificity protein 1 (Sp1) maintains basal epithelial expression of the miR-200 family: implications for epithelial-mesenchymal transition.” The Journal of biological chemistry vol. 289,16 (2014): 11194-11205. doi:10.1074/jbc.M113.529172
- Kosmider, Beata et al. “Isolation and Characterization of Human Alveolar Type II Cells.” Methods in molecular biology (Clifton, N.J.) vol. 1809 (2018): 83-90. doi:10.1007/978-1-4939-8570-8_7
- Kropski, Jonathan A et al. “Deregulated angiogenesis in chronic lung diseases: a possible role for lung mesenchymal progenitor cells (2017 Grover Conference Series).” Pulmonary circulation vol. 8,1 (2018): 2045893217739807. doi:10.1177/2045893217739807
- Kropski, Jonathan A et al. “The genetic basis of idiopathic pulmonary fibrosis.” The European respiratory journal vol. 45,6 (2015): 1717-27. doi:10.1183/09031936.00163814
- Kulkarni, Yogesh M et al. “A proteomics approach to identifying key protein targets involved in VEGF inhibitor mediated attenuation of bleomycin-induced pulmonary fibrosis.” Proteomics vol. 16,1 (2016): 33-46. doi:10.1002/pmic.201500171
- Lacedonia, Donato et al. “Downregulation of exosomal let-7d and miR-16 in idiopathic pulmonary fibrosis.” BMC pulmonary medicine vol. 21,1 188. 4 Jun. 2021, doi:10.1186/s12890-021-01550-2
- Landi, Claudia et al. “Idiopathic Pulmonary Fibrosis Serum proteomic analysis before and after nintedanib therapy.” Scientific reports vol. 10,1 9378. 10 Jun. 2020, doi:10.1038/s41598-020-66296-z

- Laporta Hernandez, Rosalía et al. “Lung Transplantation in Idiopathic Pulmonary Fibrosis.” Medical sciences (Basel, Switzerland) vol. 6,3 68. 23 Aug. 2018, doi:10.3390/medsci6030068
- Lawson, William E et al. “Increased and prolonged pulmonary fibrosis in surfactant protein C-deficient mice following intratracheal bleomycin.” The American journal of pathology vol. 167,5 (2005): 1267-77. doi:10.1016/S0002-9440(10)61214-X
- Lee, Chun Geun et al. “Vascular endothelial growth factor (VEGF) induces remodeling and enhances TH2-mediated sensitization and inflammation in the lung.” Nature medicine vol. 10,10 (2004): 1095-103. doi:10.1038/nm1105
- Lehmann, Mareike et al. “Differential effects of Nintedanib and Pirfenidone on lung alveolar epithelial cell function in ex vivo murine and human lung tissue cultures of pulmonary fibrosis.” Respiratory research vol. 19,1 175. 15 Sep. 2018, doi:10.1186/s12931-018-0876-y
- Ley, Brett, and Harold R Collard. “Epidemiology of idiopathic pulmonary fibrosis.” Clinical epidemiology vol. 5 483-92. 25 Nov. 2013, doi:10.2147/CLEP.S54815
- Li, Huimin et al. “MicroRNAs in idiopathic pulmonary fibrosis: involvement in pathogenesis and potential use in diagnosis and therapeutics.” Acta pharmaceutica Sinica. B vol. 6,6 (2016): 531-539. doi:10.1016/j.apsb.2016.06.010
- Liu, Rui-Ming, and Gang Liu. “Cell senescence and fibrotic lung diseases.” Experimental gerontology vol. 132 (2020): 110836. doi:10.1016/j.exger.2020.110836
- Lopez-de la Mora, David Alejandro et al. “Role and New Insights of Pirfenidone in Fibrotic Diseases.” International journal of medical sciences vol. 12,11 840-7. 14 Oct. 2015, doi:10.7150/ijms.11579
- Lord, Megan S et al. “The Inter-α-Trypsin Inhibitor Family: Versatile Molecules in Biology and Pathology.” The journal of histochemistry and cytochemistry : official journal of the Histochemistry Society vol. 68,12 (2020): 907-927. doi:10.1369/0022155420940067
- Lynch, Joseph P. III, and John A. Belperio. “Idiopathic Pulmonary Fibrosis.” Diffuse Lung Disease: A Practical Approach 171–194. 12 Jul. 2011, doi:10.1007/978-1-4419-9771-5_10

- Maher, Toby M et al. “Global incidence and prevalence of idiopathic pulmonary fibrosis.” Respiratory research vol. 22,1 197. 7 Jul. 2021, doi:10.1186/s12931-021-01791-z
- Malli, Foteini et al. “Endothelial progenitor cells in the pathogenesis of idiopathic pulmonary fibrosis: an evolving concept.” PloS one vol. 8,1 (2013): e53658. doi:10.1371/journal.pone.0053658
- Mamer, Spencer B et al. “VEGF-A splice variants bind VEGFRs with differential affinities.” Scientific reports vol. 10,1 14413. 2 Sep. 2020, doi:10.1038/s41598-020-71484-y
- Mammoto, Akiko, and Tadanori Mammoto. “Vascular Niche in Lung Alveolar Development, Homeostasis, and Regeneration.” Frontiers in bioengineering and biotechnology vol. 7 318. 12 Nov. 2019, doi:10.3389/fbioe.2019.00318
- Martinez, Fernando J et al. “Idiopathic pulmonary fibrosis.” Nature reviews. Disease primers vol. 3 17074. 20 Oct. 2017, doi:10.1038/nrdp.2017.74
- Matsui, Yoshio et al. “The role of vascular endothelial growth factor receptor-1 signaling in compensatory contralateral lung growth following unilateral pneumonectomy.” Laboratory investigation; a journal of technical methods and pathology vol. 95,5 (2015): 456-68. doi:10.1038/labinvest.2014.159
- McBride, William H, and Dörthe Schaue. “Radiation-induced tissue damage and response.” *The Journal of pathology* vol. 250,5 (2020): 647-655. doi:10.1002/path.5389
- Medford, Andrew R L et al. “Vascular endothelial growth factor receptor and coreceptor expression in human acute respiratory distress syndrome.” Journal of critical care vol. 24,2 (2009): 236-42. doi:10.1016/j.jcrc.2008.04.003
- Meiners, Silke et al. “Hallmarks of the ageing lung.” The European respiratory journal vol. 45,3 (2015): 807-27. doi:10.1183/09031936.00186914
- Mezquita, Belén et al. “A truncated-Flt1 isoform of breast cancer cells is upregulated by Notch and downregulated by retinoic acid.” Journal of cellular biochemistry vol. 115,1 (2014): 52-61. doi:10.1002/jcb.24632
- Miao, Chenggui et al. “MicroRNAs in idiopathic pulmonary fibrosis, new research progress and their pathophysiological implication.” Experimental lung research vol. 44,3 (2018): 178-190. doi:10.1080/01902148.2018.1455927

- Miao, Chenggui et al. “MicroRNAs in idiopathic pulmonary fibrosis, new research progress and their pathophysiological implication.” Experimental lung research vol. 44,3 (2018): 178-190. doi:10.1080/01902148.2018.1455927
- Moeller, Antje et al. “The bleomycin animal model: a useful tool to investigate treatment options for idiopathic pulmonary fibrosis?.” The international journal of biochemistry & cell biology vol. 40,3 (2008): 362-82. doi:10.1016/j.biocel.2007.08.011
- Moimas, Silvia et al. “miR-200 family members reduce senescence and restore idiopathic pulmonary fibrosis type II alveolar epithelial cell transdifferentiation.” ERJ open researchvol. 5,4 00138-2019. 16 Dec. 2019, doi:10.1183/23120541.00138-2019
- Moore, Bethany B, and Cory M Hogaboam. “Murine models of pulmonary fibrosis.” American journal of physiology. Lung cellular and molecular physiology vol. 294,2 (2008): L152-60. doi:10.1152/ajplung.00313.2007
- Morrisey, Edward E, and Brigid L M Hogan. “Preparing for the first breath: genetic and cellular mechanisms in lung development.” Developmental cell vol. 18,1 (2010): 8-23. doi:10.1016/j.devcel.2009.12.01
- Murray, Lynne A et al. “Antifibrotic role of vascular endothelial growth factor in pulmonary fibrosis.” JCI insight vol. 2,16 e92192. 17 Aug. 2017, doi:10.1172/jci.insight.92192
- Naikawadi, Ram P et al. “Telomere dysfunction in alveolar epithelial cells causes lung remodeling and fibrosis.” JCI insight vol. 1,14 e86704. 8 Sep. 2016, doi:10.1172/jci.insight.86704
- Naikawadi, Ram P et al. “Telomere dysfunction in alveolar epithelial cells causes lung remodeling and fibrosis.” JCI insight vol. 1,14 e86704. 8 Sep. 2016, doi:10.1172/jci.insight.86704
- Nemeth, Julia et al. “Insights Into Development and Progression of Idiopathic Pulmonary Fibrosis From Single Cell RNA Studies.” Frontiers in medicine vol. 7 611728. 16 Dec. 2020, doi:10.3389/fmed.2020.611728
- Newman, Stephen P. “Drug delivery to the lungs: challenges and opportunities.” Therapeutic delivery vol. 8,8 (2017): 647-661. doi:10.4155/tde-2017-0037
- Niethamer, Terren K et al. “Defining the role of pulmonary endothelial cell heterogeneity in the response to acute lung injury.” eLife vol. 9 e53072. 24 Feb. 2020, doi:10.7554/eLife.53072

- Nikolić, Marko Z et al. “From the pathophysiology of the human lung alveolus to epigenetic editing: Congress 2018 highlights from ERS Assembly 3 "Basic and Translational Science."." ERJ open research vol. 5,2 00194-2018. 10 May. 2019, doi:10.1183/23120541.00194-2018
- Niu, Gang, and Xiaoyuan Chen. “Vascular endothelial growth factor as an anti-angiogenic target for cancer therapy.” Current drug targets vol. 11,8 (2010): 1000-17. doi:10.2174/138945010791591395
- Nureki, Shin-Ichi et al. “Expression of mutant Sftpc in murine alveolar epithelia drives spontaneous lung fibrosis.” The Journal of clinical investigation vol. 128,9 (2018): 4008-4024. doi:10.1172/JCI99287
- O'Reilly, Steven. “MicroRNAs in fibrosis: opportunities and challenges.” Arthritis research & therapy vol. 18 11. 13 Jan. 2016, doi:10.1186/s13075-016-0929-x
- Paisley, Derek et al. “The pneumonectomy model of compensatory lung growth: insights into lung regeneration.” Pharmacology & therapeutics vol. 142,2 (2014): 196-205. doi:10.1016/j.pharmthera.2013.12.006
- Pandit, Kusum V et al. “Inhibition and role of let-7d in idiopathic pulmonary fibrosis.” American journal of respiratory and critical care medicine vol. 182,2 (2010): 220-9. doi:10.1164/rccm.200911-1698OC
- Pandit, Kusum V, and Jadranka Milosevic. “MicroRNA regulatory networks in idiopathic pulmonary fibrosis.” Biochemistry and cell biology = Biochimie et biologie cellulaire vol. 93,2 (2015): 129-37. doi:10.1139/bcb-2014-0101
- Parimon, Tanyalak et al. “Alveolar Epithelial Type II Cells as Drivers of Lung Fibrosis in Idiopathic Pulmonary Fibrosis.” International journal of molecular sciences vol. 21,7 2269. 25 Mar. 2020, doi:10.3390/ijms21072269
- Parimon, Tanyalak et al. “Syndecan-1 promotes lung fibrosis by regulating epithelial reprogramming through extracellular vesicles.” JCI insight vol. 5,17 e129359. 8 Aug. 2019, doi:10.1172/jci.insight.129359
- Pecot, Chad V et al. “Tumour angiogenesis regulation by the miR-200 family.” Nature communications vol. 4 (2013): 2427. doi:10.1038/ncomms3427
- Plate, K H et al. “Vascular endothelial growth factor is a potential tumour angiogenesis factor in human gliomas in vivo.” Nature vol. 359,6398 (1992): 845-8. doi:10.1038/359845a0

- Polverino, Eva et al. “The overlap between bronchiectasis and chronic airway diseases: state of the art and future directions.” The European respiratory journal vol. 52,3 1800328. 15 Sep. 2018, doi:10.1183/13993003.00328-2018
- Rafii, Shahin et al. “Angiocrine functions of organ-specific endothelial cells.” Nature vol. 529,7586 (2016): 316-25. doi:10.1038/nature17040
- Raghu, Ganesh et al. “Diagnosis of idiopathic pulmonary fibrosis with high-resolution CT in patients with little or no radiological evidence of honeycombing: secondary analysis of a randomised, controlled trial.” The Lancet. Respiratory medicine vol. 2,4 (2014): 277-84. doi:10.1016/S2213-2600(14)70011-6
- Raghu, Ganesh et al. “Diagnosis of Idiopathic Pulmonary Fibrosis. An Official ATS/ERS/JRS/ALAT Clinical Practice Guideline.” American journal of respiratory and critical care medicine vol. 198,5 (2018): e44-e68. doi:10.1164/rccm.201807-1255ST
- Rajasekaran, Subbiah et al. “MicroRNAs as potential targets for progressive pulmonary fibrosis.” Frontiers in pharmacology vol. 6 254. 5 Nov. 2015, doi:10.3389/fphar.2015.00254
- Rawlins, Emma L, and Anne-Karina Perl. “The a"MAZE"ing world of lung-specific transgenic mice.” American journal of respiratory cell and molecular biology vol. 46,3 (2012): 269-82. doi:10.1165/rcmb.2011-0372PS
- Redente, Elizabeth F et al. “Age and sex dimorphisms contribute to the severity of bleomycin-induced lung injury and fibrosis.” American journal of physiology. Lung cellular and molecular physiology vol. 301,4 (2011): L510-8. doi:10.1152/ajplung.00122.2011
- Reyfman, Paul A et al. “Single-Cell Transcriptomic Analysis of Human Lung Provides Insights into the Pathobiology of Pulmonary Fibrosis.” American journal of respiratory and critical care medicine vol. 199,12 (2019): 1517-1536. doi:10.1164/rccm.201712-2410OC
- Roberts, Jonathan R et al. “Vascular endothelial growth factor promotes physical wound repair and is anti-apoptotic in primary distal lung epithelial and A549 cells.” Critical care medicine vol. 35,9 (2007): 2164-70. doi:10.1097/01.ccm.0000281451.73202.f6
- Rock, Jason R, and Brigid L M Hogan. “Epithelial progenitor cells in lung development, maintenance, repair, and disease.” Annual review of cell and developmental biology vol. 27 (2011): 493-512. doi:10.1146/annurev-cellbio-100109-104040

- Ruaro, Barbara et al. “The History and Mystery of Alveolar Epithelial Type II Cells: Focus on Their Physiologic and Pathologic Role in Lung.” International journal of molecular sciences vol. 22,5 2566. 4 Mar. 2021, doi:10.3390/ijms22052566
- Ryan, U S, and J W Ryan. “Cell biology of pulmonary endothelium.” Circulation vol. 70,5 Pt 2 (1984): III46-62.
- Ryu, J H et al. “Smoking-related interstitial lung diseases: a concise review.” The European respiratory journal vol. 17,1 (2001): 122-32. doi:10.1183/09031936.01.17101220
- Sakai, Norihiko, and Andrew M Tager. “Fibrosis of two: Epithelial cell-fibroblast interactions in pulmonary fibrosis.” Biochimica et biophysica acta vol. 1832,7 (2013): 911-21. doi:10.1016/j.bbadis.2013.03.001
- Salton, Francesco et al. “Epithelial-Mesenchymal Transition: A Major Pathogenic Driver in Idiopathic Pulmonary Fibrosis?.” Medicina (Kaunas, Lithuania) vol. 56,11 608. 13 Nov. 2020, doi:10.3390/medicina56110608
- Salton, Francesco et al. “Epithelial–Mesenchymal Transition in the Pathogenesis of Idiopathic Pulmonary Fibrosis.” Medicina (Kaunas, Lithuania) vol. 55,4 83. 28 Mar. 2019, doi:10.3390/medicina55040083
- Sato, Seidai et al. “Anti-fibrotic efficacy of nintedanib in pulmonary fibrosis via the inhibition of fibrocyte activity.” Respiratory research vol. 18,1 172. 15 Sep. 2017, doi:10.1186/s12931-017-0654-2
- Schruf, Eva et al. “Recapitulating idiopathic pulmonary fibrosis related alveolar epithelial dysfunction in a human iPSC-derived air-liquid interface model.” FASEB journal : official publication of the Federation of American Societies for Experimental Biology vol. 34,6 (2020): 7825-7846. doi:10.1096/fj.201902926R
- Selman, Moisés et al. “Idiopathic pulmonary fibrosis: aberrant recapitulation of developmental programs?.” PLoS medicine vol. 5,3 (2008): e62. doi:10.1371/journal.pmed.0050062
- Shibuya, M et al. “Nucleotide sequence and expression of a novel human receptor-type tyrosine kinase gene (flt) closely related to the fms family.” Oncogene vol. 5,4 (1990): 519-24.
- Shibuya, Masabumi. “Vascular Endothelial Growth Factor (VEGF) and Its Receptor (VEGFR) Signaling in Angiogenesis: A Crucial Target for Anti- and Pro-Angiogenic

Therapies.” Genes & cancer vol. 2,12 (2011): 1097-105. doi:10.1177/1947601911423031

- Shibuya, Masaubmi. “Vascular endothelial growth factor receptor-1 (VEGFR-1/Flt-1): a dual regulator for angiogenesis.” Angiogenesisvol. 9,4 (2006): 225-30; discussion 231. doi:10.1007/s10456-006-9055-8
- Simpson, A B et al. “Fatal bleomycin pulmonary toxicity in the west of Scotland 1991-95: a review of patients with germ cell tumours.” British journal of cancer vol. 78,8 (1998): 1061-6. doi:10.1038/bjc.1998.628
- Suri, Gurparsad Singh et al. “Understanding idiopathic pulmonary fibrosis - Clinical features, molecular mechanism and therapies.” Experimental gerontology vol. 153 (2021): 111473. doi:10.1016/j.exger.2021.111473
- Takeda, Yoshito et al. “Efficacy and safety of pirfenidone for idiopathic pulmonary fibrosis.” Patient preference and adherence vol. 8 361-70. 21 Mar. 2014, doi:10.2147/PPA.S37233
- Tang, Changyong et al. “Neural Stem Cells Behave as a Functional Niche for the Maturation of Newborn Neurons through the Secretion of PTN.” Neuron vol. 101,1 (2019): 32-44.e6. doi:10.1016/j.neuron.2018.10.051
- Tashiro, Jun et al. “Exploring Animal Models That Resemble Idiopathic Pulmonary Fibrosis.” Frontiers in medicine vol. 4 118. 28 Jul. 2017, doi:10.3389/fmed.2017.00118
- Tetzlaff, Fabian, and Andreas Fischer. “Human Endothelial Cell Spheroid-based Sprouting Angiogenesis Assay in Collagen.” Bio-protocol vol. 8,17 e2995. 5 Sep. 2018, doi:10.21769/BioProtoc.2995
- Tian, Yaqiong et al. “Loss of PTEN induces lung fibrosis via alveolar epithelial cell senescence depending on NF-κB activation.” Aging cell vol. 18,1 (2019): e12858. doi:10.1111/acel.12858
- Tian, Yaqiong et al. “Quantitative proteomic characterization of lung tissue in idiopathic pulmonary fibrosis.” Clinical proteomics vol. 16 6. 6 Feb. 2019, doi:10.1186/s12014-019-9226-4
- Todd, Nevins W et al. “Molecular and cellular mechanisms of pulmonary fibrosis.” Fibrogenesis & tissue repair vol. 5,1 11. 23 Jul. 2012, doi:10.1186/1755-1536-5-11
- Travis, William D et al. “An official American Thoracic Society/European Respiratory Society statement: Update of the international multidisciplinary classification of the

idiopathic interstitial pneumonias.” American journal of respiratory and critical care medicine vol. 188,6 (2013): 733-48. doi:10.1164/rccm.201308-1483ST

- Tsujino, Kazuyuki et al. “Tetraspanin CD151 protects against pulmonary fibrosis by maintaining epithelial integrity.” American journal of respiratory and critical care medicine vol. 186,2 (2012): 170-80. doi:10.1164/rccm.201201-0117OC
- Tzahor, Eldad, and Kenneth D Poss. “Cardiac regeneration strategies: Staying young at heart.” Science (New York, N.Y.) vol. 356,6342 (2017): 1035-1039. doi:10.1126/science.aam5894
- Uhal, B D et al. “Alveolar epithelial cell death adjacent to underlying myofibroblasts in advanced fibrotic human lung.” The American journal of physiology vol. 275,6 (1998): L1192-9. doi:10.1152/ajplung.1998.275.6.L1192
- Urbich, Carmen et al. “Soluble factors released by endothelial progenitor cells promote migration of endothelial cells and cardiac resident progenitor cells.” Journal of molecular and cellular cardiology vol. 39,5 (2005): 733-42. doi:10.1016/j.yjmcc.2005.07.003
- Vaccaro, C A, and J S Brody. “Structural features of alveolar wall basement membrane in the adult rat lung.” The Journal of cell biology vol. 91,2 Pt 1 (1981): 427-37. doi:10.1083/jcb.91.2.427
- Valapour, M et al. “OPTN/SRTR 2019 Annual Data Report: Lung.” American journal of transplantation : official journal of the American Society of Transplantation and the American Society of Transplant Surgeons vol. 21 Suppl 2 (2021): 441-520. doi:10.1111/ajt.16495
- Vila Ellis, Lisandra et al. “Epithelial Vegfa Specifies a Distinct Endothelial Population in the Mouse Lung.” Developmental cell vol. 52,5 (2020): 617-630.e6. doi:10.1016/j.devcel.2020.01.009
- Visscher, Daniel W, and Jeffrey L Myers. “Bronchiolitis: the pathologist's perspective.” Proceedings of the American Thoracic Societyvol. 3,1 (2006): 41-7. doi:10.1513/pats.200512-124JH
- Voswinckel, R et al. “Characterisation of post-pneumonectomy lung growth in adult mice.” The European respiratory journal vol. 24,4 (2004): 524-32. doi:10.1183/09031936.04.10004904
- Walters, Dianne M, and Steven R Kleeberger. “Mouse models of bleomycin-induced pulmonary fibrosis.” Current protocols in pharmacology vol. Chapter 5 (2008): Unit 5.46. doi:10.1002/0471141755.ph0546s40

- Wang, Shuang et al. “TGF-β/Smad3 signalling regulates the transition of bone marrow-derived macrophages into myofibroblasts during tissue fibrosis.” Oncotarget vol. 7,8 (2016): 8809-22. doi:10.18632/oncotarget.6604
- Wang, Yangming et al. “DGCR8 is essential for microRNA biogenesis and silencing of embryonic stem cell self-renewal.” Nature genetics vol. 39,3 (2007): 380-5. doi:10.1038/ng1969
- Willems, Stijn et al. “Multiplex protein profiling of bronchoalveolar lavage in idiopathic pulmonary fibrosis and hypersensitivity pneumonitis.” Annals of thoracic medicine vol. 8,1 (2013): 38-45. doi:10.4103/1817-1737.105718
- Witjas, Franca M R et al. “Concise Review: The Endothelial Cell Extracellular Matrix Regulates Tissue Homeostasis and Repair.” Stem cells translational medicine vol. 8,4 (2019): 375-382. doi:10.1002/sctm.18-0155
- Wollin, Lutz et al. “Mode of action of nintedanib in the treatment of idiopathic pulmonary fibrosis.” The European respiratory journal vol. 45,5 (2015): 1434-45. doi:10.1183/09031936.00174914
- Wolters, Paul J et al. “Pathogenesis of idiopathic pulmonary fibrosis.” Annual review of pathology vol. 9 (2014): 157-79. doi:10.1146/annurev-pathol-012513-104706
- Wright, Joanne L et al. “Animal models of chronic obstructive pulmonary disease.” American journal of physiology. Lung cellular and molecular physiology vol. 295,1 (2008): L1-15. doi:10.1152/ajplung.90200.2008
- Xu, Yan et al. “Single-cell RNA sequencing identifies diverse roles of epithelial cells in idiopathic pulmonary fibrosis.” JCI insight vol. 1,20 e90558. 8 Dec. 2016, doi:10.1172/jci.insight.90558
- Yagoda, A et al. “Bleomycin, an antitumor antibiotic. Clinical experience in 274 patients.” Annals of internal medicine vol. 77,6 (1972): 861-70. doi:10.7326/0003-4819-77-6-861
- Yang, Funmei et al. “Haptoglobin reduces lung injury associated with exposure to blood.” American journal of physiology. Lung cellular and molecular physiology vol. 284,2 (2003): L402-9. doi:10.1152/ajplung.00115.2002
- Yang, Shanzhong et al. “Participation of miR-200 in pulmonary fibrosis.” The American journal of pathology vol. 180,2 (2012): 484-93. doi:10.1016/j.ajpath.2011.10.005

- Yao, Liudi et al. “Paracrine signalling during ZEB1-mediated epithelial-mesenchymal transition augments local myofibroblast differentiation in lung fibrosis.” Cell death and differentiation vol. 26,5 (2019): 943-957. doi:10.1038/s41418-018-0175-7
- Zepp, Jarod A, and Edward E Morrisey. “Cellular crosstalk in the development and regeneration of the respiratory system.” Nature reviews. Molecular cell biology vol. 20,9 (2019): 551-566. doi:10.1038/s41580-019-0141-3

- Zepp, Jarod A, and Edward E Morrisey. “Cellular crosstalk in the development and regeneration of the respiratory system.” Nature reviews. Molecular cell biology vol. 20,9 (2019): 551-566. doi:10.1038/s41580-019-0141-3

- Zhang, Yunfeng et al. “miR-200c serves an important role in H5V endothelial cells in high glucose by targeting Notch1.” Molecular medicine reports vol. 16,2 (2017): 2149-2155. doi:10.3892/mmr.2017.6792

8. Ringraziamenti

Questo lavoro è stato svolto all'interno del gruppo Cardio Vascular Biology, all'interno del centro internazionale di ingegneria genetica e biotecnologica di Trieste. Voglio ringraziare tutte le persone che hanno contribuito alla realizzazione di questa tesi con il loro aiuto, i loro commenti e il loro supporto emotivo e professionale.

Il primo ringraziamento va al Prof. Marco Confalonieri per aver dato l'opportunità a questa ragazza "sanguigna" (come ama definirmi) di iniziare questa avventura, per tutto il suo supporto sia emotivo che professionale, per le sue parole di conforto quando le cose andavano male e la voglia di continuare veniva a mancare, per avermi spedita tre mesi in America ad accrescermi scientificamente e culturalmente, per le liti e le discussioni, ed infine per non aver mai smesso di credere nelle mie potenzialità.

Il secondo ringraziamento va alla Prof. Serena Zacchigna, che mi ha ospitata nel suo laboratorio sin dal primo giorno. Grazie per tutti i rimproveri, le discussioni, i sorrisi e i pianti durante questi 3 anni. Grazie per la tua pazienza e la tua conoscenza scientifica. Se non fosse stato per te probabilmente oggi non sarei così forte e determinata.

Vorrei, inoltre ringraziare tutti i membri CVB, Simone, Andrea, Maristella e Barbara. Tutti loro hanno contribuito a rendere questi anni impressi nella mia mente. Grazie Andrea per avermi mandata dalla psicologa. Grazie Tea per avermi insegnato ad amare i cavalli. Grazie Matteo e William. Grazie Pietro, miglior studente mai avuto.

Nina, Roman e Alessia, cosa dire? Ho trovato una famiglia. Grazie per gli immensi sfoghi, grazie per essere sempre stati dalla mia parte, grazie davvero per tutto, perché senza di voi non avrei mai potuto farcela.

Grazie al dott. Mario Santagiuliana, per il meraviglioso viaggio a Dallas che ci ha resi due amici, grazie per il tuo sostegno e grazie per tutto l'aiuto datomi in questi 3 anni.

Grazie a Luca Braga per tutte le immagini acquisite e i pomeriggi a fare analisi.

Grazie ai miei amici, in primis Michela, la mia persona. Abbiamo iniziato questo percorso insieme, piangendo, ridendo e disperandoci. Grazie per tutto quello che hai fatto e che continui a fare, grazie per la correzione della mia tesi, grazie perché ESISTI.

Lo stesso ringraziamento va rivolto a Claudio e Ilaria, due capisaldi di questi 3 anni. Anche se non ce lo diciamo mai, grazie davvero di tutto, partendo dalla quarantena e dalle scappate per cercare di passare una serata insieme alla mia persistente e infinita ipocondria. Grazie!

Grazie Annalisa, per tutte le chiamate, per tutte le ore spese a sapere come sto, ad essere sempre la prima ad aspettare che io arrivi giù. Grazie di cuore.

A Davide, che completa la mia vita. A te che mi hai sopportato in questi anni sempre con il sorriso e dandomi la forza di andare avanti. A te che hai riempito la mia vita di dolcezza, sopportando tutti i momenti di follia, urla, grida e pianti.

Ed infine, grazie Mamma, Papà e Tommaso. A voi a cui devo la persona che sono diventata, che con mille sacrifici mi avete portata avanti un passo alla volta. A voi che devo non solo questa tesi ma tutta la mia intera vita. Grazie.
Ed alla fine: Ce l'ho FATTAAAAAAAA!!!!